NASA Technical Memorandum 104545

Preliminary Calibration Plan for the Advanced Particles and Field Observatory (APAFO) Magnetometer Experiment

C.V. Voorhies, R.A. Langel, J. Slavin,
E.R. Lancaster, and S. Jones

July 1991

NASA

NASA Technical Memorandum 104545

Preliminary Calibration Plan for the Advanced Particles and Field Observatory (APAFO) Magnetometer Experiment

C.V. Voorhies, R.A. Langel, J. Slavin
Goddard Space Flight Center
Greenbelt, Maryland

E.R. Lancaster and S. Jones
ST Systems Corporation
Lanham, Maryland

National Aeronautics and
Space Administration

Goddard Space Flight Center
Greenbelt, MD

1991

ABSTRACT

Pre-launch and post-launch calibration plans for the APAFO magnetometer experiment are presented. A study of trade-offs between boom length and spacecraft field is described; the results are summarized. The pre-launch plan includes: calibration of the Vector Fluxgate Magnetometer (VFM), Star Sensors, and Scalar Helium Magnetometer (SHM); optical bench integration; and acquisition of basic spacecraft field data. Post-launch calibration has two phases. In phase one, SHM data are used to calibrate the VFM, total vector magnetic-field data are used to calibrate a physical model of the spacecraft field, and both calibrations are refined by iteration. In phase two, corrected vector data are transformed into geocentric coordinates, previously undetected spacecraft fields are isolated, and initial geomagnetic field models are computed. Provided the SHM is accurate to the required 1.0 nT and can be used to calibrate the VFM to the required 3.0 nT accuracy, the trade-off study indicates that a 12-m boom and a spacecraft field model uncertainty of 5% together allow the 1.0-nT spacecraft field error requirement to be met.

CONTENTS

INTRODUCTION

The APAFO magnetometer experiment consists of a three-axis vector fluxgate magnetometer and a scalar helium magnetometer together with two star sensors. These are mounted on an optical bench at the end of a boom in order to reduce any magnetic fields from the spacecraft, its systems and other investigations. At present, the length of the boom is baselined at 12 m (see Figure 1). The scalar magnetometer sensor will be provided by E. Smith of the Jet Propulsion Laboratory (JPL); the vector magnetometer sensor and the electronics for both magnetometers will be provided by M. Acuna of Goddard Space Flight Center (GSFC); the star sensors will be provided by T. Potemra of The Johns Hopkins University Applied Physics Laboratory (APL). All three are APAFO Co-Investigators. The optical bench and boom will be provided by vendors to be selected during Phase C.

The error budget for the magnetometer experiment, in nanoTeslas (nT), is as follows:

	SCALAR		VECTOR	
	Req.	Goal	Req.	Goal
Instrument	1.0	0.7	3.0	1.5
Spacecraft Field	1.0	0.5	1.0	0.5
Position and Time	1.3	0.5	2.0	1.0
APAFO Field Error	0.2	0.1	0.2	0.1
Attitude Error	---	---	3.0	2.0
Rss	1.93	1.0	4.8	2.74

It is our intention to meet the goal and not merely the requirement. To do so in practice we must attempt to make the errors less than the goal. Toward that end, we suppose for now that the APAFO field error, i.e. that error due to stray magnetic fields from the instruments mounted at the optical bench, can be reduced to 0.1 nT or less. We may then proceed to consider the other sources of error.

The purview of this report, then, are the instrument and spacecraft field contributions to the error budget. For this mission, the basic in-flight standard of accuracy is the scalar helium magnetometer (SHM). It is believed that the SHM can be built and calibrated pre-launch such that its basic accuracy is within 0.7 nT. This report shows that if this is accomplished then the meeting of the error budget goal for spacecraft field and APAFO field is feasible, provided an adequate model of the spacecraft field is derived and provided that the input information needed in that model is present in the spacecraft telemetry.

To accomplish this will require certain steps be taken both prior to launch and in orbit to calibrate both the magnetometers and the spacecraft field model. These procedures are the topic of this report.

PRE-LAUNCH CALIBRATION

Vector Fluxgate Magnetometer (VFM)

1. Internal calibration parameters will be established by comparison with an absolute instrument at the GSFC magnetic test site.

2. The relationship of the internal magnetometer axes to a coordinate system determined by an externally mounted optical cube must be experimentally determined.

APAFO Magnetic Fields

An attempt will be made to determine parameters for fields exceeding 0.1 nT at the SHM due to the VFM and star sensors and for fields exceeding 0.1 nT at the VFM due to the star sensors.

Star Sensors

APL and their external vendors shall furnish calibration parameters relating the field of view of the sensor to a coordinate system determined by an externally mounted optical cube.

Scalar Helium Magnetometer (SHM)

The accuracy of the SHM shall be determined by laboratory measurement of the various parameters contributing to instrument error. This error budget is made up of:

Light Shift	0.5 nT
Noise	0.15 nT
Servo Error	0.1 nT
Readout Error	0.07 nT
Electronic Offset	0.05 nT

which gives a maximum error of 0.87 nT or an rss error of 0.54 nT.

In addition, the overall error shall be verified by direct comparison with a Proton Precession Magnetometer over its range of operation and over a comprehensive selection of field directions with respect to the magnetometer axis.

Integrated Optical Bench

Optical alignments shall be determined between the four optical cubes: one each on the two star sensors, one on the VFM and one on the SHM. This should be accomplished in the GSFC optical facility according to a plan submitted by the contractor responsible for integration and test.

Optical alignment accuracies are expected to be within 1 arc-second, 3σ.

Spacecraft

1. The locations of the magnetic torquers, solar panels, and any other magnetic sources likely to cause a field >0.1 nT at the optical bench, shall be measured relative to the base of the APAFO boom to an accuracy of about 3-5 cm.

2. The pole-strength of the magnetic torquers as a function of the current applied shall be measured to at least 1%.

3. As possible, the magnetic characteristics of other magnetic sources, including investigator instruments, shall be specified (measured) as a function of their operational state.

4. The housekeeping telemetry shall include, as possible,
   a) Torquer current,
   b) Solar panel current, position and other state information,
   c) Main bus current,
   d) Pertinent state information from other identified magnetic sources.

5. The boom will need to be deployed to a position whose accuracy should be known to about 2-3 cm.

POST-LAUNCH CALIBRATION

It cannot be assumed that the pre-launch APAFO magnetometer calibration will be unchanged by launch, boom deployment, and long-duration exposure to the space environment. In-flight magnetometer calibration is necessary to monitor and correct for changes during launch and on orbit. Post-launch calibration will take place periodically during the mission. The frequency of the various steps in this calibration will be determined after launch when it is found how rapidly the calibration parameters are changing. Calibration must enable accurate calculation of the geophysical parameters (the ambient magnetic flux density vector) from APAFO data both during and between calibrations despite variable spacecraft fields, small boom motions, and VFM drift. Periodic in-flight calibration of the VFM against the SHM is used to derive the VFM calibration parameters. These periodically updated parameters enable calculation of total vector magnetic-field values between calibration runs; however, calculation of the ambient field also requires elimination of the spacecraft field from the observed total field. This requires a model of the spacecraft field which itself must be calibrated.

Post-launch calibrations will consist of two phases, each with several steps. The first phase consists of those steps necessary to determine the VFM calibration parameters and the spacecraft field model parameters. The second phase consists of those steps necessary to confirm and/or modify transformations between spacecraft and Earth-centered coordinates and to model any previously unaccounted-for fields originating on the spacecraft.

PHASE ONE

At present this phase will be described as a multi-step iterative process. It is easier to comprehend and describe when viewed in this manner. However, in practice the procedure may be integrated. The actual procedure to be followed will be determined in a Phase C study.

Phase One: Notation and Coordinates

Begin by introducing time, t, dependent coordinate systems and position vectors therein:

$\mathbf{r}(t) \equiv$ position of the ESA/PPF spacecraft coordinate system origin in Earth-centered spherical polar coordinates.

$\mathbf{x}^o(t) \equiv$ position of the optical bench coordinate system origin in the spacecraft coordinate system ($x \simeq -12m, y \simeq 8m, z \simeq 0m$).

$\mathbf{x}^j(t) \equiv$ position of the j^{th} sensor in spacecraft coordinates.

$\mathbf{x}^{*j}(t) \equiv$ position of the j^{th} sensor in optical bench coordinates.

$\mathbf{x}^*(t) \equiv$ nominal position of the observation in optical bench coordinates, the 'center' of the SHM ($\mathbf{x}^* = \mathbf{x}^{*5}$).

Assume a rigid optical bench: $\mathbf{x}^{*j}(t) = \mathbf{x}^{*j}$ and $\mathbf{x}^{*}(t) = \mathbf{x}^{*}$. Boom flex, twist, and stretch indicated by time-varying $\mathbf{x}^{o}(t)$ admit time-varying $\mathbf{x}^{j}(t)$ despite steady $\mathbf{x}^{*j}$.

The true magnetic flux density vector $\mathbf{B}$ is the sum of the ambient field $\mathbf{B}^{A}$ which would exist in the absence of the spacecraft, the spacecraft field $\mathbf{B}^{S}$, and the platform or bench field $\mathbf{B}^{P}$ generated by APAFO instrumentation and equipment:

$$\mathbf{B}(\mathbf{x}^{*j},t) = \overset{A}{\mathbf{B}}(\mathbf{x}^{*j},t) + \overset{S}{\mathbf{B}}(\mathbf{x}^{*j},t) + \overset{P}{\mathbf{B}}(\mathbf{x}^{*j},t) \ . \qquad (0)$$

The transformation of (0) between coordinate systems is a tri-axial, time-dependent rotation. The default coordinate system is the optical bench coordinate system, which must be transformed into a celestial reference frame using bench-mounted star cameras and then into a terrestrial reference frame using ESA/PPF position data. For APAFO we consider, for generality, one quadraxial VFM ($j = 1,2,3,4$) and a single cell SHM magnetometer ($j = 5$) on the bench. Note that quadraxial rather than triaxial fluxgates would be appropriate to the 4-coil/2-ring core, null-in-plane design. Each VFM coil is considered as defining one sensor axis. Two sensor axes ($j = 1$ and $j = 4$) will be very nearly parallel. Onboard or inboard magnetometers ($j > 5$) could improve spacecraft field estimation and elimination, but are not expected.

Assume digital data is received from functioning magnetometers in the form of bit streams:

$\bar{u}_{jk}(t_i) \equiv k^{th}$ bit of the offset field generator code for the j^{th} VFM sensor at time t_i ($j \leq 4$; $k \leq 7$); these bits define the integer $g_j(t_i)$: $(-64 \leq g_j(t_i) \leq 63)$.

$\bar{f}_j(t_i) \equiv$ fine measurement from the j^{th} VFM sensor fine reading - a 16-bit integer $-32768 \leq f_j \leq 32767$ ($j \neq 5$).

$\bar{f}_5(t_i) \equiv$ fine reading from the SHM (a 19- or 21-bit positive integer).

$\bar{I}_r(t_i) \equiv$ signed integer representing measured current energizing the r^{th} torque rod ($r = 1,2$).

$\bar{I}_4(t_i) \equiv$ positive integer representing current from the solar array.

$C \pm \sigma C \equiv$ He scalar calibration coefficient $\pm$ uncertainty therein.

$\sigma f_j(t_i) \equiv$ precision of $\bar{f}_j(t_i)$ ($\pm$ 0.5 in the least significant bit if f_j represents a rounding to the nearest integer; truncation would merely contribute to VFM biases).

$\sigma I_r \equiv$ precision of $\bar{I}_r$; and $\sigma I_4 \equiv$ precision of $\bar{I}_4$.

Note the σ prefix indicates the uncertainty in the ensuing quantity. The goal is to use these data, which by design must represent the simultaneously measured field at times t_i ($i = 1,2,3,\ldots I$) during the calibration run $t_o \leq t_i \leq t_f$, to calibrate the magnetometer system.

Phase One: Method

The present method extends the work of Lancaster et al., "Magsat Vector Magnetometer Calibration Using Magsat Geomagnetic Field Measurements" Nov. 1980; NASA Technical Memorandum 82046. The main problems considered are how to:

(I) Calibrate the VFM (j=1,2,3,4) against the SHM (j = 5).

(II) Calibrate the spacecraft field model so as to obtain initial estimates of $\mathbf{B}^S(\mathbf{x}^*,t)$ and $\mathbf{B}^A(\mathbf{x}^*,t)$ both during and between calibration runs.

(III) Correct and improve (I) and (II) by iterative refinement.

At present, only the magnetic torquers are considered primary spacecraft field sources. In the initial iteration of Step (I), pre-launch calibration parameters of the VFM will serve as the starting, or a-priori, model. Also, pre-launch calibration parameters for the spacecraft field sources may be utilized in Step (I) for the calculation of field gradients between the SHM and the VFM.

The present assumptions in Step (I) are: (1) that the SHM accuracy is $\pm$ 0.7 nT or better for its entire operating range; (2) that the VFM can be calibrated, using the SHM, to an accuracy of 1 nT, 1σ, in the magnitude of its measurement and to an accuracy of 2 nT, 1σ, in the accuracy of its measurement of each component. The procedure for accomplishing this is described in this section and is based upon a similar procedure used for Magsat as described by Lancaster et al. (1980). Results of applying the procedure to the Magsat data are described by Langel et al. (1981).

As will be pointed out, full calibration of the VFM (Step (I)) requires that, during the collection of data for a calibration run, the ambient field along each VFM axis swing through its full range while data are available from the scalar instrument. Such full-range calibration is highly desirable but not essential. What is essential is that the appropriate combinations of VFM calibration parameters be determined such that all VFM states encountered during normal measurement of the Earth's field will be calibrated. This should be achievable with appropriate geometric orientation of the VFM and SHM axes. Such locations will be determined in Phase C of the project.

The more ambitious goal of full-range VFM calibration should also be pursued. Such calibration may require a planned attitude maneuver of the spacecraft for a short period of time (say, about 10 minutes) upon rare (say, once every 6 months) occasions during the mission. Attitude maneuvers needed to maintain orbit attitude and ground-track repeat cycle may prove adequate for this purpose.

Problem (I) is solved with estimates of steady calibration parameters, p_n, and the time-varying total vector field values at the bench, $\mathbf{B}(\mathbf{x}^*,t_i)$, with components B_{ik} (k = 1,2,3). These estimates are to be obtained by iterating an optionally constrained, weighted, linearized least-squares calibration algorithm on data acquired at I discrete times t_i during each calibration interval $t_o \leq t_i \leq t_f$. VFM drift is identified as any change in the p_n which contributes more than about 0.2 nT change in measurement value between calibration runs. Problem (II) is solved with estimates of primary spacecraft field calibration parameters M_{lr}. These estimates may be derivable from routinely collected data but should be verified during times when a distinct, rapidly varying torque rod current signal can be separated from the more slowly varying ambient field. Problem (III) is solved by using results from (II) to correct (I).

An advantage of this method is that VFM calibration need not depend upon either the spacecraft field parameterization or the twist, flex, or stretch of the boom. This could be achieved by solving (I) alone with data corresponding to times of weak or steady spacecraft field (e.g., in shadow with all torque rods off). Each step also poses a smaller computational problem than would a simultaneous approach. The main disadvantages are as follows. (a) During iterated VFM calibration runs, effects of field gradients across the VFM caused by the spacecraft and bench instrumentation are treated as due in part to a spacecraft field model; the second and higher VFM calibration iterations thus depend weakly upon spacecraft field parameterization. (b) A steady field gradient appears indistinguishable from VFM bias. (c) Unmodeled boom motion may degrade spacecraft field calibration and thus, ambient field estimation.

Problem (a) influences admissible t_i, boom length, and bench fields, and the utility of the method. Problem (b) is addressed by the Phase two calibration. As to problem (c), simultaneous attitudes for both the APAFO bench and the spacecraft derived from star cameras mounted on the bench and onboard the spacecraft are to give their relative orientations to about 121 arc-seconds rss; with a mechanical model of the boom, this relative orientation might be used to estimate boom-end position and remove the effects of translation (as well as rotation) through the spacecraft field. Such estimation could be difficult due to complex forcing and boom overtones; the boom should be designed to keep such effects small. The accuracy of the spacecraft field corrections, and the utility of VFM data to calibrate a spacecraft field model, are here considered limited by effects of boom-tip translation--as distinct from the relative orientation of bench and spacecraft coordinate systems. Fortunately, knowledge of the latter allows tagging of unexpected, off-nominal, boom-tip positions.

The method seems well suited to a long-boom, far-field case in which secondary spacecraft field gradients across the bench are weak and effects of VFM translation; i.e., from boom motions, through the spacecraft field are usually small. The major difficulty is the potential inadequacy of the spacecraft field parameterization due to insufficient ground-based spacecraft field measurements, unmodeled sources, or uncertainty in the deployed position of the bench relative to the spacecraft.

Phase One: Step I, Vector Fluxgate Calibration (VFC)

This section extends the work of Lancaster et al., 1980 on the MAGSAT calibration. From the He scalar magnetometer

$$|B(x^{*5},t_i)| = [C \pm \sigma C][f_5(t_i) \pm \sigma f_5(t_i)] \equiv C[f_5(t_i) \pm \sigma_5(t_i)] \quad (1)$$

where $C\sigma_5$ is the root-sum-square uncertainty in the scalar field.

At any given time the measured field value along the j^{th} sensor axis is, for $j \leq 4$, assumed to be of the form

$$\bar{y}_j = \sum_{k=1}^{K} w_{jk}\bar{U}_{jk} + \sum_{l=1}^{L} w^*_{jl}N_{jl} + a_j(\bar{f}_j - b_j) \quad (2)$$

where

$\bar{U}_{jk} \equiv -\bar{u}_{jk}$ for $k \leq 6$ and $\bar{U}_{j7} = \bar{u}_{j7}$ for $K = 7$.

$w_{jk} \equiv$ calibration coefficient for the k^{th} offset generator bit of the j^{th} sensor coil.

$N_{jl} \equiv N_{jl}(\bar{u}_{jk})$ is the l^{th} non-linear function representing the non-linear response of the j^{th} sensor coil. The form of the $N_{jl}(\bar{u}_{jk})$ must be specified by ground calibration.

$w^*_{jl} \equiv$ calibration coefficient for N_{jl} --for the lth non-linear response functional of the j^{th} sensor coil. We anticipate $w^*_{jl}N_{jl} = 0_{jl}$.

$a_j \equiv$ scale factor for the j^{th} sensor fine reading.

$b_j \equiv$ bias of the j^{th} sensor.

It is convenient to introduce the generic measured form

$$\bar{y}_j = a_j[\bar{f}_j - b_j] + \sum_{m=1}^{M} c_{jm}F_{jm}(\bar{u}_j) \qquad (j \leq 4) \quad (3a)$$

$$\bar{y}_5 = C\bar{f}_5 \quad (3b)$$

where: a_j, b_j $\bar{f}_j$, $\bar{f}_5$, and C are as before; $\bar{u}_j$ is the K element vector of bits from the offset field generator code of the j^{th} sensor; the c_{jm} are the offset field calibration coefficients (w_{jk} or w^*_{jl}); and $F_{jm}(\bar{u}_j)$ is the m^{th} known calibration function for the j^{th} sensor (just U_{jk} if $L = 0$ and $M = K$). For MAGSAT, $L = 2$ and N_{j1} and N_{j2} were respectively the third and fifth power of signed $g_j(u_j)$. For APAFO, we expect $K = 7$, guess $L = 1$, and anticipate f_j to be a 16-bit result of an A to D conversion ($-32768 < f_j < 32767$). If so, there would be 10 sensor parameters per coil (a_j, b_j, and $M = 8$ c_{jm}) and 40 sensor parameters to determine. If $L = 0$; then $M = K = 7$, $c_{jm} = w_{jm}$, $F_{jm}(u_j) = U_{jm}$ and there may be but 36 sensor parameters to determine.

The measured fluxgate field values (3a) are, within the precision of digitized measurement ($\sigma_j = \sigma f_j = \pm 0.5$ for $j \leq 4$), theoretically indistinguishable from the result of a system response matrix ρ_{jk} operating on the true field components $B_k(\mathbf{x}^{*j})$

$$y_j = \sum_{k=1}^{3} \rho_{jk} B_k(\mathbf{x}^{*j}) = \sum_{k=1}^{3} G_{jk}(\mathbf{B},\mathbf{a};\mathbf{h}) a_{jk} B_k \ . \tag{4a}$$

The matrix notation for (4a) is $\mathbf{y} = \rho\mathbf{B}$. The measured scalar field (3b) is, within the absolute accuracy of measurement ($C\sigma_5$ from (1)), theoretically indistinguishable from the true scalar intensity

$$y_5 = [\sum_{k=1}^{3} (B_k(\mathbf{x}^{*5})^2]^{1/2} \ . \tag{4b}$$

In (4a-b)

$B_k(\mathbf{x}^{*j}) \equiv k^{th}$ field component at j^{th} sensor in bench coordinates.

$a_{jk} \equiv \cos\theta_{jk}$ and θ_{jk} is the angle between the j^{th} sensor axis and the k^{th} APAFO bench coordinate system axis.

Note $\sum_{k=1}^{3} (a_{jk})^2 = 1$, so

$$a_{11} = (1 - a_{12}^2 - a_{13}^2)^{1/2} \qquad a_{33} = (1 - a_{31}^2 - a_{32}^2)^{1/2}$$
$$a_{22} = (1 - a_{21}^2 - a_{23}^2)^{1/2} \qquad a_{43} = (1 - a_{41}^2 - a_{42}^2)^{1/2} \ . \tag{5}$$

G_{jk} accounts for possibly non-linear cross-coupling and may depend upon the 3 elements B_l of $\mathbf{B}(\mathbf{x}^{*j})$, the elements a_{jk} of matrix $\mathbf{a}$, and parameter matrix $\mathbf{h}$ (see Appendix A). The functional form of $G_{jk}(\mathbf{B},\mathbf{a};\mathbf{h})$ and the numerical values of $\mathbf{h}$ must be specified by ground calibration. For APAFO we anticipate linear cross-coupling, $G_{jk} \simeq 1$ and $\rho_{jk} \simeq a_{jk}$ (M. Acuña, 1990 pers. comm.; see Appendix A).

ρ_{jk} is the 4x3 system response matrix (see Appendix A). If G_{jk} depends on $B_k(\mathbf{x}^{*j},t_i)$, then ρ_{jk} is implicitly time dependent; this is not anticipated, but the possibility is admitted here.

Now 4 of the 12 a_{jk} would follow from (5) and values for the other 8; yet all 12 ρ_{jk} are needed. Thus, 40 + 12 = 52 true calibration parameters need to be estimated along with $B_k(\mathbf{x}^{*j},t_i)$. (See Appendix A; for linear response, there would be 36 + 12 = 48 parameters to estimate.)

With (3a-b), measured values $\bar{y}_j$ calculated from the bits, the true values of the sensor parameters, and C would be true values to within instrumental precision; with (4a-b), true values y_j follow from true values for ρ_{jk} and $B_k(\mathbf{x}^{*j})$. True values cannot be assumed; yet given (3) and (4), the difference between true and measured values can be minimized provided

the calibration parameters are steady during each calibration run and provided an expression can be identified which links $\mathbf{B}(\mathbf{x}^{*j},t_i)$ to $\mathbf{B}(\mathbf{x}^{*5},t_i)$ for $j \leq 4$.

Assume that the ambient field is, at any t, homogeneous across the bench. Then the bias field (defined for $j \leq 4$),

$$\boldsymbol{\delta}(\mathbf{x}^{*j},t) \equiv \mathbf{B}(\mathbf{x}^{*5},t) - \mathbf{B}(\mathbf{x}^{*j},t) \tag{6}$$

is due solely to $\mathbf{B}^P + \mathbf{B}^S$. If $\boldsymbol{\delta}$ were steady, then it would be indistinguishable from steady VFM biases and no extra steps are needed. To see this note $\mathbf{B}(\mathbf{x}^{*5},t_i)$ would be $\mathbf{B}(\mathbf{x}^{*j},t_i) + \boldsymbol{\delta}(\mathbf{x}^{*j})$, so at each t_i

$$B_k(\mathbf{x}^{*5}) = \sum_{l=1}^{3} (\boldsymbol{\rho}^T\boldsymbol{\rho})^{-1}{}_{kl} \sum_{j=1}^{4} \rho_{jl} y_j + \delta_k(\mathbf{x}^{*j})$$

would be indistinguishable from adding $b_j^* \equiv \sum_{n=1}^{3} a_j^{-1}\rho_{jn}\delta_n$ to b_j:

$$B_k(\mathbf{x}^{*5}) = \sum_{l=1}^{3} (\boldsymbol{\rho}^T\boldsymbol{\rho})^{-1}{}_{kl} \sum_{j=1}^{4} \rho_{jl}(y_j + a_j b_j^*)$$

where matrix inversion preceeds assignation of element indicies.

Now $\boldsymbol{\delta}$ may be steady to within mission goals during certain select intervals (preferred VFC times), but might not be at all t. Indeed, $\boldsymbol{\delta}$ will not be steady enough when time-varying spacecraft field gradients are too steep at the end of the boom. For ESA/PPF torquer rods amounting to a point dipole of maximum moment 495 Atm^2, the radial gradient of the radial field over 0.5-m amounts to differences of at most,3.9 nT at 14 m (the radial field is at most,36 nT; see, e.g.,Figure 2). The transverse gradient of the radial field, the radial gradient of the transverse field, and the transverse gradient of the transverse field,respectively,give at most 1/3, 1/2, and 1/6 of this extreme value. In the more realistic case of a dipole of moment (350, 0, -350) Atm^2 at the origin, the field at (12, 7.5, 0) m differs from that at (12, 8, 0) m by (1.7, 0.5, 0.7) nT, but only 1.6 nT scalar.

Corrections for time-varying bias fields of such magnitude are needed. The corrected value of f_j would be measured f_j minus $\Sigma_k\, a_j^{-1}\rho_{jk}\delta_k$ --with all quantities evaluated at t_i. Such corrections require values for a_j, possibly time-varying $\boldsymbol{\rho}$, and time-varying $\boldsymbol{\delta}$ in the bench coordinate system. The latter require information on the spacecraft field and on the relative orientations and positions of the bench and spacecraft coordinate systems--perhaps from outboard and onboard star cameras. Now 14 m from a 495-Atm^2 dipole-a 0.5° relative orientation error in a spacecraft field of at most 36 nT implies a spacecraft field error of at most (36 nT)$\times$sin0.5° = 0.3 nT; the implied error in the bench bias field correction is negligible (being at most (3.9 nT)$\times$sin0.5° = 0.034 nT). Such small rotations through the spacecraft field need not alter bench bias corrections appreciably, so it is argued that these particular corrections may presume a rigid boom. Here it is first supposed that $\boldsymbol{\delta}$ is steady, but that step (II) will allow a correction for the part of $\boldsymbol{\delta}$ due to the time-varying primary spacecraft field. Corrections for the part of $\boldsymbol{\delta}$ due to bench instrumentation might be achieved using ground calibrated models for said instruments.

Because sensors j = 1 and j = 4 have nearly parallel axes, there are two quasi-independent VFM calibration configurations. Configuration 1 uses j = 1,2,3 (and 5). Configuration 2 uses j = 2,3,4 (and 5). Baseline Configuration 0 uses j = 1,2,3,4 (and 5). Each configuration can be used to estimate the calibration parameters and the uncorrected geophysical parameters ($\mathbf{B}^A + \mathbf{B}^S + \mathbf{B}^P$). Comparison of these results enables: validation, estimation of calibration uncertainty, and a check on formal error estimates. Such comparisons may also prove sensitive to a selected (z) component of bench fields due to the 7-cm separation of coils 1 and 4.

With the understanding that b_j is now the bias due to both the j^{th} sensor and any uncorrected steady bias field, and with B_k now regarded as $B_k(\mathbf{x}^{*5})$, the 3 configurations give:

Configuration 0 ($j = 1,2,3,4$): $y_j = \sum_{k=1}^{3} \rho_{jk} B_k$ implies $B_k = \sum_{l=1}^{3} (\boldsymbol{\rho}^T \boldsymbol{\rho})^{-1}_{kl} \sum_{j=1}^{4} \rho_{jl} y_j$

Configuration 1 ($j = 1,2,3$): $y_j = \sum_{k=1}^{3} {}^1\rho_{jk} B_k$ implies $B_k = \sum_{l=1}^{3} ({}^1\boldsymbol{\rho}^{-1})_{kl} \sum_{j=1}^{3} {}^1\rho_{jl} y_j$

Configuration 2 ($j = 2,3,4$): $y_j = \sum_{k=1}^{3} {}^2\rho_{jk} B_k$ implies $B_k = \sum_{l=1}^{3} ({}^2\boldsymbol{\rho})^{-1}_{kl} \sum_{j=2}^{4} {}^2\rho_{jl} y_j$

where ${}^1\rho_{jl}$ and ${}^2\rho_{jl}$ are the relevant 3x3 sub-matricies. Only Baseline Configuration 0 is treated here because all calibration parameters are obtained and because Configurations 1 and 2 are easier; moreover, sensors (1,4) have the strongest cross-coupling and are but quasi-independent. Either Configuration 1 or 2 suffice because the resulting B_k at many t_i overdetermine the calibration parameters for the remaining sensor; yet the opportunity for validation offered by multiple configurations is not to be overlooked. It seems wise to mount the VFM so that the nearly parallel sensors detect mostly the geocentrically radial ambient field component.

Assume simultaneous measurements at I times t_i. With the functional forms of F_{jm} and G_{jk} specified, and measured bits $\bar{u}_j$ at times t_i denoted $\bar{u}_{ij}$ from telemetry, we need to estimate

(i) 52 steady calibration parameters $p_n = \{a_j, b_j, c_{jm}, \rho_{jk}\}$

(ii) 3I uncorrected field parameters $B_{ik} = B_k(\mathbf{x}^{*5}, t_i)$

from the single scalar calibration coefficient and the 5I measurements: $\{\bar{f}_{ij}, \bar{u}_{ij}\}$ (4I) and f_{i5} (1I). As sensors j = 1 and j = 4 are nearly parallel, it seems there are but 4I pieces of information to estimate the 3I + 52 parameters. So I > 17 is essential, and $I \simeq 10^3$ is anticipated. The 5I equations are

$$\bar{y}_{ij} = a_j[\bar{f}_{ij} - b_j] + \sum_{m=1}^{M} c_{jm} F_{jm}(\bar{u}_{ij}) \qquad (j \leq 4) \qquad (7a)$$

$$\simeq a_j[f_{ij} - b_j] + \sum_{m=1}^{M} c_{jm} F_{jm}(\bar{u}_{ij}) = \sum_{k=1}^{3} \rho_{jk} B_{ik} = y_{ij}$$

$$\bar{y}_{i5} = C\bar{f}_{i5} \simeq [\sum_{k=1}^{3} (B_{ik})^2]^{1/2} = y_{i5} \qquad (7b)$$

where the approximations hold only to within the precision (7a) or absolute accuracy (7b) of measurement--and only then if both the theory on the right and the instrument model on the left are correct. The precision of measurement is accommodated by weights.

For the optionally constrained, weighted, iterated, linearized least-squares approach anticipated, we need: measured $\bar{f}_{ij}(j=1,2,3,4,5)$ and $\bar{u}_{ij}$, C, the functional forms of F_{jm} and G_{jk}; the uncertainty estimates σ_j in the measured $\bar{f}_{ij}$ (again, nominally ± 0.5 bit for $j \leq 4$, and $\sigma 5$ from (1)), and some initial guess of the calibration parameters--the measured values from the ground calibration. The idea is that minimizing the difference, albeit weighted-sum squared, between measured and theoretical true values of y_{ij} estimates true y_{ij}.

Following Lancaster et al., focus on f_{ij} rather than y_{ij}. From (7), the theoretical true values f_{ij} are

$$f_{ij} = a_j^{-1}[\sum_{k=1}^{3} \rho_{jk}B_{ik} - \sum_{m=1}^{M} c_{jm}F_{jm}(\bar{u}_{ij})] + b_j \qquad (j \leq 4) \qquad (8a)$$

$$f_{i5} = C^{-1}[\sum_{k=1}^{3} (B_{ik})^2]^{1/2} \; . \qquad (8b)$$

The partial derivatives of f_{ij} with respect to calibration parameters p_n and uncorrected geophysical parameters B_{ik} are, respectively

$$\frac{\partial f_{ij}}{\partial p_n} \equiv s_{ijn} \qquad \frac{\partial f_{ij}}{\partial B_{ik}} \equiv r_{ijk}$$

with subscripts i (1→I) for time, sensor j (1→5), calibration parameter n (1→52) and field component k (1→3) in bench coordinates.

Now $\partial f_{i5}/\partial p_n = 0_{i5n}$, so the only non-trivial s_{ijn} have $j \leq 4$ and, by (8), are

$$\frac{\partial f_{ij}}{\partial a_j} = -a_j^{-2}[\sum_{k=1}^{3} \rho_{jk}B_{ik} - \sum_{m=1}^{M} c_{jm}F_{jm}(\bar{u}_{ij})] = -(f_{ij} - b_j)/a_j \qquad (9a)$$

$$\frac{\partial f_{ij}}{\partial b_j} = 1 \qquad (9b)$$

$$\frac{\partial f_{ij}}{\partial c_{jm}} = -a_j^{-1}F_{jm}(\bar{u}_{ij}) \qquad (9c)$$

$$\frac{\partial f_{ij}}{\partial \rho_{jk}} = a_j^{-1} \sum_{l=1}^{3} [\frac{\partial \rho_{jl}}{\partial \rho_{jk}} B_{il}] = \sum_{l=1}^{3} a_j^{-1} \delta_{kl} B_{il} = a_j^{-1} B_{ik} \ . \qquad (9d)$$

Note (9d) anticipates linear cross-coupling and treats the elements of ρ as independent. For non-linear cross-coupling (9d) would be replaced by

$$\frac{\partial f_{ij}}{\partial a_{jk}} = a_j^{-1} \sum_{l=1}^{3} [\frac{\partial \rho_{jl}}{\partial a_{jk}} B_{il}] = \sum_{l=1}^{3} a_j^{-1} \{[G_{jl}(\frac{\partial a_{jl}}{\partial a_{jk}}) + (\frac{\partial G_{jl}}{\partial a_{jk}}) a_{jl}] B_{il}\}$$

where some of the $\partial a_{jl}/\partial a_{jk}$ are zero by (5). For no cross-coupling, all G_{jl} would be 1 and all $\partial G_{jl}/\partial a_{jk}$ would be zero; for non-linear MAGSAT cross-coupling, 3 of 9 G_{jl} differed from unity, $\partial G_{jl}/\partial a_{j'k}$ was zero unless $j = j'$ --in which case $\partial \rho_{jl}/\partial a_{jk}$ depended only upon $\mathbf{B}_i$ and the ground based values of $\mathbf{h}$. The replacement for (9d) would thus suppose $j = j'$ and estimate the 8 independent a_{jk} rather than 12 ρ_{jk}.

The only non-trivial r_{ijk} are, according to (8)

$$\frac{\partial f_{ij}}{\partial B_{ik}} = a_j^{-1} \sum_{l=1}^{3} [\rho_{jl} \delta_{lk} + \frac{\partial \rho_{jl}}{\partial B_{ik}}] B_{il} \qquad (10a)$$

$$\frac{\partial f_{i5}}{\partial B_{ik}} = (C^2 f_{i5})^{-1} B_{ik} \ . \qquad (10b)$$

The partials (9-10) imply $s_{ijn} = s_{ijn}(p_n, B_{il}; f_{ij}, F_{jm}(\bar{u}_{ij}))$ and $r_{ijk} = r_{ijk}(p_n, B_{il}; f_{ij}, F_{jm}(\bar{u}_{ij}))$. The inverse problem is thus non-linear: refined estimates of p_n and B_{ik} require prior values for p_n and B_{ik}. In the iterative linearized method of estimation anticipated, all partial derivatives are evaluated at the best previous values of p_n and B_{ik} (and f_{ij})--be it an initial guess or a subsequent estimate.

For quantity q, denote: true value q; guess $\tilde{q}$; measurement $\bar{q}$; and estimate $\hat{q}$. The expected VFM change upon launch enjoys zero mean, so initial guesses of a_j, b_j, c_{jm}, and a_{jk} are pre-launch values 'measured' during ground calibration ($\tilde{p}_n = \bar{p}_n$). For purely linear cross-coupling an initial guess of B_{ik} follows from $\tilde{p}_n$ and telemetry. To obtain $\tilde{B}_{ik}$ for non-linear cross-coupling, guess $\tilde{B}^0_{ik}$ (e.g., suppose either linear response or the values indicated by position and attitude in a 29,500-nT geocentric axial dipole) and use it with $\tilde{a}_{jk}$ and $\mathbf{h}$ to compute $\tilde{G}^0_{jk}$, hence $\tilde{\rho}^0_{jk}$. Then use $\tilde{\rho}^0_{jk}$ and $\tilde{y}_{ij}$ to compute $\tilde{B}^1_{ik}$ and iterate until satisfactory values for $\tilde{B}_{ik}$ and $\tilde{\rho}_{jk}$ are obtained. Either way, these guesses give

$$\tilde{y}_{ij} = \tilde{a}_j [f_{ij} - \tilde{b}_j] + \sum_{m=1}^{M} \tilde{c}_{jm} F_{jm}(\bar{u}_{ij}) \qquad (j \leq 4) \qquad (11a)$$

$$\tilde{B}_{ik} = \sum_{l=1}^{3} [\tilde{\rho}^T \tilde{\rho}]^{-1}_{kl} \sum_{j=1}^{4} \tilde{\rho}_{jl} \tilde{y}_{ij} \tag{11b}$$

$$\tilde{f}_{i5} = C^{-1}[\sum_{k=1}^{3} (B_{ik})^2]^{1/2} \neq \bar{f}_{i5} \tag{11c}$$

where the anticipated inequality on the far right of (11c) is to be eliminated, along with the guesswork, by calibration.

Let $\mathbf{f} \equiv \{f_{ij}, f_{i5}\}$ be the column vector of 5I true fine readings, $\mathbf{z} \equiv \{p_n, B_{ik}\}$ the vector of 3I+52 true calibration and total field components, and let $\Gamma \equiv \{s_{ijn}, r_{ijk}\}$ be the matrix of the partial derivatives $\partial\mathbf{f}/\partial\mathbf{z}$ (evaluated at true $\mathbf{z}$) with 5I+52 rows and 3I+52 columns. Let $\mathbf{W}$ be the 5Ix5I matrix of fine measurement weights--the expectation value $\{\sigma_{ij}\sigma_{ik}\}^{-1}$ (noting that the σ_{ij} are expected to be independent and steady so that $\mathbf{W}$ is a diagonal matrix of constant elements).

We seek to minimize $(\mathbf{f} - \mathbf{f})^T\mathbf{W}(\mathbf{f} - \mathbf{f})$. Unfortunately, constraints may be needed to hold estimates of a few p_n near previous estimates (if not ground-based values). The reason is that some data bits comprising some $\bar{u}_j$ are not expected to change independently during some calibration runs due to VFM attitude in the largely dipolar ambient field. This problem is exacerbated by the loss of scalar signal (LOSS) encountered when the field vector is inclined by more than 60^o relative to the single SHM cell axis. Two suitably oriented SHM cells will prohibit LOSS events during intervals of nominal spacecraft attitude. During such runs, the corresponding p_n (a few of the 28 w_{jk}) cannot be estimated. Either these special parameters must be fixed to their previous values and the corresponding rows and columns of Γ deleted or, perhaps more simply, a constraint can be added to the objective function which keeps them near their previous values. The added constraint is of the form $(\mathbf{z} - \bar{\mathbf{z}})\mathbf{\Lambda}(\mathbf{z} - \bar{\mathbf{z}})$ where $\bar{\mathbf{z}}$ is the previous estimate--regarded as a 'measured' value. "Nearness" is judged by the elements of the damping matrix $\mathbf{\Lambda}$ which, in turn, is a modification of the information matrix from the previous calibration $\mathbf{\Omega}^{-1}$.

The previous calibration covariance $\mathbf{\Omega}$ is generally a full matrix and is the expectation value $\{(\sigma\mathbf{z})(\sigma\mathbf{z})^T\}$, but only its upper left-hand portion contains the expectation value $\{(\sigma\mathbf{p})(\sigma\mathbf{p})^T\}$ (i.e., the covariance of $\mathbf{p}$ from the previous estimate). The information matrix $\mathbf{\Omega}^{-1}$ will normally be the expected weight or confidence matrix. However, if the parameters change too much, this weighting may need to be modified or reduced. In the extreme case of drastic change from the previous calibration one would assign zero confidence to all previous estimates of B_{ik} and p_n --excepting those which cannot be estimated due to LOSS or attitude restrictions and are, perforce, kept close to the previous estimate. This can be achieved by setting all elements of $\mathbf{\Omega}^{-1}$ to zero except the few elements in the upper left corresponding to the targeted $\{\sigma p_n \sigma p_m\}$. For example, if only p_7 is to be constrained, then only $\Lambda_{77} = \lambda\{\sigma p_7 \sigma p_7\}^{-1}$ would be non-trivial. Alternately, if all p_n are to be constrained, then the non-trivial elements would fill the upper left-hand portion of $\mathbf{\Lambda}$. The damping parameter $\lambda \leq 1$ may reflect reduced confidence in the relevance of the previous

calibration. We aim to set $\lambda = 0$ during the initial, on-orbit check-out and on other selected occasions. It is also possible that we may instead use the fact that some p_n enjoy hard prior bounds (e.g., $|a_{jk}| \leq 1$).

In view of (2), a set of t_i which fails to span zero-crossings of the offset field (the 7-bit u_j changing from 1111111 to 0000000) will not sample a flip of at least one u_{jk} (i.e., u_{j7}); then at least w_{j7} is not resolved. With appropriate orientation of the SHM axis, resolution might be achieved by carefully selecting the t_i. If a polar orbiting sensor (say $j = x$) is always nearly parallel to the geomagnetic X component of a roughly axial dipolar field with a -30000-nT equatorial field, then both u_{x7} and u_{x6} will flip--but they will always flip together. Then calibration coefficients (w_{x7}, w_{x6}) are not separable as they cannot be determined independently. This indeterminacy might be considered irrelevant: a single determinable calibration coefficient could replace the two. A similar situation exists for w_{y7}, w_{y6}, perhaps w_{y5}, and conceivably w_{y4}; no such situation is expected for Z.

Determination of the set of all calibration parameters requires exercise of all relevant offset field generator bits for all sensors; unfortunately, it may not occur at times when scalar data is available. Full exercise of all bits with scalar data is requested periodically to separate and identify drift in all w_{jk}. More frequent exercise is desirable to determine more nearly current values of Ω. If the x,y,z sensor axes are nearly parallel to the X,Y,Z geomagnetic components (as are the nominal spacecraft coordinates when ascending above the Northern Hemisphere), then full exercise is expected to occur naturally on the z (j=1,4) axis, might not occur naturally on the x (j=2) axis, and will not occur naturally on the y (j=3) axis. As to LOSS, consider a polar orbit through an axial dipole field. If the SHM axis points in the x (ram) direction, the LOSS cones would be poleward of $\pm 40.9^{\circ}$ latitude; if the SHM points in the z (down) direction, the LOSS band in such a field would be equatorward of $\pm 16.1^{\circ}$; if the SHM is oriented at 45°, the LOSS zones in such a field would span 61.8°N to 7.6°N in the descending (day) arc and 61.8° S to 7.6°S in the ascending (night) arc. The 98°, rather than 90°, orbital inclination, 11° dipole tilt, and non-dipole field will shift the LOSS zones. The first effect bars data poleward of $\pm 82^{\circ}$ --suggesting an off-nadir SHM attitude; the second effect would seem to narrow any equatorial LOSS zone. A detailed simulation seems appropriate in view of non-dipole fields. Depending upon the SHM orientation, some separation of the more significant w_{jk} may be achieved by attitude maneuvers: a 90° roll at high latitude likely results in LOSS, but a 45° roll may allow separation of many w_{yk}.

With $\bar{\mathbf{z}}$ denoting the previous value for $\mathbf{z}$, the total objective function to be minimized is

$$\Delta^2 \equiv (\mathbf{f} - \bar{\mathbf{f}})^T \mathbf{W} (\mathbf{f} - \bar{\mathbf{f}}) + (\mathbf{z} - \bar{\mathbf{z}}) \mathbf{\Lambda} (\mathbf{z} - \bar{\mathbf{z}}) \ . \tag{12}$$

The linearizations

$$\mathbf{z} \simeq \hat{\mathbf{z}} \tag{13a}$$

$$\mathbf{f} \simeq \hat{\mathbf{f}} = \tilde{\mathbf{f}} + \mathbf{\Gamma} (\mathbf{z} - \hat{\mathbf{z}}) \tag{13b}$$

yield $\mathbf{f} - \bar{\mathbf{f}} \simeq \hat{\mathbf{f}} - \bar{\mathbf{f}} = \tilde{\mathbf{f}} - \bar{\mathbf{f}} + \tilde{\Gamma}(\hat{\mathbf{z}} - \tilde{\mathbf{z}})$ and

$$\Delta^2 \simeq [(\tilde{\mathbf{f}} - \bar{\mathbf{f}}) + \tilde{\Gamma}(\hat{\mathbf{z}} - \tilde{\mathbf{z}})]^T \mathbf{W} [(\tilde{\mathbf{f}} - \bar{\mathbf{f}}) + \tilde{\Gamma}(\hat{\mathbf{z}} - \tilde{\mathbf{z}})] + [(\hat{\mathbf{z}} - \tilde{\mathbf{z}}) - (\bar{\mathbf{z}} - \tilde{\mathbf{z}})]^T \mathbf{A} [(\hat{\mathbf{z}} - \tilde{\mathbf{z}}) - (\bar{\mathbf{z}} - \tilde{\mathbf{z}})] \quad . \tag{13c}$$

Δ^2 as approximated by (13c) is minimal if, and only if,

$$\tilde{\Gamma}^T \mathbf{W} [(\tilde{\mathbf{f}} - \bar{\mathbf{f}}) + \tilde{\Gamma}(\hat{\mathbf{z}} - \tilde{\mathbf{z}})] + \mathbf{A} [(\hat{\mathbf{z}} - \tilde{\mathbf{z}}) - (\bar{\mathbf{z}} - \tilde{\mathbf{z}})] = \mathbf{0} \tag{14a}$$

or, with $\tilde{\mathbf{d}} \equiv \bar{\mathbf{f}} - \tilde{\mathbf{f}}$

$$\hat{\mathbf{z}} = \tilde{\mathbf{z}} + [\tilde{\Gamma}^T \mathbf{W} \tilde{\Gamma} + \mathbf{A}]^{-1} [\tilde{\Gamma}^T \mathbf{W} \tilde{\mathbf{d}} + \mathbf{A}(\bar{\mathbf{z}} - \tilde{\mathbf{z}})]. \tag{14b}$$

It is stressed that the vast majority of the elements of $\mathbf{A}$ are zero--notably all those corresponding to any value for B_{ik}. The few non-trivial elements of $\mathbf{A}$ corresponding to the unresolved p_n also correspond to guesses $\tilde{\mathbf{z}}$ which are equal to the previous value $\bar{\mathbf{z}}$. So $\mathbf{A}(\bar{\mathbf{z}} - \tilde{\mathbf{z}}) = \mathbf{0}$. The inversion of the 3I + 52 square matrix $[\tilde{\Gamma}^T \mathbf{W} \tilde{\Gamma} + \mathbf{A}]$ is formidable with $\mathbf{A} = \mathbf{0}$, but must be done in occasional full-range calibrations. The routine inversion with non-trivial upper left $\mathbf{A}$ from the pxp sub-matrix of $\mathbf{\Omega}^{-1}$ is described by Lancaster et al., 1980; then inversion of even the 3Ix3I sub-matrix associated with the B_{ik} is avoided by partitioning it into I, 3x3 matricies.

With the first estimate of true $\mathbf{z}$, we can estimate $\hat{\Gamma} = \partial \mathbf{f}/\partial \mathbf{z}|_{\hat{\mathbf{z}}}$, set $\hat{\mathbf{d}} \equiv \bar{\mathbf{f}} - \hat{\mathbf{f}}$, and calculate the refined estimate

$$\hat{\hat{\mathbf{z}}} = \hat{\mathbf{z}} + [\hat{\Gamma}^T \mathbf{W} \hat{\Gamma} + \mathbf{A}^*]^{-1} [\hat{\Gamma}^T \mathbf{W} \hat{\mathbf{d}} + \mathbf{A}^*(\bar{\mathbf{z}} - \hat{\mathbf{z}})] \quad . \tag{15}$$

Note $\mathbf{A}^*$ may differ from $\mathbf{A}$ because $\mathbf{\Omega}^{*-1}$ may differ from $\mathbf{\Omega}^{-1}$ in view of $\hat{\mathbf{z}}$ and the likelihood that exposure to the space environment cause p_n to deviate from previous values. Indeed, $\bar{\mathbf{z}}$ itself in (15) might be replaced with $\hat{\mathbf{z}}$ or higher iterates if they prove that p_n evolves due to fluxgate drift and cosmic radiation. Of course, weights $\mathbf{W}$ are dictated by instrumental precision and are thus fixed. Extreme care is required in the selection of $\mathbf{A}^*$. If estimate $\hat{\mathbf{z}}$ from (14b) differs enough from guess $\tilde{\mathbf{z}}$, then estimate $\hat{\Gamma}$ can be far from guess $\tilde{\Gamma}$; similarly, if estimate $\hat{p}_n$ differs enough from previous value $\bar{p}_n$, then the previous $\mathbf{\Omega}$ can be a poor estimate of current calibration covariance and both $\hat{p}_n$ and $\mathbf{A}$, worthless. The former case demands iteration; the latter case indicates attempting to exercise all bits, setting $\mathbf{\Omega}^{*-1}$ and $\mathbf{A}^*$ to zero, and redetermining all p_n. Clearly, no confidence in prior estimates of the calibration parameters is warranted if a micrometeor impact reorients the instruments!

Phase One: Step II, Spacecraft Field Parameterization

This section outlines a parameterization for the spacecraft fields, both primary and secondary. This could readily be translated into a least-squares problem. Included in the parameterization are the torquer rod fields, fields from the solar array, and fields induced both in conductors via Faraday's law and in magnetically permeable materials by ambient fields. Further study will be undertaken in Phase C to refine this parameterization and to translate it into operational software.

However, the outlined procedure may be unnecessarily complex. For example, it is hoped that induced fields will be negligible and that the solar panels will be so wired as to eliminate their magnetic field. In any case, a model including the magnetic torquers and, probably, the solar panels will be required. For the present discussion, a model formulation for induced fields will be included but not practically developed. To determine if they may be ignored during the mission, an appropriate magnetic survey of the spacecraft should be conducted prior to launch. Otherwise, a model such as the one presented must be implemented prior to launch to include this contingency in our plans.

In addition to these assumptions are the following:

1) Torquer rod, solar panel and other currents will be available in the telemetry with sufficient accuracy and time resolution to permit spacecraft field calibration and application of that calibration to correct the measured field.

2) Changing states of spacecraft and instrument systems will be known via telemetry.

3) Boom motion can be ignored. As will be shown, this assumption is justified as long as boom angles relative to nominal are less than 0.6^{o}, and possibly if they are less than 2.5^{o}. Boom model studies should be conducted to confirm that these limits are not likely to be exceeded. Note that if boom motions do exceed these values, but do so in a way that can be geometrically modeled (i.e., following the 1st normal mode), then the combination of stellar attitude measurements on the main spacecraft and on the APAFO optical bench should allow a correction for boom motion.

4) It is assumed that the torquer rod field strength depends linearly upon the applied current with no appreciable hysteresis. This implies the use of ultra-soft, low-hysteresis rods. If necessary, the model could be made to account for small non-linearities. The rods must be checked pre-launch for linearity and hysteresis.

Given these conditions, it should be possible to calibrate the fields from the torquer rods and solar panels to within 1% and the entire spacecraft field to within 5%.

Many spacecraft field parameterizations are possible, but the purpose of the spacecraft field model is to enable accurate calculation of the ambient field by correcting VFM calibration and the total field measured. This implies that the spacecraft field parameterization must represent the

spatio-temporal variation of real spacecraft field sources. We anticipate a full complement of spacecraft field sources: bi-axial torque rods rated at 350 Atm^2 each; solar array panel current; other designed currents; currents induced in the spacecraft and the APAFO equipment (boom, bench, etc.) by the time-varying spacecraft and ambient fields; induced magnetization; and permanent magnetization. The torque rods are considered primary sources; the solar array and induced fields are considered secondary sources. Figure 2 shows the spacecraft field as a function of boom length for two torquers of 350 Atm^2 in the configuration of Figure 1. Other sources may be weak, but must be anticipated unless pre-launch measurements of the field near the spacecraft indicate they are indeed absent. Ground-based spacecraft field calibration must determine the relations converting torquer rod and solar array current telemetry to the magnetic field produced at the expected bench location.

Application of Step (I) yields initial estimates of the total magnetic field at the outboard location in bench coordinates at times t_i. It also gives calibration parameters for estimating the field at other observation times. At any observation time t_j the spacecraft field in bench coordinates is

$$B^S_{jk} = \sum_{l=1}^{3} R_{jkl} B^S{}'_{jl} \qquad (16)$$

where $B^{S}{}'_{jl}$ is the l^{th} component of the spacecraft field at t_j in spacecraft coordinates and the R_{jkl} are elements of the matrix $\mathbf{R}(t_n)$ which rotates the spacecraft coordinate system into the bench coordinate system at t_n. Clearly $\mathbf{R}$ is time dependent due to boom motion. The reverse rotation of bench coordinates into spacecraft coordinates is denoted $\mathbf{S}(t_j)$. The R_{jkl} can be derived from the attitudes determined by the bench star cameras and by the ESA/PPF onboard star cameras. ESA/PPF attitude knowledge is put at 0.01^o (one sigma), but pointing accuracy at the torquer rods is put at 0.033^o during disturbed times (120 arcseconds, or about ± 0.6 mm positioning at the ends of a 1 m rod); the star camera axis to VFM optical cube pointing accuracy is put at better than 12.5 arcseconds rss (perhaps 5 seconds). So the relative orientation of the torque rods and bench coordinates should be determinable to about 121 arc-seconds rss.

At present, it seems that boom motion through the spacecraft field (as distinct from the ambient field) might be a negligible source of error due to the small amplitude of the spacecraft field at the bench. The rigid boom approximation,

$$B^S_{nk} \simeq \sum_{l=1}^{3} R_{kl} B^S{}'_{nl} \qquad (17)$$

where the R_{kl} are the mean values of the R_{jkl}, may thus prove useful. To see this, recall that for the realistic example in section (I), a "torque rods" magnetic dipole of moment (350,0,-350) Atm^2 at the origin

generates a field at (12,7.5,0) m which differs from that at (12,8,0) m by (1.73,0.50,0.69) nT, but only 1.63 nT scalar. The field at (12,8,0) is (12.56,16.15, 11.67) nT, or 23.56 nT scalar. These realistic values suggest that the 36-nT worst-case spacecraft field estimate is a little too pessimistic. Also recall that a 0.5° relative orientation error in a 36-nT spacecraft field gives at most a 0.3-nT error in the spacecraft field estimate. This approaches the 0.5-nT APAFO goal. Now, relative orientation fluctuations of ±0.5° due to flex of a parabolic 12-m boom imply ±5-cm translations of the bench through the spacecraft field. These in turn imply a spacecraft field correction about ±10% of those noted above for the 0.5-m displacement, or about 0.4 nT in the worst case. Because errors of 0.3 nT and 0.4 nT yield 0.5-nT rss, fluctuations in the relative bench-spacecraft orientation of up to 0.5° are clearly magnetically tolerable (i.e., negligible). In contrast, fluctuations over ± 1° may prevent meeting the 1.0-nT spacecraft field requirement.

In fact, a 2.86° fluctuation in the relative orientation (known to ±121 in) of the bench to the spacecraft due to boom flex would imply a 30-cm translation at the tip of a parabolic 12-m boom (60 cm for a linear boom). In the realistic example, this would imply a 1.0-nT correction to the x component of the spacecraft field. But the parabolic boom model cannot be assumed reliable because the orientation fluctuation may be caused by an overtone rather than the fundamental, roughly parabolic, flexural mode. Thus the desired correction cannot be made with certainty and the 1.0-nT spacecraft field requirement cannot be met. Clearly if elements of R_{jkl} differ from the mean R_{kl} so much as to imply a ±2.8° fluctuation, the data must be flagged for a potentially serious, off-nominal relative bench-spacecraft orientation. The point here is that even ±0.5° fluctuations seem large, yet are quite tolerable; thus the rigid boom approximation may in fact prove quite useful.

Parameterization. The chief spacecraft field at a position $\mathbf{x}$ in spacecraft coordinates is here represented as

$$B^{S}{}'_{jl}(\mathbf{x}) = B^{rods}_{jl}(\mathbf{x}) + B^{solar}_{jl}(\mathbf{x}) + B^{in}_{jl}(\mathbf{x}) + B_{ol}(\mathbf{x}) \qquad (18)$$

where B^{in}_{jl} is the induced field and B_{ol} is the steady spacecraft field due to both permanent magnetization and steady currents.

Torque Rods. In spacecraft coordinates the magnetic field in nT at $\mathbf{x}$ (in meters) generated by the thin solenoid (two point monopoles) model of a torque rod with fixed ends at $\mathbf{x}^+$ and $\mathbf{x}^-$ separated by $D = |\mathbf{x}^+ - \mathbf{x}^-|$ is

$$B^{rod}(\mathbf{x}) = \frac{10^2 NIA}{D}\left[\frac{\mathbf{x} - \mathbf{x}^+}{|\mathbf{x} - \mathbf{x}^+|^3} - \frac{\mathbf{x} - \mathbf{x}^-}{|\mathbf{x} - \mathbf{x}^-|^3}\right] \qquad (19a)$$

where N is the number of turns, I is the solenoid current in Amperes, and A is the cross-sectional area of the rod in m^2. NIA is the absolute Amperian magnetic dipole moment. The field due to two solenoids is, at time t_n,

$$B_{nl}^{\text{rods}}(\mathbf{x}) = \sum_{r=1}^{2} \frac{10^2 N_r A_r}{D_r} \left[\frac{x_l - x_{rl}^{+}}{|\mathbf{x} - \mathbf{x}_r^{+}|^3} - \frac{x_l - x_{rl}^{-}}{|\mathbf{x} - \mathbf{x}_r^{-}|^3}\right] I_{nr} \qquad (19b)$$

$$\equiv \sum_{r=1}^{2} M_{lr}(\mathbf{x}) I_{nr} .$$

If $\mathbf{x}$ is time dependent, then so is $M_{lr}(\mathbf{x})$; such dependency would be omitted in the rigid boom approximation. Prior values for M_{lr} at $\mathbf{x}^*$ may be taken from ground-based design and pre-launch testing, but estimates of the 6 elements of $\mathbf{M}$ need to be made in-flight.

The relations between the true magnetic dipole moments and the torque rod currents are not known and must be specified; at the very least, a soft, high-permeability rod core implies that the true magnetic dipole moment will greatly exceed the vacuum core value unless either $N_r A_r$ is regarded as an effective turn-area or I_{nr} includes the effect of magnetization. The linear relation

$$I_{nr} \simeq \alpha_r(\bar{I}_{nr} - \beta_r) \qquad (19c)$$

may prove adequate for electromagnet-type rods--with α_r regarded as the permeability gain and β_r the offset or bias of rod r; a cubic or higher order polynomial will be used as needed. Hysteresis in the rod cores may be observable, but no correction for it is planned due to the complicated time history of rod currents. It seems that ultra-soft, low-hysteresis rod cores are required; even then, a hyperbolic tangent may be needed to mimic an approach to rod core saturation.

Solar Array. In practice, the solar array fields could be made negligible by suitable back-wiring. If not, then a model is required. For a rotating solar array, the angle of rotation will need to be known for the model. If instead of complete back-wiring, adjacent panels in the solar array are intended to cancel one another, additional information will be needed. In particular, the multi-panel geometry should be specified and the telemetry signal should give information about which panels are operable and, if possible, what current is output from each panel.

The solar array wiring and current flow design are not yet known, so detailed modeling of the field produced by the solar array is not yet possible; however, we anticipate a representation in terms of two or more rectangular current loops. For example, in the special case where the solar array field reduces to the 2 counter-circulating current loops of area A_4 which are far ($|\mathbf{x}-\mathbf{x}_4|^2 >> A_4$) from the bench, the array field is well approximated by two anti-parallel point magnetic dipoles of moments $\pm KI_{j4}A_4\mathbf{m}$ located at $\mathbf{x}_1$ and $\mathbf{x}_2$:

$$\mathbf{B}^{\text{solar}}(t_j) = 10^2 K A_4 \left[\frac{(\mathbf{n}_1 \cdot \mathbf{m})\mathbf{n}_1 - \mathbf{m}}{|\mathbf{x} - \mathbf{x}_1|^3} - \frac{(\mathbf{n}_2 \cdot \mathbf{m})\mathbf{n}_2 - \mathbf{m}}{|\mathbf{x} - \mathbf{x}_2|^3}\right] I_{j4} \qquad (20a)$$

where $\mathbf{n}_1 = (\mathbf{x}-\mathbf{x}_1)/|\mathbf{x}-\mathbf{x}_1|$ and $\mathbf{n}_2 = (\mathbf{x}-\mathbf{x}_2)/|\mathbf{x}-\mathbf{x}_2|$ are the unit-normal vector point from the dipoles towards the field point at $\mathbf{x}$, and where K is the fraction of I_{j4} flowing around the loops. Now $\mathbf{m}$, $\mathbf{n}_1$, $\mathbf{n}_2$, $\mathbf{x}_1$, and $\mathbf{x}_2$ are all time dependent because the solar array rotates relative to the spacecraft so as to face sunward; yet 'estimates' for all these quantities can be derived from ESA/PPF design, orbital data, and ephemeris data.

More generally, if a linear relation between true and telemetered solar array current is presumed, then, at time t_j,

$$B_{j1}^{\text{solar}}(\mathbf{x}) = Q_{j1}I_{j4} = Q_{j1}\alpha_4(\bar{I}_{j4} - \beta_4) \ . \qquad (20b)$$

Nominal Q_{j1} is expected to have a distinct, ephemeris specified time variation which repeats every orbit; special calculation of the Q_{j1} is needed for off-nominal attitude. Refinement of these calculated Q_{j1} is not anticipated; instead we expand the coefficient α_4 into the 3 component α_{14}:

$$B_{j1}^{\text{solar}}(\mathbf{x}) = Q_{j1}\alpha_{14}(\bar{I}_{j4} - \beta_4) \ . \qquad (20c)$$

In-flight estimates of α_{14} which deviate significantly from a single α_4 indicates inadequacy of either the solar array model leading to the form of Q_{j1} or in the prior estimate of it.

Induced Fields. In the spacecraft coordinate system, Faraday's law implies that the time rate of change of ambient, torque rod, and solar array fields are equivalent to the negative curl of an induced electric field. This induced electric field drives electrical currents in every electrical conductor onboard the spacecraft. These currents generate the "Faraday" induced spacecraft field which, by Lenz's law, opposes the inducing field. In addition, the spacecraft and ambient fields induce magnetization in permeable materials onboard the spacecraft (notably the torque rod cores); this induced magnetization generates the "Henry" induced spacecraft field.

Ideally, an explicit model of Faraday induced fields might begin with the position and electrical conductivity $\sigma(\mathbf{x})$ of every conductor onboard the spacecraft and an estimate of the electric field $\mathbf{E}$ induced by the total space-time-varying magnetic field; proceed through evaluation of the current density $\mathbf{J}$ induced in the conductors by the induced electric field and calculation of the induced magnetic field via the Biot-Savart law; and wind up in iterative correction of the total time-varying field for the Faraday induced field. Similarly, an explicit Henry induced field model might begin with the position and permeability $\mu(\mathbf{x})$ of all magnetizable materials onboard the spacecraft. Alternately, one might solve the vector magnetic diffusion equation (e.g., $\partial_t \mathbf{B} = -\nabla\times\sigma^{-1}\nabla\times\mu^{-1}\mathbf{B}$ for linear $\mathbf{J} = \sigma\mathbf{E}$ and $\mathbf{B} = \mu\mathbf{H}$). The short magnetic diffusion times expected for thin ESA/PPF conductors indicate a Faraday induced field which is in phase with the time-rate of change of the inducing magnetic field at the ultra-low

frequencies of interest. Similarly, magnetically soft materials will have an induced magnetization, and Henry induced field, which is in phase with the ULF inducing magnetic field.

Only the induced field at the bench is of interest, so we bypass the exhaustive explicit procedure by supposing that the Faraday induced field at $\mathbf{x}$ consists of a part proportional to the time rates of change of: the torque rod field (which is in turn proportional to the torque rod current); the solar array field; and the ambient field. Similarly, the Henry induced field may be bypassed in favor of a simple transfer function. In this "lumped element" approach to induced spacecraft fields, the parameterization of the induced field at the bench is

$$B^{in}_{j1} = \sum_{r=1}^{2} D_{1r}\partial_t I_{jr} + E_{1k}\partial_t B^{A}_{jk} + F_{14}[P_{j1}\partial_t I_{j4} + (\partial_t P_{j1})I_{j4}]$$

$$+ \sum_{r=1}^{2} T_{1r}I_{jr} + \sum_{k=1}^{3} U_{1k}B^{A}_{jk} + V_{14}C_{j1}I_{j4} \qquad (21)$$

here $\partial_t I_{jr} = (I_{j,r} - I_{j-1,r})/(t_j - t_{j-1}) = \alpha_r \partial_t \bar{I}_{jr}/\partial t$ and $\partial_t I_{j4} = (I_{j,4} - I_{j-1,4})/(t_j - t_{j-1}) = \alpha_4 \partial I_{j4}/\partial t$. The ambient field in the spacecraft coordinate system can initially be taken as the rotated total field from the calibrated VFM: $B^{A}_{jk} \simeq \Sigma_n S_{jmn} B_{jn}(\mathbf{x}^5)$; similarly, $\partial_t B^{A}_{jk} \simeq \Sigma_n S^{*}_{jmn}[B_{j,n}(\mathbf{x}^5) - B_{j-1,n}(\mathbf{x}^5)]/(t_j - t_{j-1})$. (Although the rigid boom approximation may be adequate, use of time-dependent $S(t_j)$ reduces contributions from boom twist through the ambient field; corrections to $\partial_t B^{A}_{jk}$ due to the time-varying spacecraft field at $\mathbf{x}^5$ can be included on higher iterations). In principle, the elements of (D,E,F) could be derived from the Biot-Savart law by integrating over the result of geometric operations on the induced current density; similarly (T,U,V) would follow from the curl of a dummy integral over the result of a geometric operator on the induced magnetization. P_{j1} and C_{j1} account for the time variation of the solar array orientation. For simplicity, P_{j1} is taken as Q_{j1} evaluated at an $\mathbf{x}$ near the base of the solar array boom (where the solar panel field is much stronger than at the center of conductivity); C_{j1} is taken as Q_{j1} evaluated at an $\mathbf{x}$ near the torque rods (where virtually all the permeability is located). In the unlikely event that a spatial parameterization of the induced field is needed for bench gradient corrections, fields mapped by (D,E,F) might be treated as follows: (D) a point dipole located closer to the torque rods than to the center of conductivity of the spacecraft; (E) a point dipole at the center of conductivity; (F) a point quadrupole much closer to the base of the solar array boom than to the center of conductivity. The fields mapped by (T,U,V) might be treated as: (T) two-point dipoles near the center of permeability; (U) a point dipole at the center of permeability; (V) a point quadrupole between the solar array boom base and the center of permeability. It might further be supposed that the center of permeability would coincide with the torque rods, while the center of conductivity would coincide with the center of mass.

The spacecraft field model parameterization is now

$$B^{S}{}'_{j1} = \sum_{r=1}^{2} M_{1r}\alpha_r(\bar{I}_{jr} - \beta_r) + Q_{j1}\alpha_{14}(\bar{I}_{j4} - \beta_4)$$

$$+ \sum_{r=1}^{2} D_{1r}\alpha_r\partial_t\bar{I}_{jr} + \sum_{k=1}^{3} E_{1k}\partial_t B^{A}_{jk} + F_{14}[P_{j1}\alpha_{14}\partial_t\bar{I}_{j4} + (\partial_t P_{j1})\alpha_{14}(\bar{I}_{j4}-\beta_4)]$$

$$+ \sum_{r=1}^{2} T_{1r}\alpha_r(\bar{I}_{jr}-\beta_r) + \sum_{k=1}^{3} U_{1k}B^{A}_{jk} + V_{14}C_{j1}\alpha_{14}(\bar{I}_{j4}-\beta_4) + B_{o1} \ . \qquad (22a)$$

The effects of M_{1r} are virtually indistinguishable from those of T_{1r}, as are those of Q_{j1}, $F_{14}\partial_t P_{j1}$, and $V_{14}C_{j1}$:

$$B^{S}{}'_{j1} = \sum_{r=1}^{2} [M_{1r}+T_{1r}]\alpha_r(\bar{I}_{jr} - \beta_r) + [Q_{j1}+F_{14}(\partial_t P_{j1})+V_{14}C_{j1}]\alpha_{14}(\bar{I}_{j4} - \beta_4)$$

$$+ \sum_{r=1}^{2} D_{1r}\alpha_r\partial_t\bar{I}_{jr} + \sum_{k=1}^{3} E_{1k}\partial_t B^{A}_{jk} + F_{14}P_{j1}\alpha_{14}\partial_t\bar{I}_{j4} + \sum_{k=1}^{3} U_{1k}B^{A}_{jk} + B_{o1} \qquad (22b)$$

Torque rod offsets β_r are indistinguishable from any other steady spacecraft field. So, grouping together time-varying rod, solar array, and ambient field effects and steady field effects,

$$B^{S}{}'_{j1} = \sum_{r=1}^{2} \{[M_{1r} + T_{1r}]\alpha_r(\bar{I}_{jr} - \beta_r) + D_{1r}\alpha_r(\partial_t\bar{I}_{jr})\}$$

$$+ \{[Q_{j1} + F_{14}(\partial_t P_{j1}) + V_{14}C_{j1}]\alpha_{14}(\bar{I}_{j4} - \beta_4) + F_{14}P_{j1}\alpha_{14}(\partial_t\bar{I}_{j4})\}$$

$$+ \sum_{k=1}^{3} \{U_{1k}(B^{A}_{jk}) + E_{1k}(\partial_t B^{A}_{jk})\} + \{B_{o1} - [M_{1r} + T_{1r}]\alpha_r\beta_r\} \qquad (22c)$$

or, more simply

$$B^{S}{}'_{j1} = \sum_{r=1}^{2} \{M'_{1r}(\bar{I}_{jr}) + D'_{1r}(\partial_t\bar{I}_{jr})\}$$

$$+ \{[Q_{j1} + F_{14}(\partial_t P_{j1}) + V_{14}C_{j1}]\alpha_{14}(\bar{I}_{j4} - \beta_4) + F_{14}P_{j1}\alpha_{14}(\partial_t\bar{I}_{j4})\}$$

$$+ \sum_{k=1}^{3} \{U_{1k}(B^{A}_{jk}) + E_{1k}(\partial_t B^{A}_{jk})\} + \{B'_{o1}\} \ . \qquad (22d)$$

Here Q_{j1}, P_{j1}, $\partial_t P_{j1}$, and C_{j1} are considered known from solar array design, orbital, and ephemeris data; the command current and its time rate of change are known from telemetry; and the guesses for $B^{A}{}_{jk}$ and $\partial_t B^{A}{}_{jk}$ follow from step I, VFM telemetry, and the dual star-camera specification of $S(t_j)$. The 24 spacecraft field calibration parameters TBD are: 6 M'_{1r} for

the direct torque rod field and its Henry induced counterpart; 6 D'_{1r} for the Faraday field induced by the torque rod field; 3 α_{14} for direct, 3 F_{14} for Faraday induced, and 3 V_{14} for Henry induced solar array fields; 3 U_{1k} for Henry induced and 3 E_{1k} for Faraday induced fields associated with spacecraft flight through the ambient field; and 3 components of the steady spacecraft field B'_{o1}. Note that a suitably wired solar array would eliminate 9 parameters and costly evaluation of **Q**, **P**, and **C**.

Special Calibration Periods. To ease detection of a roughly 30-nT spacecraft field superimposed upon a ambient field exceeding 30,000 nT, it is useful to subtract an initial ambient field model and correlate variations in the residuals with those in I_{jr}, I_{j4}, and their time derivatives. Unfortunately, the torque rod currents are expected to be strongly correlated with the ambient field exerting the designed torque. So, as a check on the routine calibration, special calibration periods would be desirable for this primary spacecraft field source during which the torque rods are pulsed in a preset pattern.

The pulsing pattern considered is a series of abrupt changes in the command current from one level to another level, with the command held fixed at each level for an interval Δt. Start with both rods off. Raise one rod to level I_o for Δt, lower it to zero for Δt, then lower it to $-I_o$, and finally raise it to zero for Δt. Then repeat the sequence at levels $\pm 2I_o$, $\pm 3I_o$, ... $\pm I_{max}$. Then repeat this pattern for the other bar. With Δt = 1 s and the VFM in campaign mode, induced transients can be monitored with 128 VFM samples and at least two scalar samples will be acquired. Longer Δt is needed if transients are a problem. Clearly ΔT should be much larger than the inductive time constant of the torque rods. If the rods are pulsed in shadow, the times of zero-level rod current could be ideally suited to VFM calibration.

In the rigid boom approximation, the zero-current VFM measurements would be fitted with a low-order polynomial in time; this model would be subtracted from the entire measurement sequence, and the 6 elements of $[M_{1r}+T_{1r}]\alpha_r \equiv M'_{1r}$ estimated by a least-squares fit to the residual field - which is simply modeled as $M'_{1r}I_{jr}$. Rod core remanance should appear as residuals at the zero-current times which share the sign of the previous command current.

Boom flex, twist and stretch will contaminate the residuals to a low order polynomial due to VFM rotation through the ambient field; this signal may well exceed that of the torque rods. If the spacecraft/torque rods attitude is known only to 121" rss, the total field ought not be rotated into spacecraft coordinates prior to elimination of some ambient field model, lest attitude errors of up to 50,000sin(120") $\simeq$ 30 nT be introduced. So, for a flexible boom, first rotate the VFM samples into celestial coordinates using the bench star-camera data only (12.5" rss); then fit a low-order polynomial through the zero-current samples; next rotate the residuals into spacecraft coordinates; and finally estimate M'_{1r} from the residuals in spacecraft coordinates using least squares. Any prior information on M_{1r} must be distinguished from that on M'_{1r}.

The low-order temporal polynomial fitted to celestially oriented, zero rod current level, 'ambient' field values might be abandoned in favor of simply averaging or otherwise interpolating the (celestially oriented) field values during the zero current level times adjacent to the pulse of interest. This reduces presumption regarding ambient field smoothness and, perhaps more importantly, allows the pulsing to occur at high latitudes - where the crossings of auroral current sheets would be poorly represented by a low-order polynomial. Pulsing the rods at high latitudes could also provide useful zero current level times for VFC calibration. Furthermore, hysteretic remanance in the rod cores (which may appear in the residuals to a low-order polynomial) might be reduced by suitably weighting the average (or other interpolate).

Clearly $4\Delta t$ must not equal the fundamental period of the boom; selecting Δt equal to this period may improve spacecraft field calibration. Alternately, sufficient time should be allowed between torquer steps for induced boom transients to die out. Special calibration periods conducted with the boom either in constant shadow or constant sunlight should enjoy minimal thermal boom transients.

Phase One: Step III, Iteration

The initial spacecraft field estimate from (II) is just the torque rod direct and Henry induced field $B'S_{j1} = \Sigma_r M'_{1r} I_{jr}$; in bench coordinates this is $BS_{jk} = \Sigma_{1r} S_{jk1} M'_{1r} I_{jr}$, or about $\Sigma_{1r} S_{k1} M'_{1r} I_{jr}$ in the rigid boom approximation. To correct the VFM calibration for the time-varying bench bias field caused by the torque rods, not only the orientation, but the positions $\mathbf{x}^j = \mathbf{x}^o + R\mathbf{x}^{*j}$ of the VFM and the SHM must be known in spacecraft coordinates. It can be assumed that shifts in VFM and SHM positions on the bench itself would appear as off-nominal calibration parameters or LOSS events; indeed, if steady, they might be deduced and used to obtain corrected $\mathbf{x}^{*j}$. The key question thus regards the position of bench itself $\mathbf{x}^o$: did the boom deploy as designed? Clearly, if the R_{k1} differ significantly from designed values, the designed boom twist or deployment angle was not achieved - suggesting a deviation from the designed bench position. Moreover, if the elements of M'_{1r} differ from the values of $M_{1r}\alpha_r$ anticipated at the designed bench location by more than explicable in terms of $T_{1r}\alpha_r$, then one may infer that the value of $\mathbf{x}^o$ differs from the designed value. Then the values of the 3 components of $\mathbf{x}$ (or rather $\mathbf{x}^5$) can be calculated from the 6 estimates M'_{1r} using (19b) on the suppositions that $M'_{1r} = M_{1r}\alpha_r$ and that both the α_r and the torque rod positions are as designed. Of course, R_{1k}, and $\mathbf{x}^{*5}$ are regarded as known, so the determination of $\mathbf{x}^5$ implies $\mathbf{x}^o$. Thus the position of the bench in the primary spacecraft field can be estimated in the unlikely event of an off-nominal boom deployment.

With $M'_{lr}I_{jr}$ having the $\mathbf{x}$ dependence indicated by (19b,c), and supposing $\boldsymbol{\beta}_r = 0_r$, the primary spacecraft field can be evaluated at the positions of the VFM as well as the nominal SHM position. In bench coordinates, the difference between the two values estimates the time varying part of the bench bias field $\boldsymbol{\delta}$. As described in section I, this implies a correction to the $\bar{f}_{ij}$; the corrected $\bar{f}_{ij}$ can then be used to derive corrected calibration parameters $\hat{p}_n$ and corrected total $\hat{B}_{ik}$ as in section I. The value of B^S_{jl} is then subtracted from the $\hat{B}_{jk}$ derived using the corrected calibration parameters to obtain the next estimate of the ambient field, B^A_{jk}, in bench coordinates.

PHASE TWO

During phase II the coordinate transformation from the VFM to an earth centered system will be confirmed, previously undetected spacecraft fields will be isolated, and initial models of the geomagnetic field computed.

This phase uses procedures developed for reduction of Magsat data. It depends upon the fact that the platform is earth oriented and therefore any unmodeled spacecraft fields are rotating relative to the field of the earth. The basic assumptions are that the magnetometer coordinate system does not change relative to the star sensors and that any unmodeled spacecraft fields are constant during the period of analysis.

This phase is accomplished using a spacecraft vector magnetometer measurement model in the software used to derive models of the geomagnetic field, i.e., the computer code FIT.

The magnetic field vector in earth fixed cartesian coordinates is represented as

$$\mathbf{B}_G = T_{CS} \begin{pmatrix} X \\ Y \\ Z \end{pmatrix} \tag{23}$$

where
$$X = -B_\theta \cos\delta - B_r \sin\delta \tag{24a}$$
$$Y = B_\phi \tag{24b}$$
$$Z = B_\theta \sin\delta - B_r \cos\delta \tag{24c}$$

$$\begin{aligned} &(T_{CS})_{11} = -\cos(\theta-\delta)\cos\phi;\ (T_{CS})_{22} = \cos\phi;\ (T_{CS})_{33} = -\cos(\theta-\delta) \\ &(T_{CS})_{12} = -\sin\phi;\ (T_{CS})_{13} = -\sin(\theta-\delta)\cos\phi \\ &(T_{CS})_{21} = -\cos(\theta-\delta)\sin\phi;\ (T_{CS})_{23} = -\sin(\theta-\delta)\sin\phi \\ &(T_{CS})_{31} = \sin(\theta-\delta);\ (T_{CS})_{32} = 0 \end{aligned} \tag{25}$$

$$\mathbf{B} = -\nabla V(r, \theta, \phi, g_n^m, h_n^m), \tag{26}$$

where r, θ, ϕ are the usual geocentric coordinates, δ is now the difference between geodetic and geocentric latitude, and the g_n^m and h_n^m are the usual spherical harmonic coefficients in a geomagnetic model.

For the satellite vector measurements, the field vector in earth fixed coordinates is assumed related to the orthogonal magnetometer axes, the bench coordinate system, fixed to the spacecraft boom by

$$\mathbf{B}_G = T_{GS} T_{SM} \mathbf{B}_M \tag{27}$$

T_{GS} is a function of the spacecraft attitude and position and relates the spacecraft coordinates to earth fixed coordinates. As presently configured, FIT can either assume this tranformation is known or solve for its parameters. The assumed spacecraft coordinate system in FIT is such that the z axis is along the satellite velocity vector, the x axis is in the cross-track direction and the y axis completes the orthogonal system.

Note that this system differs from the APAFO system described elsewhere. The transformation T_{GS} is then calculated from the spacecraft inertial position and velocity, $\mathbf{x}_S$ and $\dot{\mathbf{x}}_S$, and the Greenwich hour angle at the data times. T_{SM} is a function of Euler angles ϵ defining the transformation from the orthogonal vector magnetometer axes to the spacecraft coordinate axes. The definition of the orientation parameters ϵ_1, ϵ_2, ϵ_3 which describes the relationship between the magnetometer coordinate system and the spacecraft system are as follows:

1) rotate by ϵ_2 about the z axis
2) rotate by ϵ_3 about the new x axis
3) rotate by ϵ_1 about the new z axis

The transformation matrix elements are then given by:

$$
\begin{aligned}
(T_{SM})_{11} &= \cos\epsilon_1\cos\epsilon_2-\cos\epsilon_3\sin\epsilon_2\sin\epsilon_1;\\
(T_{SM})_{12} &= \cos\epsilon_1\sin\epsilon_2+\cos\epsilon_3\cos\epsilon_2\sin\epsilon_1;\\
(T_{SM})_{13} &= \sin\epsilon_1\sin\epsilon_3\\
(T_{SM})_{21} &= -\sin\epsilon_1\cos\epsilon_2-\cos\epsilon_3\sin\epsilon_2\cos\epsilon_1;\\
(T_{SM})_{22} &= -\sin\epsilon_1\sin\epsilon_2+\cos\epsilon_3\cos\epsilon_2\cos\epsilon_1;\\
(T_{SM})_{23} &= \cos\epsilon_1\sin\epsilon_3;\\
(T_{SM})_{31} &= \sin\epsilon_3\sin\epsilon_2;\ (T_{SM})_{32} = -\sin\epsilon_3\cos\epsilon_2;\ (T_{SM})_{33} = \cos\epsilon_3
\end{aligned}
\tag{28}
$$

To account for the possibility that the axes of the magnetometer are non-orthogonal, we relate the field vector projected on non-orthogonal unit vectors $\mathbf{u}_1$, $\mathbf{u}_2$, $\mathbf{u}_3$ to the orthogonal magnetometer axes. We assume that the $\mathbf{u}_1$ vector is aligned along the x axis of the magnetometer, the $\mathbf{u}_2$ vector lies in the x-y plane of the magnetometer system, and the $\mathbf{u}_3$ vector has arbitrary orientation.

Let $\mathbf{B}_M$ represent the magnetic field vector in the orthogonal system and $\mathbf{B}_{NO} = (B_1, B_2, B_3)$ denote the projections of $\mathbf{B}_M$ along the $\mathbf{u}_1$, $\mathbf{u}_2$, $\mathbf{u}_3$ vectors. Then

$$
\begin{aligned}
B_1 &= B_{Mx}\\
B_2 &= B_{Mx}\sin\alpha + B_{My}\cos\alpha\\
B_3 &= B_{Mx}\sin\beta\cos\gamma + B_{My}\sin\beta\sin\gamma + B_{Mz}\cos\beta
\end{aligned}
\tag{29}
$$

$$
\text{or } \mathbf{B}_{NO} = T_{nm}\mathbf{B}_M \tag{30}
$$

where

$$
\begin{aligned}
(T_{NM})_{11} &= 1;\ (T_{NM})_{12} = (T_{NM})_{13} = (T_{NM})_{23} = 0;\\
(T_{NM})_{21} &= Y_1;\ (T_{NM})_{22} = [1-Y_1^2]^{1/2};\\
(T_{NM})_{31} &= Z_1;\ (T_{NM})_{32} = Z_2\\
(T_{NM})_{33} &= [1 - Z_1^2 - Z_2^2]^{1/2}
\end{aligned}
\tag{31}
$$

and

$$
Y_1 = \sin\alpha;\ Z_1 = \sin\beta\cos\gamma;\ Z_2 = \sin\beta\sin\gamma \tag{32}
$$

The parameters Y_1, Z_1, and Z_2 represent the non-orthogonal measurements to the orthogonal system, while the Euler angles ϵ_1, ϵ_2, ϵ_3 relate the magnetometer system to the bench coordinates. Expressions for the partial derivatives used in FIT are found in the FIT documentation.

The actual measurement of the magnetometer along an axis u_j is a voltage, v_j, and the field measurement, in nT, is

$$B_j = S_j v_j + \delta_j \tag{33}$$

where the S_j and δ_j represent a slope parameter and bias, respectively. For convenience we choose to represent the voltage measurement in the form

$$v_j = \mu_j B_j + \eta_j \tag{34}$$

where μ_j and η_j model the slope and bias parameters. Then

$$\mathbf{v} = T_{Slope} \mathbf{B}_{NO} + \boldsymbol{\mu} \tag{35}$$

The scalar magnetometer measurement is also represented with a bias parameter,

$$v_S = |B_G| + \eta_S \tag{36}$$

The vector magnetometer measurement model is then:

$$\mathbf{v} = T_{Slope} T_{NM} (T_{SM})^T (T_{GS})^T \mathbf{B}_G + \boldsymbol{\eta}. \tag{37}$$

Given a proper distribution of data, which takes one to two days to accumulate, and the assumptions mentioned above, the FIT program is then able to solve for the slope, non-orthogonality, bias offset and Euler angle parameters simultaneously with its solution for the spherical harmonic coefficients.

In practice with Magsat, the slope and non-orthogonality parameters were equal to their nominal values, as expected, and were not solved for. However the Euler angles and bias parameters were an important part of the Magsat calibration. It is anticipated that this may also be the situation for APAFO. Phase one calibration should account for slope and non-orthogonality; indeed, finding $\alpha = \beta = \gamma = 0$ in equations (29) would help confirm this (as well as optical bench and star sensor rigidity).

If the spacecraft coordinate system used in T_{SM} is fixed to the ESA/PPF spacecraft, then $(\epsilon_1, \epsilon_2, \epsilon_3)$ will be time-dependent due to boom flex and twist. Routine evaluation of these changing Euler angles may be a costly, and unecessary, source of attitude transfer error. If the boom indeed proves stable to within 0.5^o, then it seems that dual star sensor determination of the orientation between the APAFO bench and the spacecraft will only be needed during calibration runs and, of course, independent boom stability checks. For routine evaluation of T_{SM} and T_{GS}, the "S" coordinate system could then be fixed to the bench mounted APAFO star

sensors. Then T_{SM} would represent the post-launch orientation of the bench system (fixed to the VFM optical cube) relative to the APAFO star sensors and will be steady to within the thermal stability of the bench systems. Given the position of a point on the spacecraft in geocentric coordinates and the values of T_{GS} from the APAFO star sensors, the position of the APAFO bench in geocentric coordinates can be determined to sufficient accuracy in the rigid boom approximation.

BOOM LENGTH/SPACECRAFT FIELD TRADE-OFFS

Introduction

The purpose of the boom is to place the magnetometer at sufficient distance from the spacecraft so that spacecraft fields are negligible. For APAFO this is not feasible. Rather, the boom length will be such that the spacecraft fields can be modeled with sufficient accuracy as to make them negligible. An error analysis study has been conducted to determine the trade-offs involved.

This study is a preliminary error analysis for the APAFO magnetic field experiment. A vector magnetometer and a scalar magnetometer are located at the end of a boom. The spacecraft fields are due to currents in two torque rods and these currents are known at discrete time intervals. The positive x-axis is along the axis of the boom, which is perpendicular to the y-axis along the longitudinal axis of the spacecraft. The z-axis completes the right-handed reference system. The torquing rods are on the y-axis at (0.0, 7.2, 0.0) meters. One rod has its axis parallel to the x-axis. The other rod has its axis parallel to the z-axis. The length of the boom is expected to be 12 meters. See Figure 1.

The total magnetic field is measured by a vector magnetometer and a scalar magnetometer at the end of the boom. When the boom is in its unbent nominal position, the vector magnetometer is located at (x, 0, 0) with axes parallel to the corresponding axes of the spacecraft reference frame. Star cameras are located on the spacecraft and at the end of the boom. At a given instant of time the ambient magnetic field is assumed to be constant in the neighborhood of the spacecraft; i.e., for an unbent boom the ambient field vector components are the same at the torque rods, the magnetometers and the star cameras. The maximum gradient of the Earth's field is expected to be less than 28 nT/km, 24 nT/km in the horizontal plane. For a maximum distance of 20 m this gives a maximum field difference of 0.56 nT, 0.48 nT in the horizontal plane. The ambient field difference across an optical bench of 2 m would be less than 0.06 nT.

For this study,the spacecraft magnetic field is modeled by two magnetic dipoles, which have their origins at the centers of the torque rods. The field from these dipoles along the boom is shown in Figure 2. The dipole axes are coincident with rod axes and have corresponding polarities. Activation of the torquer rods will cause the boom to bend and oscillate relative to the spacecraft. Thus the position and orientation of the magnetometers and the outboard star cameras in the spacecraft coordinate system will change with time. In this study,the boom is assumed to have a parabolic shape in its fundamental vibrational mode and other modes are not considered.

It is assumed that four independent magnetometer measurements are known at a fixed time: one scalar magnetometer measurement and three vector magnetometer component measurements. It is also assumed that apriori values are known for the parameters in the magnetic field models and the parabolic

boom model. Standard deviations are taken as known for the measurement and a priori errors. This information is used to compute a covariance matrix for the above parameters and the components of the ambient field using a weighted least-squares estimation scheme.

The error sources considered in this study are

1. magnetometer measurements (4),
2. torque rod magnetic dipole moments (2),
3. orientation of the vector magnetometer relative to the spacecraft (3).

The estimable parameters are

1. dipole moments for torquer rods (2),
2. orientation angles for the vector magnetometer relative to spacecraft (3),
3. ambient magnetic field vector components (3).

These parameters are not actually estimated in this study. Rather, the covariance matrix from the parameter estimation equations is computed using assigned values for the parameters and the standard deviations on the magnetometer measurements and the a priori parameter values. If the estimation process itself were performed, we would be solving in a weighted least-squares sense for eight parameters from nine data values (see error sources above). From the covariance matrix we obtain the standard estimates of error for the 8 parameters which would result if we actually solved for them. From this matrix we can also obtain the cross-correlations for the estimated errors in the parameters.

We emphasize that the procedure described above is limited to data observed at a single fixed time. This is because models for the parameters as a continuous function of time are not assumed to be known.

p_1 = x-component of the total magnetic field
p_2 = y-component of the total magnetic field
p_3 = z-component of the total magnetic field
p_4 = magnitude of the total magnetic field.

All the p_i's (i = 1 to 4) are in the vector magnetometer reference frame.

q_1 = magnetic dipole moment for torque rod parallel to spacecraft x-axis
q_2 = magnetic dipole moment for torque rod parallel to spacecraft z-axis
q_3 = α, the angle of rotation of the vector magnetometer about the x-axis of the spacecraft
q_4 = β, the angle of rotation of the vector magnetometer about the y-axis of the spacecraft
q_5 = γ, the angle of rotation of the vector magnetometer about the z-axis of the spacecraft

q_6 = x-component of the ambient magnetic field
q_7 = y-component of the ambient magnetic field
q_8 = z-component of the ambient magnetic field

q_6, q_7 and q_8 are in the vector magnetometer reference frame.

In a solution for the eight parameters, allowing for a priori errors, a covariance matrix is obtained from which can be extracted the standard deviations of the estimated quantities. This covariance matrix is given by

$$K = P^T M^{-1} P + N^{-1}$$

where P^T is the transpose of P. For the problem at hand P is a 4 x 8 matrix whose element in the i^{th} row and j^{th} column is $\partial p_i/\partial q_j$ evaluated for the nominal values of the parameters. The p_i (i = 1 to 4) are the measured quantities. The q_j (j = 1 to 8) are the model parameters: 2 torquer bar magnetic moments, 3 boom bending angles, and 3 ambient field vector components.

M is a 4 x 4 diagonal matrix, the i^{th} diagonal element being σ_i^2, the variance of the i^{th} measurement (i = 1 to 4). N is an 8 x 8 diagonal matrix, the i^{th} diagonal element being s_i^2, the apriori variance of the i^{th} model parameter.

Some of the questions which motivated this study are

1. How accurately can the ambient field be determined?
2. How does the ambient field accuracy vary with boom length?
3. How does the ambient field accuracy vary with dipole model accuracy?
4. What are the primary sources of error?

The mathematical theory supporting this study is presented in the following sections. In the final section, graphical results are given to support the answers given there to the foregoing questions.

The Magnetic Dipole Model

As a first approximation, the magnetic field produced by a torque rod may be represented by that of a magnetic dipole at the center of the rod and the positive dipole axis along the positive rod axis. The field of a dipole is obtained from the scalar magnetic potential

$$V = \mathbf{m}\cdot\mathbf{u}/4\pi u^3 = m\cos\delta/4\pi u^2, \text{ where} \qquad (38)$$

$\mathbf{m}$ = magnetic dipole moment vector,
m = magnetic dipole moment ($m = |\mathbf{m}|$),
$\mathbf{u}$ = vector from the dipole origin to the point considered,
u = magnitude of $\mathbf{u}$ ($u = |\mathbf{u}|$),
δ = angle between the positive dipole axis and $\mathbf{u}$,
$\mathbf{m}\cdot\mathbf{u}$ = scalar product of $\mathbf{m}$ and $\mathbf{u}$.

The magnetic dipole field is

$\mathbf{B} = -\mu_o$ grad V, where (39)

μ_o = permeability of free space.

B can be broken into components

$B_u = -\mu_o \partial V/\partial u = 2 B_o \cos\delta$, (40)

$B_\delta = -(\mu_o/u) \partial V/\partial\delta = B_o \sin\delta$, where (41)

$B_o = \mu_o m/4\pi u^3$ teslas. (42)

Since $\mu_o = 4\pi \times 10^{-7}$ Henrys/meter, we have

$B_o = 10^{-7} m/u^3$ teslas.

We convert this to nanoteslas by multiplying by 10^9. Thus

$B_o = 100\ m/u^3$ nanoteslas.

The units for m are ampere meters^2 (Am^2) if the magnetic dipole field is assumed to be produced by a single small closed loop of electric current. When the field is produced by multiple loops of current, it may be convenient to use ampere turns meters^2 (Atm^2) as units for m.

x,y,z : coordinates of magnetometers in the spacecraft rectangular coordinate system

v_1,v_2,v_3 : coordinates of a magnetic dipole center in the spacecraft rectangular coordinate system

u_1,u_2,u_3 : coordinates of the magnetometers relative to the dipole in the spacecraft rectangular coordinate system

$u_1 = x - v_1$ (43)

$u_2 = y - v_2$ (44)

$u_3 = z - v_3$ (45)

m_1,m_2,m_3: components of magnetic dipole moment vector **m** in the spacecraft rectangular coordinate system

m,θ,λ : spherical coordinates of **m**

$m_1 = m \sin\theta \cos\lambda$ (46)

$m_2 = m \sin\theta \sin\lambda$ (47)

$m_3 = m \cos\theta$ (48)

From (38) we get

$$V = (m_1u_1 + m_2u_2 + m_3u_3)/4\pi u^3. \tag{49}$$

For the torque rod with an axis parallel to the x-axis in the spacecraft reference frame, we have from (46) through (49),

$$V = (q_1/4\pi)u_1/u^3. \tag{50}$$

The components of the magnetic field vector produced by this rod at the point (x, y, z) are then

$$a_1 = -\partial V/\partial x = -100q_1(1-3u_1^2/u^2)/u^3 \text{ nT}, \tag{51}$$

$$a_2 = -\partial V/\partial y = 300q_1u_1u_2/u^5 \text{ nT}, \tag{52}$$

$$a_3 = -\partial V/\partial z = 300q_1u_1u_3/u^5 \text{ nT}. \tag{53}$$

The computation of the covariance matrix requires values of the following partial derivatives.

$$c_1 = \partial a_1/\partial q_1 = a_1/q_1 \tag{54}$$

$$c_2 = \partial a_2/\partial q_1 = a_2/q_1 \tag{55}$$

$$c_3 = \partial a_3/\partial q_1 = a_3/q_1 \tag{56}$$

$$a_{11} = \partial a_1/\partial x = 300\ q_1u_1(3 - 5u_1^2/u^2)/u^5 \tag{57}$$

$$a_{12} = \partial a_1/\partial y = 300\ q_1u_2(1 - 5u_1^2/u^2)/u^5 \tag{58}$$

$$a_{13} = \partial a_1/\partial z = 300\ q_1u_3(1 - 5u_1^2/u^2)/u^5 \tag{59}$$

$$a_{21} = \partial a_2/\partial x = a_{12} \tag{60}$$

$$a_{22} = \partial a_2/\partial y = 300\ q_1u_1(1 - 5u_2^2/u^2)/u^5 \tag{61}$$

$$a_{23} = \partial a_2/\partial z = -1500q_1u_1u_2u_3/u^7 \tag{62}$$

$$a_{31} = \partial a_3/\partial x = a_{13} \tag{63}$$

$$a_{32} = \partial a_3/\partial y = a_{23} \tag{64}$$

$$a_{33} = \partial a_3/\partial z = 300\ q_1u_1(1 - 5u_3^2/u^2)/u^5 \tag{65}$$

For the magnetic dipole with an axis parallel to the z-axis in the spacecraft reference frame, we have from (46) through (49),

$$V = (q_2/4\pi)u_3/u^3. \tag{66}$$

The components of the magnetic field vector produced by these dipoles at the point (x, y, z) are then

$$b_1 = -\partial V/\partial x = 300q_2u_1u_3/u^5 \text{ nT} \tag{67}$$

$$b_2 = -\partial V/\partial y = 300q_2u_2u_3/u^5 \text{ nT} \tag{68}$$

$$b_3 = -\partial V/\partial z = -100q_2(1-3u_3^2/u^2)/u^3 \text{ nT}. \tag{69}$$

The computation of the covariance matrix will require values of the following partial derivatives.

$$d_1 = \partial b_1/\partial q_2 = b_1/q_2 \tag{70}$$

$$d_2 = \partial b_2/\partial q_2 = b_2/q_2 \tag{71}$$

$$d_3 = \partial b_3/\partial q_2 = b_3/q_2 \tag{72}$$

$$b_{11} = \partial b_1/\partial x = 300\ q_2u_3(1 - 5u_1^2/u^2)/u^5 \tag{73}$$

$$b_{12} = \partial b_1/\partial y = -1500q_2u_1u_2u_3/u^7 \tag{74}$$

$$b_{13} = \partial b_1/\partial z = 300\ q_2u_1(1 - 5u_3^2/u^2)/u^5 \tag{75}$$

$$b_{21} = \partial b_2/\partial x = b_{12} \tag{76}$$

$$b_{22} = \partial b_2/\partial y = 300\ q_2u_3(1 - 5u_2^2/u^2)/u^5 \tag{77}$$

$$b_{23} = \partial b_2/\partial z = 300\ q_2u_2(1 - 5u_3^2/u^2)/u^5 \tag{78}$$

$$b_{31} = \partial b_3/\partial x = b_{13} \tag{79}$$

$$b_{32} = \partial b_3/\partial y = b_{23} \tag{80}$$

$$b_{33} = \partial b_3/\partial z = 300\ q_2u_3(3 - 5u_3^2/u^2)/u^5 \tag{81}$$

Let (h_1, h_2, h_3) = total spacecraft magnetic field in the spacecraft reference frame and $h_{ij} = \partial h_i/\partial x_j$. Then

$$h_1 = a_1 + b_1 \tag{82}$$

$$h_2 = a_2 + b_2 \tag{83}$$

$$h_3 = a_3 + b_3 \tag{84}$$

$$h_{11} = a_{11} + b_{11} \tag{85}$$

$$h_{12} = a_{12} + b_{12} \tag{86}$$

$$h_{13} = a_{13} + b_{13} \tag{87}$$

$$h_{21} = a_{21} + b_{21} \tag{88}$$

$$h_{22} = a_{22} + b_{22} \tag{89}$$

$$h_{23} = a_{23} + b_{23} \tag{90}$$

$$h_{31} = a_{31} + b_{31} \tag{91}$$

$$h_{32} = a_{32} + b_{32} \tag{92}$$

$$h_{33} = a_{33} + b_{33}. \tag{93}$$

A Model for the Boom Shape

When torques are applied to the spacecraft, the boom will change shape, deviating from its static nominal position relative to the spacecraft. The foot of the boom will remain fixed but the rest of the boom will oscillate about the nominal position. For this study, only the fundamental mode is considered and the shape of the boom is assumed to be parabolic. The nominal position of the boom is along the positive x-axis of the spacecraft reference frame with the foot of the boom at (0,0,0). The projection of the boom at any given time into the xy-plane is here described by the equation

$$y = ax^2, \tag{94}$$

where a is a constant to be determined from the data. See Figure 3.

If the tangent line at the end of the boom is projected into the xy-plane, it makes an angle γ with the nominal boom axis and $dy/dx = \tan\gamma$. Let d = length of the boom and assume the projection of the magnetometers onto the x-axis is x = d, since the deviation of the magnetometers from the x-axis will be small. Values for γ can be computed from star camera observations at the magnetometers and on the spacecraft.

Differentiating (94) with respect to x gives

$$dy/dx = 2ax. \tag{95}$$

For small γ, at the end of the boom x = d and $dy/dx = \tan\gamma \simeq \gamma$. Thus

$$a = \tan\gamma/2d = \gamma/2d. \tag{96}$$

Substituting this in (94) gives

$$y = \gamma d/2 \tag{97}$$

at the end of the boom.

The projection of the boom into the xz-plane is here described by the equation

$$z = bx^2, \tag{98}$$

where b is a constant to be determined from the data. Using the same reasoning as before, with γ replaced by β, we find

$$b = \beta/2d, \tag{99}$$

$$z = \beta d/2 \tag{100}$$

at the end of the boom.

Measurements of β can be computed from star camera observations at the magnetometers and on the spacecraft.

The boom may also twist about the x-axis through an angle α at the end of the boom. Measurements of α can be computed from star camera observations at the magnetometers and on the spacecraft.

When the boom is bent from its nominal position, the values recorded by the magnetometers differ from those which would have been recorded in the nominal position. The y and z components of the magnetic field change due to the new position but the x component is, in effect, unchanged due to the smallness of the angles γ and β. The perturbed position of the outboard magnetometers is (x,y,z) where

$$x = d, \tag{101}$$

$$y = \gamma\, d/2 = q_5 d/2, \tag{102}$$

$$z = \beta\, d/2 = q_4 d/2. \tag{103}$$

The bending and twisting of the boom produces a reorientation of the vector magnetometer in the magnetic field. We assume, however, that the ambient field is estimated in the magnetometer coordinate system. This is equivalent to holding the magnetometers fixed in position and orientation and letting the spacecraft field sources move and twist.

The vector magnetometer rotates about the x-axis through an angle α, about the y-axis through an angle β, and about the z-axis through and angle γ. Since the angles are small, we can replace $\sin\alpha$ by α and $\cos\alpha$ by 1 and similarly for β and γ.

We see now that the total magnetic field at the magnetometers is

$$P_1 = q_6 + h_1 - q_5 h_2 + q_4 h_3, \tag{104}$$

$$P_2 = q_7 + h_2 + q_5 h_1 - q_3 h_3, \tag{105}$$

$$P_3 = q_8 + h_3 - q_4 h_1 + q_3 h_2, \tag{106}$$

where α, β, and γ have been replaced by q_3, q_4 and q_5. (h_1,h_2,h_3) is the spacecraft magnetic field at (x,y,z) after translation [see (101), (102), (103)] but before rotation through angles $(\alpha,\beta,\gamma) = (q_3,q_4,q_5)$. (q_6, q_7, q_8) is the ambient magnetic field vector and (p_1, p_2, p_3) is the total magnetic field vector in the vector magnetometer reference frame.

The computation of the covariance matrix requires values of the partial derivatives of the total magnetic field at the vector magnetometer [see (101) to (106)].

We differentiate p_1, p_2, and p_3 in (104), (105), and (106) with respect to q_3, q_4, and q_5 and then replace q_3, q_4, and q_5 by their nominal values. For this study, the nominal values of q_3, q_4, and q_5 are taken as 0, although in general, this will not be the case. For example

$$\partial p_1/\partial q_4 = (\partial h_1/\partial q_4) - q_5(\partial h_2/\partial q_4) + q_4(\partial h_3/\partial q_4) + h_3,$$

$$\partial h_1/\partial q_4 = (\partial h_1/\partial x)(\partial x/\partial q_4) + (\partial h_1/\partial y)(\partial y/\partial q_4) + (\partial h_1/\partial z)(\partial z/\partial q_4) = h_{13}d/2$$

[See (101), (102), (103)],

$$\partial p_1/\partial q_4 = h_{13}d/2 + h_3.$$

The other partial derivatives are obtained in a similar way, giving

$$p_{13} = \partial p_1/\partial q_3 = 0, \tag{107}$$

$$p_{14} = \partial p_1/\partial q_4 = h_{13}d/2 + h_3, \tag{108}$$

$$p_{15} = \partial p_1/\partial q_5 = h_{12}d/2 - h_2, \tag{109}$$

$$p_{23} = \partial p_2/\partial q_3 = -h_3, \tag{110}$$

$$p_{24} = \partial p_2/\partial q_4 = h_{23}d/2, \tag{111}$$

$$p_{25} = \partial p_2/\partial q_5 = h_{22}d/2 + h_1, \tag{112}$$

$$p_{33} = \partial p_3/\partial q_3 = h_2, \tag{113}$$

$$p_{34} = \partial p_3/\partial q_4 = h_{33}d/2 - h_1, \tag{114}$$

$$p_{35} = \partial p_3/\partial q_5 = h_{32}d/2. \tag{115}$$

Obviously, $p_{16} = p_{27} = p_{38} = 1$.

The magnitude of the total magnetic field vector is

$$p_4 = (p_1^2 + p_2^2 + p_3^2)^{1/2}. \tag{116}$$

If we let g_1, g_2, g_3, and g_4 be the nominal values of p_1, p_2, p_3, and p_4, then

$$g_1 = q_6 + h_1, \tag{117}$$

$$g_2 = q_7 + h_2, \tag{118}$$

$$g_3 = q_8 + h_3, \tag{119}$$

$$g_4 = (g_1^2 + g_2^2 + g_3^2)^{1/2}. \tag{120}$$

From (116) we get the partial derivatives

$$p_4(\partial p_4/\partial q_i) = p_1(\partial p_1/\partial q_i) + p_2(\partial p_2/\partial q_i) + p_3(\partial p_3/\partial q_i),\ i = 1 \text{ to } 8. \tag{121}$$

With nominal values for the parameters, p_i, (121) gives, for i = 3,4,5,

$$p_{43} = (h_2 q_8 - h_3 q_7)/g_4, \tag{122}$$

$$p_{44} = [(g_1 h_{13} + g_2 h_{23} + g_3 h_{33})d/2 + h_3 q_6 - h_1 q_8]/g_4, \tag{123}$$

$$p_{45} = [(g_1 h_{12} + g_2 h_{22} + g_3 h_{32})d/2 + h_1 q_7 - h_2 q_6]/g_4, \tag{124}$$

From (104), (82), (54), and (67), with nominal values for q_4 and q_5, we get

$$p_{11} = c_1 = a_1/q_1. \tag{125}$$

In a similar way,we get from (104), (105), and (106)

$$p_{12} = d_1 = b_1/q_2, \tag{126}$$

$$p_{21} = c_2 = a_2/q_1, \tag{127}$$

$$p_{22} = d_2 = b_2/q_2, \tag{128}$$

$$p_{31} = c_3 = a_3/q_1, \tag{129}$$

$$p_{32} = d_3 = b_3/q_2. \tag{130}$$

With nominal values for the parameters, p_i, (121) gives, for i = 1 and 2,

$$p_{41} = (g_1 p_{11} + g_2 p_{21} + g_3 p_{31})/g_4, \tag{131}$$

$$p_{42} = (g_1 p_{12} + g_2 p_{22} + g_3 p_{32})/g_4. \tag{132}$$

From (104), (105), and (106) we get

$$p_{16} = 1, \quad p_{17} = 0, \quad p_{18} = 0, \tag{133}$$

$$p_{26} = 0, \quad p_{27} = 1, \quad p_{28} = 0, \tag{134}$$

$$p_{36} = 0, \quad p_{37} = 0, \quad p_{38} = 1. \tag{135}$$

With nominal values for the parameters, (121) gives, for i = 6, 7, and 8,

$$p46 = g1/g4, \quad p47 = g2/g4, \quad p48 = g3/g4. \tag{136}$$

Results

In the study, the spacecraft field was assumed to be due to two torquer rods with moments equal to 350 Am^2 each. The accuracy to which these moments are assumed known is σ_T. σ_T was allowed to assume the values 3.5, 17.5 and 35 Am^2 or 1%, 5% and 10%, respectively. The variation of σ_T, then, is a measure of how well the spacecraft field is known. Further, the angles between the torquer rods and the magnetometer platform were assumed to be known to an accuracy of σ_a, which for this study was assumed to be 0.6^o for a 12-meter boom. Both torquer bar moments and angles are assumed to be known a priori. For σ_a equal to 0.6^o, the angular accuracy did not affect the error analysis.

The measurement accuracies, denoted σ_{vm} for the VFM and σ_{sm} for the SHM, were studied in the following combinations: (1) σ_{vm} = 3.0 nT, σ_{sm} = 2.0 nT; (2) σ_{vm} = 3.0 nT, σ_{sm} = 1.0 nT; (3) σ_{vm} = 2.0 nT, σ_{sm} = 1.0 nT. For each of these combinations, a set of calculations were performed and results showing the following were plotted:

a) Uncertainty in the earth's field vs. boom length for fixed σ_T (3.5, 17.5, 35 Am^2). Figures 4, 5, 6; 14, 15, 16; 24, 25, 26.
b) Uncertainty in the earth's field vs. σ_T for fixed boom length (6, 12m). Figures 7,8; 17, 18; 27, 28.
c) Uncertainty in spacecraft field vs. boom length for fixed σ_T (3.5, 17.5, 35 Am^2). Figures 9, 10, 11; 19, 20, 21; 29, 30, 31.
d) Uncertainty in spacecraft field vs. σ_T for fixed boom length (6, 12m). Figures 12, 13; 22, 23; 32, 33.

The x-component curve shapes are strongly influenced by the vanishing of the x-component of the input spacecraft field roughly 5 m out the boom. The y-component curve shapes are strongly influenced by the extrema in the y-component of the input spacecraft field roughly 4 m out the boom.

Conclusions

From these results it is possible to draw the following conclusions:

1. Given minimal spacecraft field; i.e. long boom or very small σ_T, the accuracy of determination of Earth's field is limited by the calibration accuracy of the VFM. The more accurately the VFM can be calibrated via the SHM, the more accurate the final measurements will be. (See, Figures 4, 14, and especially 24.)
2. There is a distinct trade-off between knowledge of the spacecraft field, σ_T, and boom length. If the spacecraft field were known perfectly no boom would be necessary. The actual trade-off depends, of course, on the actual strength of the spacecraft field. In this study, only the fields from the two torquer rods are included.

3. For the spacecraft field strength studied, if the field is known to 5% (17.4 Am^2), and if the VFM can be calibrated to 3.0-nT using SHM data good to but 2.0 nT, then a 12-m boom is long enough to meet the 1.0-nT spacecraft field requirement (Figure 10). If the SHM data meets the 1.0-nT requirement, then a 12-m boom is long enough to meet some goals, but not all. It is long enough to meet the requirements. (Figure 25, also see Figure 15).
4. For the spacecraft field strength studied, if the field is known to 10% (35 Am^2) a 12-m boom is <u>not</u> long enough to meet the goals but <u>is</u> long enough to meet the requirement. (Figure 26, also see 16).
5. If the spacecraft field is known to 1%, then a 5-m boom length might be adequate.

There will, of course, be other sources than the torquer rods. Some of those sources will probably not be anticipated prior to launch. The ability to accurately model the spacecraft field is the single most important factor in determining the necessary boom length. For known sources, this accuracy depends crucially on the adequacy of the model and on the accuracy and timeliness of the telemetry readout. The data rate required for the solid earth measurements is one per second. If telemetry readouts of the crucial spacecraft quantities are more widely spaced than this, or are not simultaneous with vector readouts, then some sort of interpolation will be required which will reduce the accuracy.

If sufficient attention is given pre-launch so that the model of the torquer rods, the solar panels, and any other comparable sources is certainly known and characterized by the available telemetry to better than 1%, then the boom length could probably be shortened. The actual length would be subject to study but it is anticipated that it would not be shorter than 5 m.

MEETING THE ERROR BUDGET

Two items from the error budget are pertinent, instrument error and spacecraft field.

	SCALAR		VECTOR	
	Req.	Goal	Req.	Goal
Instrument	1.0	0.7	3.0	1.5
Spacecraft Field	1.0	0.5	1.0	0.5
Rss	1.41	0.86	3.16	1.6

Meeting the goals is feasible with the 12 m boom length, provided the vector instrument can be calibrated in-flight to 1.5 nT. Meeting the requirement should be possible provided the vector instrument can be calibrated in-flight to 3.0 nT. These both assume that the spacecraft field can be modeled to better than 5%. As already noted, if a 1% model is possible, then the boom can probably be shortened.

APPENDIX A

The MAGSAT tricoil system response was characterized by non-linear sensor cross-coupling, so G_{jk}, hence ρ_{jk}, was a function of **B** and 12 parameters h_{nm} determined by ground calibration alone. The APAFO 4-coil system response is expected to have but weak linear cross-coupling because the field is to be nulled in each ring core plane rather than along but one axis. One might expect $G_{jk} = 1_{jk}$ and $\rho_{jk} = a_{jk}$; however, the offset (and sense) coils 1 at $\mathbf{x}^{*1}$ generate a stray sensor field $\mathbf{B}^c(\mathbf{x}^{*j},t)$ at sensor $j \neq 1$; this field is distinguished from other ambient, spacecraft, and platform fields which comprise $\mathbf{B}(\mathbf{x}^{*j},t)$ (due to proximity; the He scalar and the star cameras may generate a stray field at the fluxgate sensors and vice-versa which must meet mission requirements). So $y_j = \Sigma_k[a_{jk}(B_k + B^c{}_k)] \neq \Sigma_k[a_{jk}B_k]$. But $\mathbf{B}^c$ depends upon the coil currents, so $B^c{}_k = B^c{}_k(p_{n(1\neq j)}, F(\bar{u}_{i1}), \bar{r}_{i1})$ and the true field $\mathbf{B} + \mathbf{B}^c$ nulled by sensor j depends in part upon the coil currents, hence calibration, of the other sensors (Heisenberg strikes again). To the extent that design ensures coil currents which are directly proportional to the true field being offset and $|B^c{}_k| << |B_k|$, $B^c{}_k = \Sigma_1[b_{k1}B_1]$ --where B_1 is assumed to be homogeneous across the fluxgates and b_{k1} is determined by the geometric configuration of the fluxgates (notably the relative orientation and separation of the coils). Then $y_j \equiv \rho_{jk}B_k = \Sigma_k[a_{jk}(B_k + \Sigma_1 b_{k1}B_1)] = \Sigma_{k,1}[a_{jk}B_k + a_{jk}b_{k1}B_1]$, where ρ_{jk} is the response function operator. Reordering the summation and relabeling gives $\rho_{jk} = a_{jk} + \Sigma_1 a_{j1}b_{1k}$; thus the dependence of ρ on **B** can be ignored for an effectively linear response. Nevertheless, even if the response of sensor j were linear with no current in other coils, the presence of current in the other coils is expected to cause a response of sensor j. It follows that ρ should differ from an optical determination of **a**. Alternately, the effective sensor axis might be thought of as differing from the geometric axis of the coil; however, equations (5) for **a** need not apply to ρ and 12 independent elements of ρ, rather than 8 independent elements of **a**, need to be estimated.

It may be possible to ensure that the dependence of ρ_{jk} on **B** is negligible for the weak fields expected, but it seems wise to prepare for the contrary. Ground-based calibration must determine whether or not ρ_{jk} depends upon **B**, and, if so, the functional form of such dependence--including numerical values of **h**. Here it is assumed that $\rho_{jk} = \rho_{jk}(\mathbf{B},\mathbf{a};\mathbf{h})$ with **h** given and ρ_{jk} and **B** to be estimated iteratively.

REFERENCES

Lancaster, E.R., et al., Magsat vector magnetometer calibration using Magsat geomagnetic field measurements, NASA/GSFC Tech. Memo. TM 82046, 1980.

Langel, R.A., et al., Magsat data processing: A report for investigators, NASA/GSFC Tech. Memo. TM 82160, 1981.

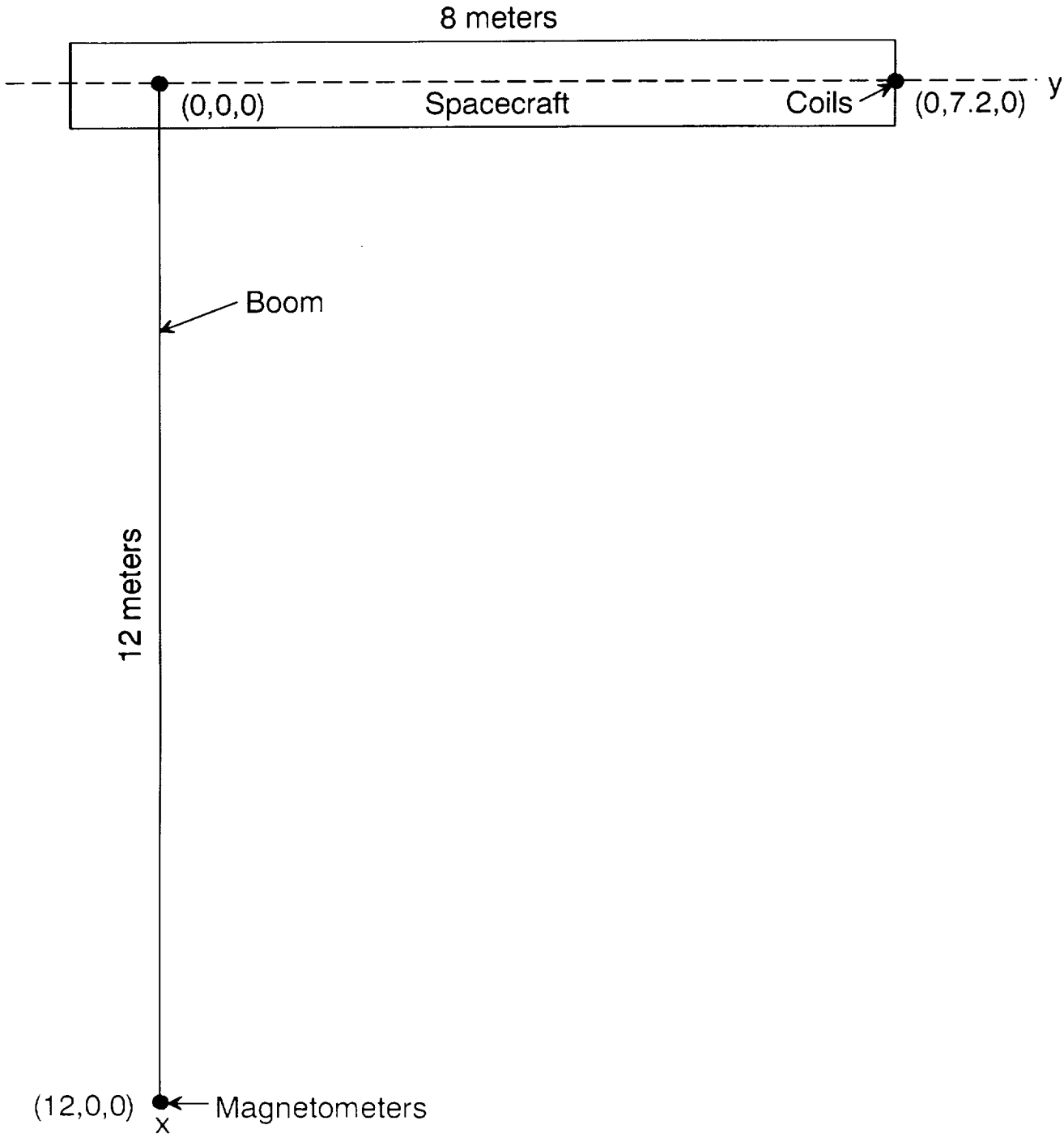
8 meters
(0,0,0)
Spacecraft
Coils
(0,7.2,0)
y
Boom
12 meters
(12,0,0)
x
Magnetometers

Figure 1.

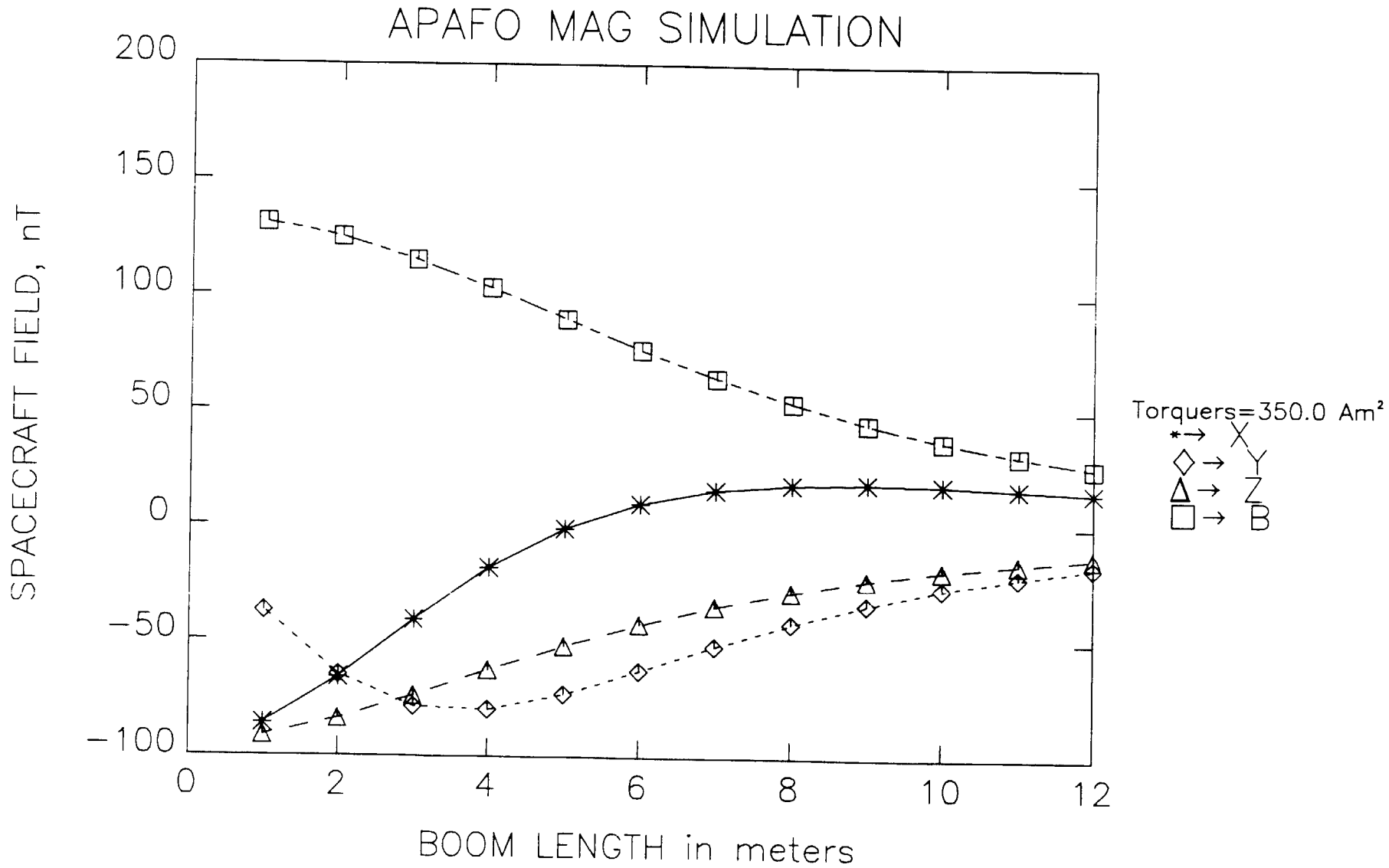
APAFO MAG SIMULATION
SPACECRAFT FIELD, nT
200
150
100
50
0
−50
−100
0
2
4
6
8
10
12
BOOM LENGTH in meters
Torquers=350.0 Am²
X
Y
Z
B

Figure 2.

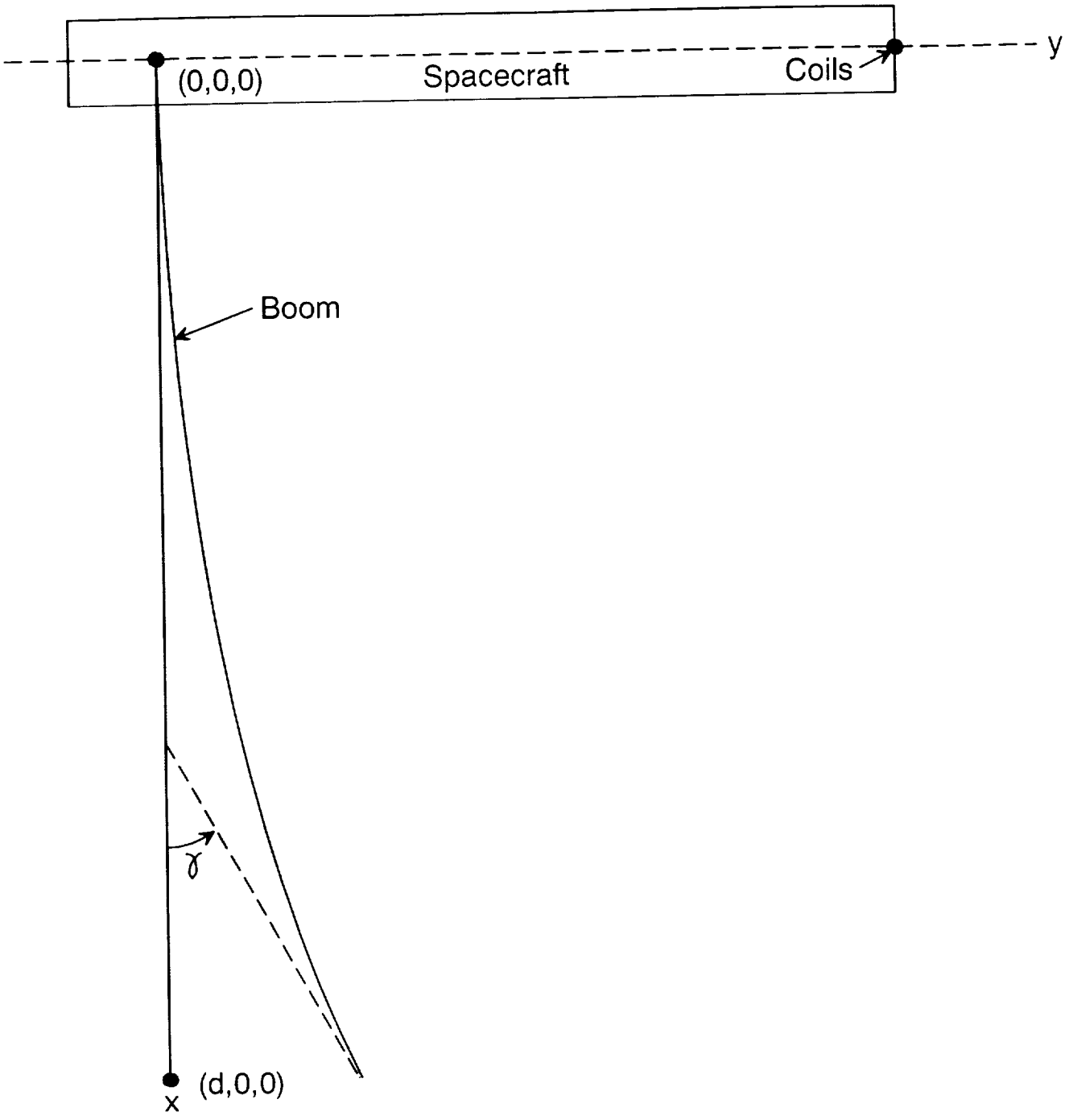

Figure 3.

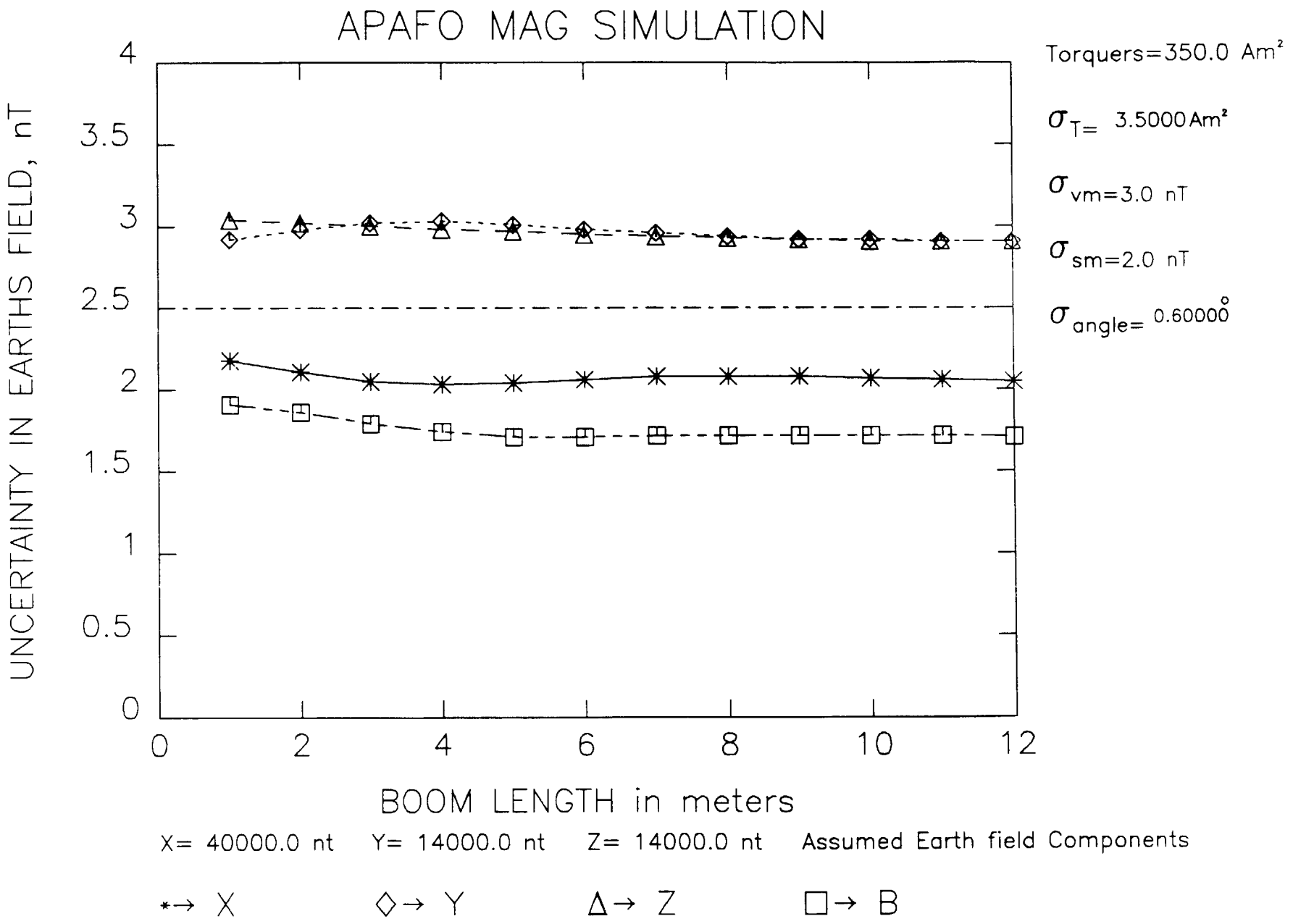
APAFO MAG SIMULATION
Torquers=350.0 Am²
σT= 3.5000Am²
σvm=3.0 nT
σsm=2.0 nT
σangle= 0.60000°
UNCERTAINTY IN EARTHS FIELD, nT
0
0.5
1
1.5
2
2.5
3
3.5
4
0
2
4
6
8
10
12
BOOM LENGTH in meters
X= 40000.0 nt Y= 14000.0 nt Z= 14000.0 nt Assumed Earth field Components
*→ X ◇→ Y Δ→ Z □→ B

Figure 4.

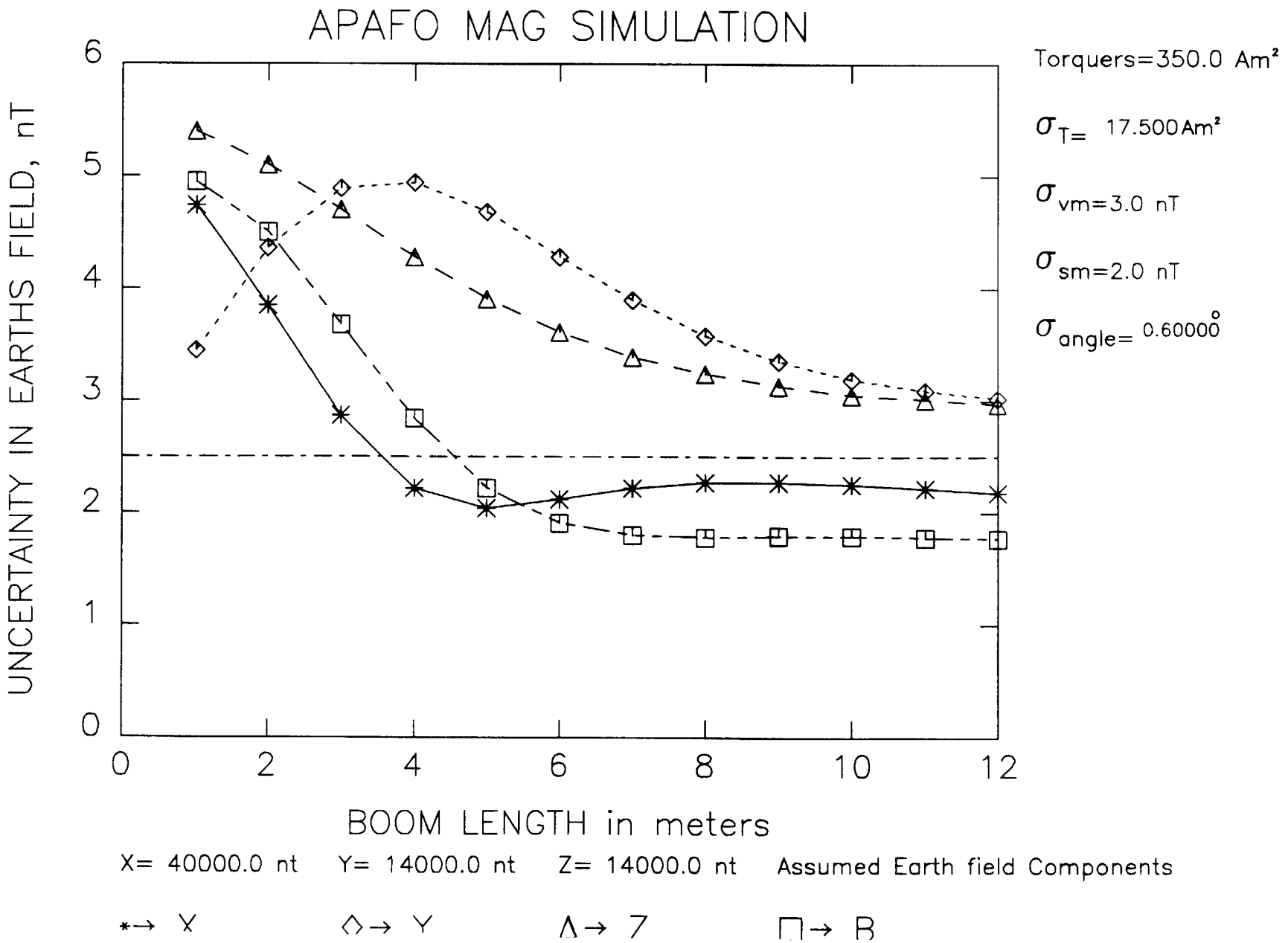
APAFO MAG SIMULATION
UNCERTAINTY IN EARTHS FIELD, nT
BOOM LENGTH in meters
0
1
2
3
4
5
6
0
2
4
6
8
10
12
Torquers=350.0 Am²
σT= 17.500Am²
σvm=3.0 nT
σsm=2.0 nT
σangle= 0.60000°
X= 40000.0 nt
Y= 14000.0 nt
Z= 14000.0 nt
Assumed Earth field Components
*→ X
◇→ Y
Λ→ Z
□→ B

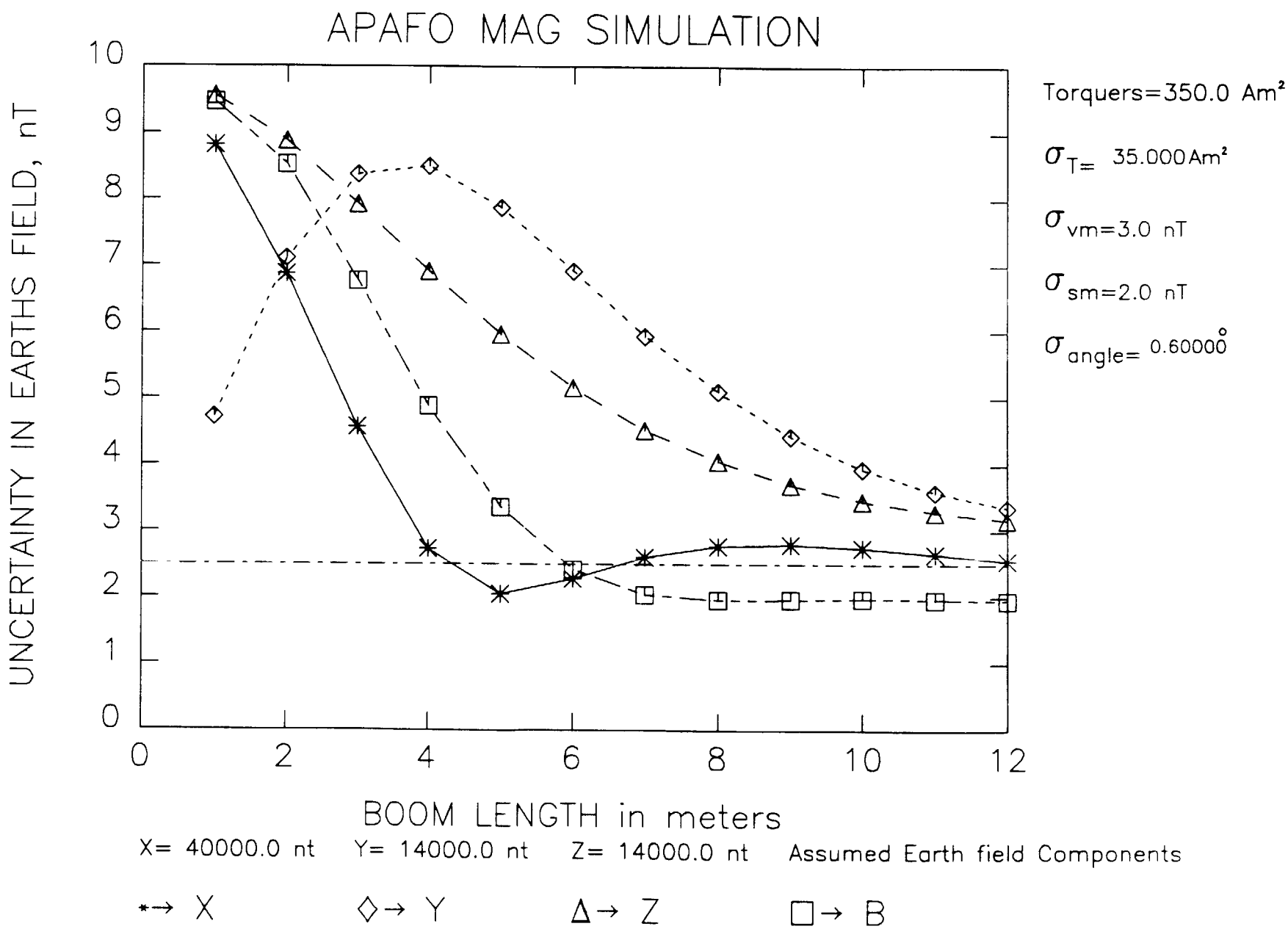
APAFO MAG SIMULATION
UNCERTAINTY IN EARTHS FIELD, nT
BOOM LENGTH in meters
0
1
2
3
4
5
6
7
8
9
10
0
2
4
6
8
10
12
Torquers=350.0 Am²
σT= 35.000Am²
σvm=3.0 nT
σsm=2.0 nT
σangle= 0.60000°
X= 40000.0 nt
Y= 14000.0 nt
Z= 14000.0 nt
Assumed Earth field Components
X
Y
Z
B

Figure 6.

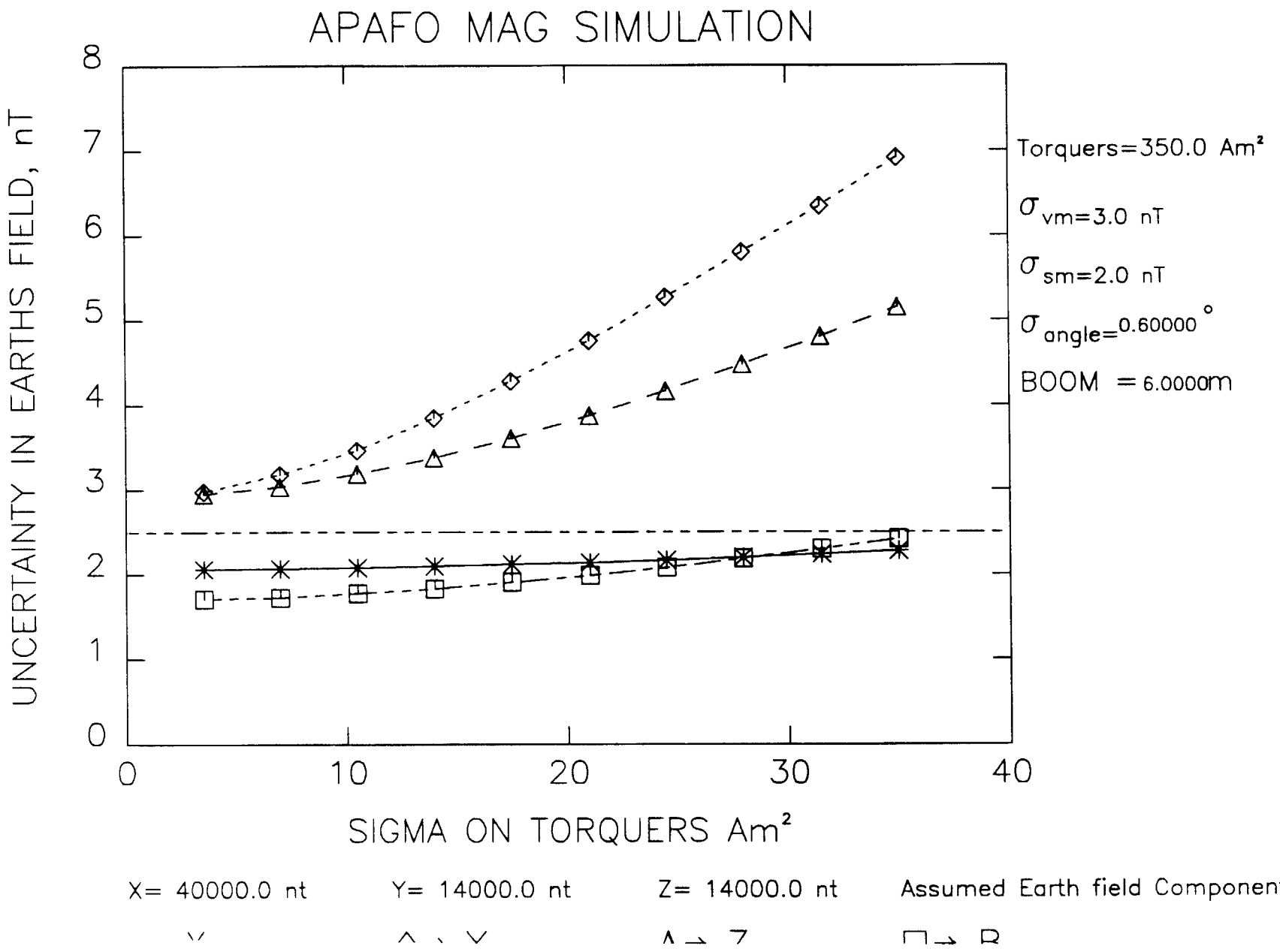

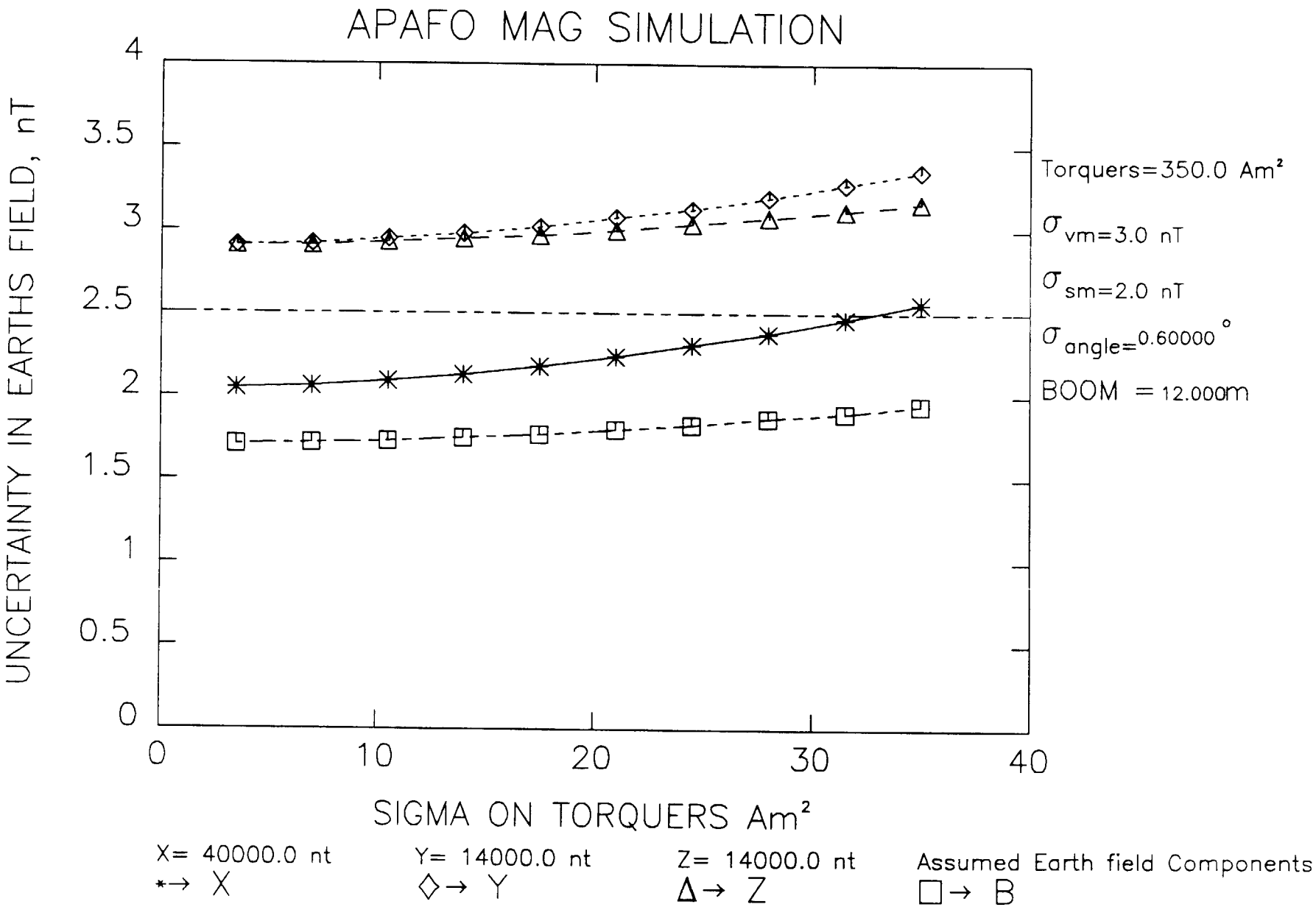
APAFO MAG SIMULATION
UNCERTAINTY IN EARTHS FIELD, nT
SIGMA ON TORQUERS Am²
0
0.5
1
1.5
2
2.5
3
3.5
4
0
10
20
30
40
Torquers=350.0 Am²
σvm=3.0 nT
σsm=2.0 nT
σangle=0.60000°
BOOM =12.000m
X= 40000.0 nt
*→ X
Y= 14000.0 nt
◇→ Y
Z= 14000.0 nt
Δ→ Z
Assumed Earth field Components
□→ B

Figure 8.

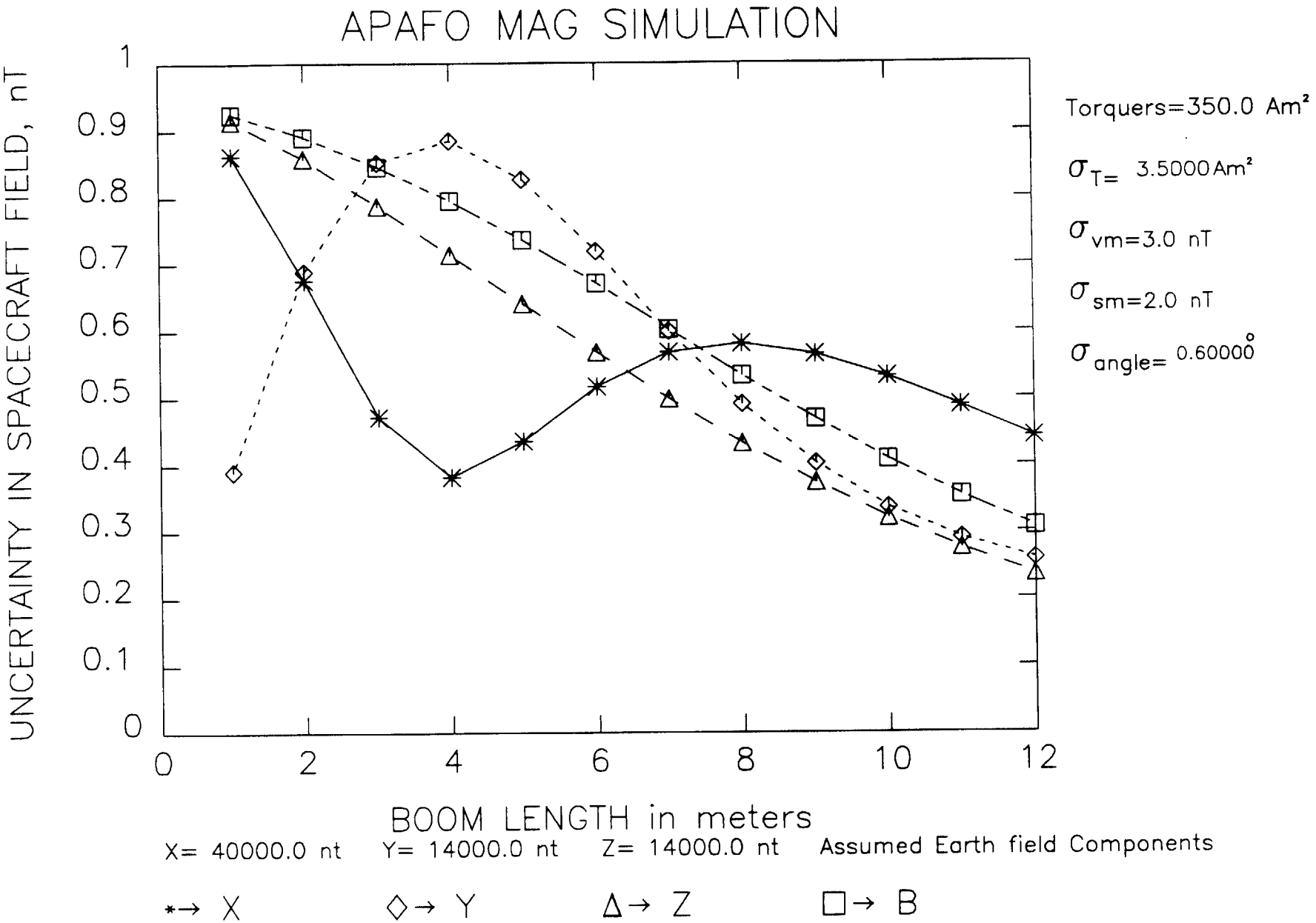
APAFO MAG SIMULATION
UNCERTAINTY IN SPACECRAFT FIELD, nT
1
0.9
0.8
0.7
0.6
0.5
0.4
0.3
0.2
0.1
0
0
2
4
6
8
10
12
BOOM LENGTH in meters
Torquers=350.0 Am²
σT= 3.5000Am²
σvm=3.0 nT
σsm=2.0 nT
σangle= 0.60000°
X= 40000.0 nt Y= 14000.0 nt Z= 14000.0 nt Assumed Earth field Components
*→ X
◇→ Y
Δ→ Z
□→ B

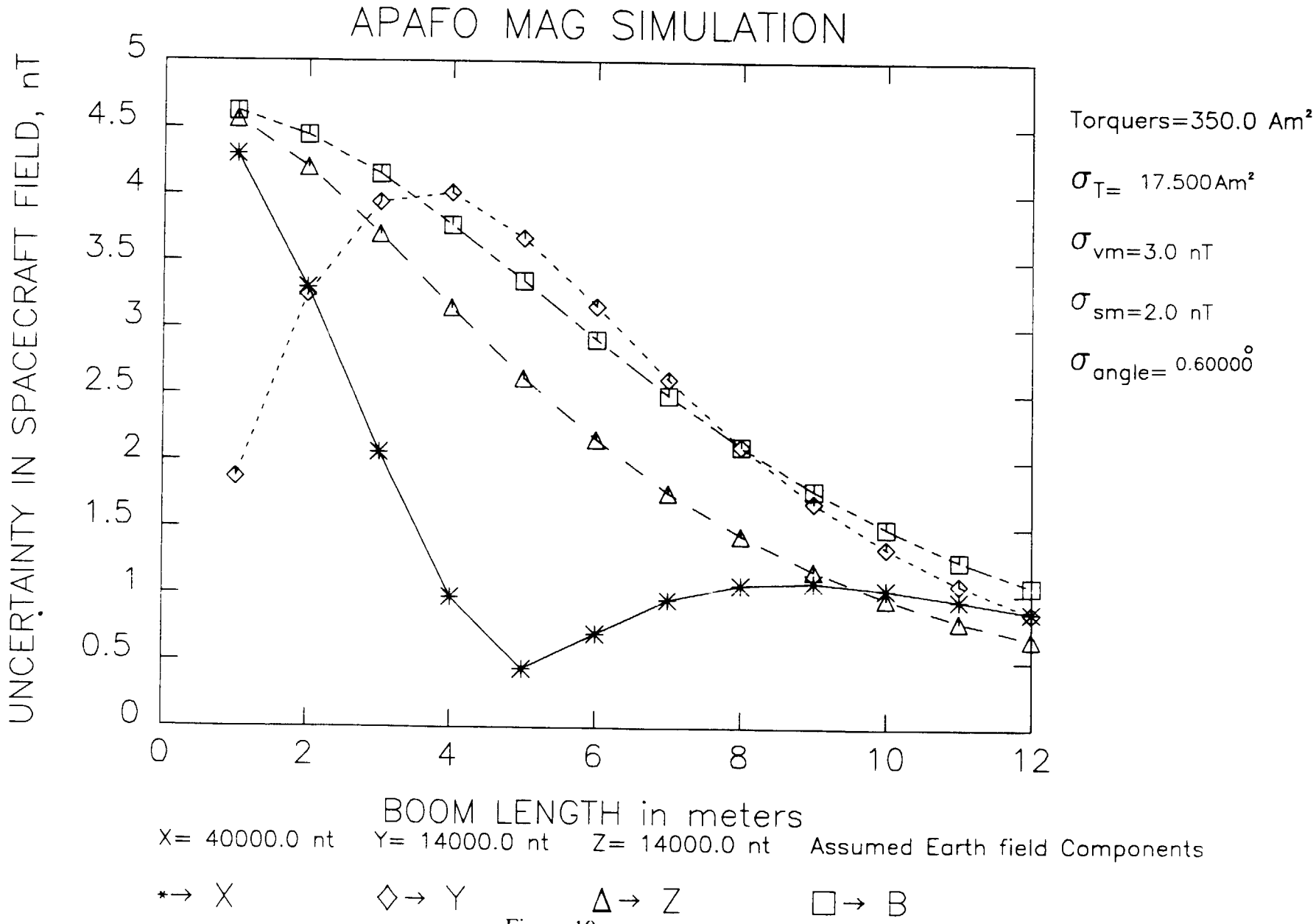
APAFO MAG SIMULATION
UNCERTAINTY IN SPACECRAFT FIELD, nT
0
0.5
1
1.5
2
2.5
3
3.5
4
4.5
5
0
2
4
6
8
10
12
BOOM LENGTH in meters
Torquers=350.0 Am²
σT= 17.500Am²
σvm=3.0 nT
σsm=2.0 nT
σangle= 0.60000°
X= 40000.0 nt
Y= 14000.0 nt
Z= 14000.0 nt
Assumed Earth field Components
*→ X
◇→ Y
Δ→ Z
□→ B

Figure 10.

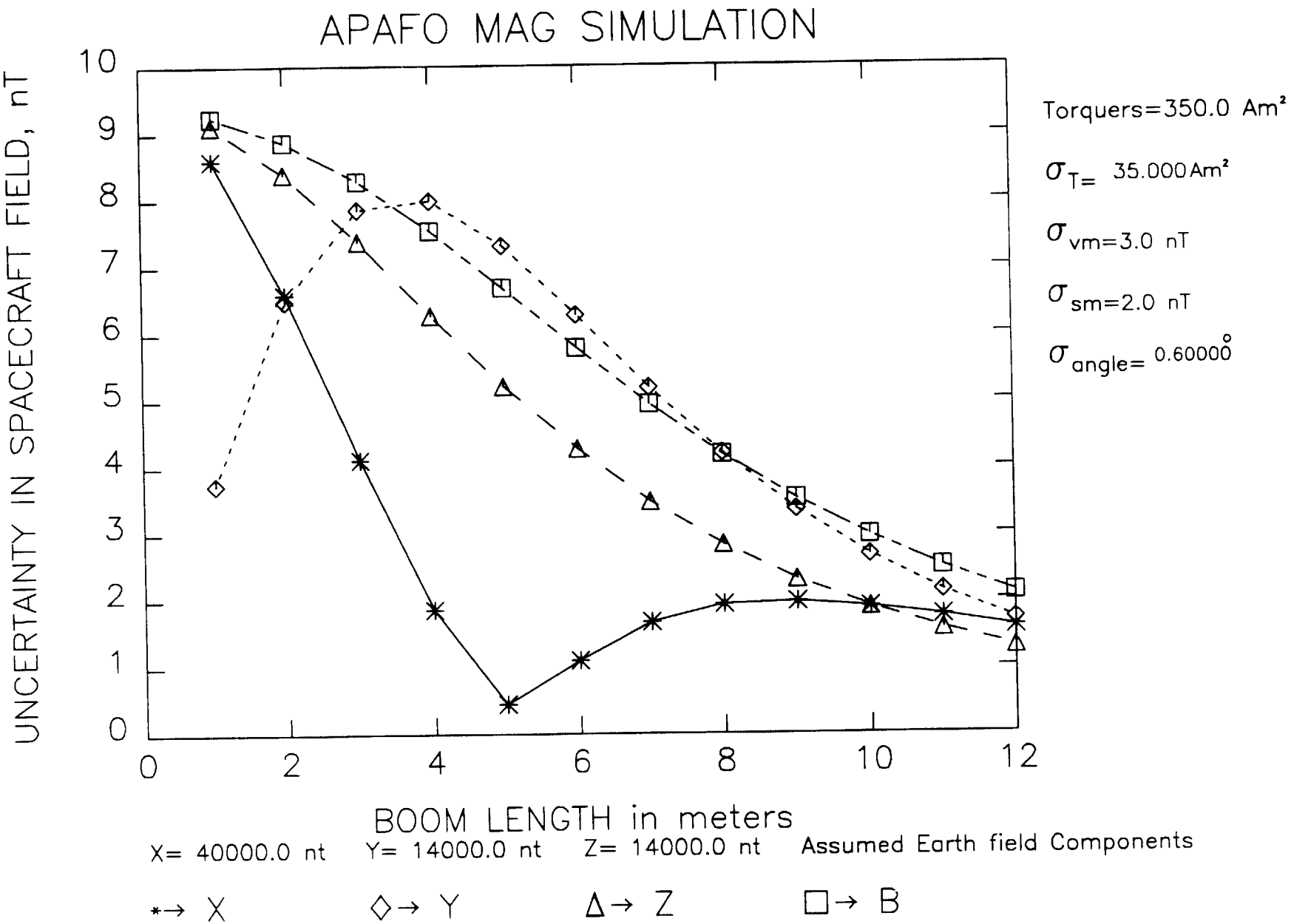
APAFO MAG SIMULATION
UNCERTAINTY IN SPACECRAFT FIELD, nT
BOOM LENGTH in meters
0
2
4
6
8
10
12
0
1
2
3
4
5
6
7
8
9
10
Torquers=350.0 Am²
σT= 35.000Am²
σvm=3.0 nT
σsm=2.0 nT
σangle= 0.60000°
X= 40000.0 nt
Y= 14000.0 nt
Z= 14000.0 nt
Assumed Earth field Components
*→ X
◇→ Y
Δ→ Z
□→ B

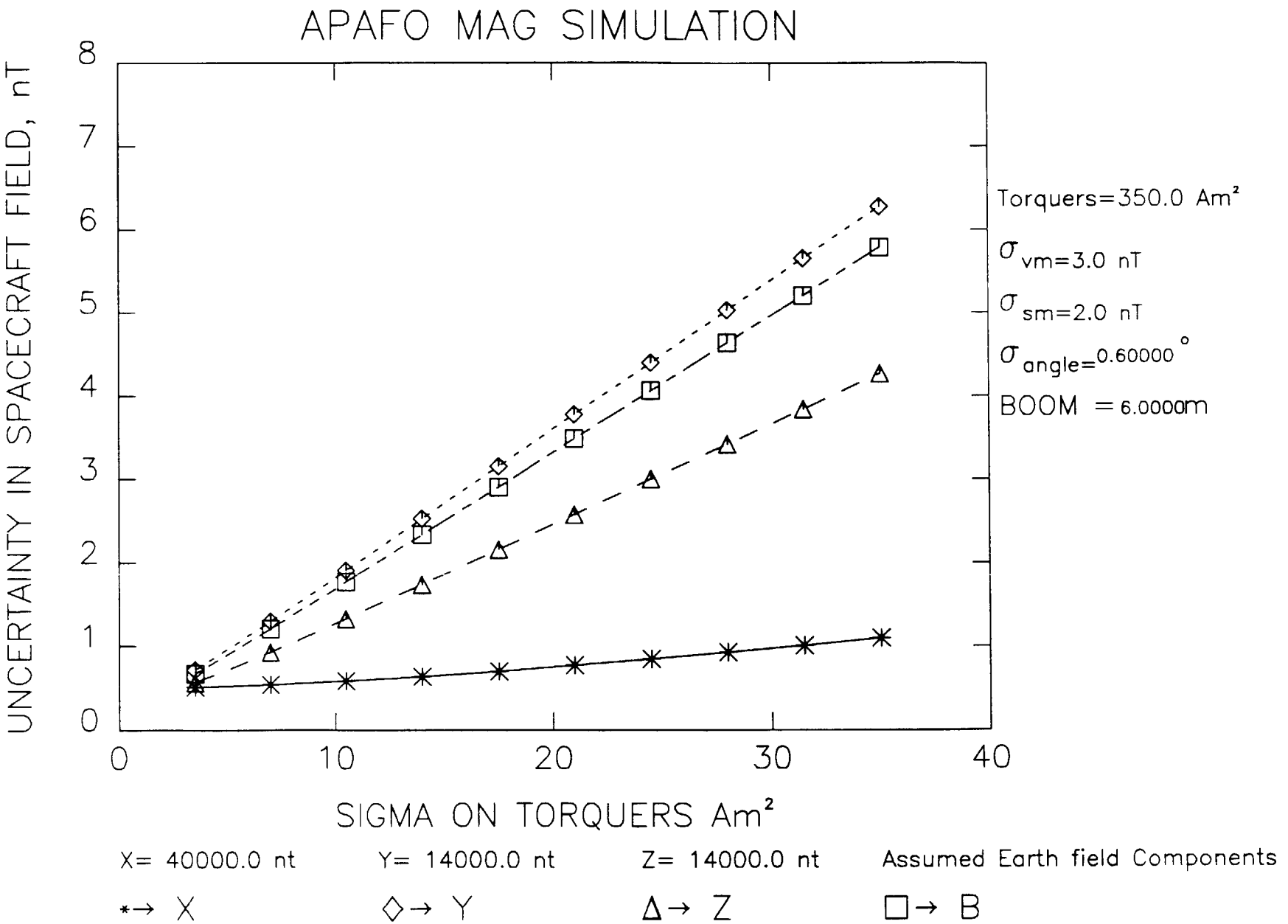
APAFO MAG SIMULATION
UNCERTAINTY IN SPACECRAFT FIELD, nT
SIGMA ON TORQUERS Am²
0
1
2
3
4
5
6
7
8
0
10
20
30
40
Torquers=350.0 Am²
σ vm=3.0 nT
σ sm=2.0 nT
σ angle=0.60000 °
BOOM =6.0000m
X= 40000.0 nt
Y= 14000.0 nt
Z= 14000.0 nt
Assumed Earth field Components
*→ X
◇→ Y
Δ→ Z
□→ B

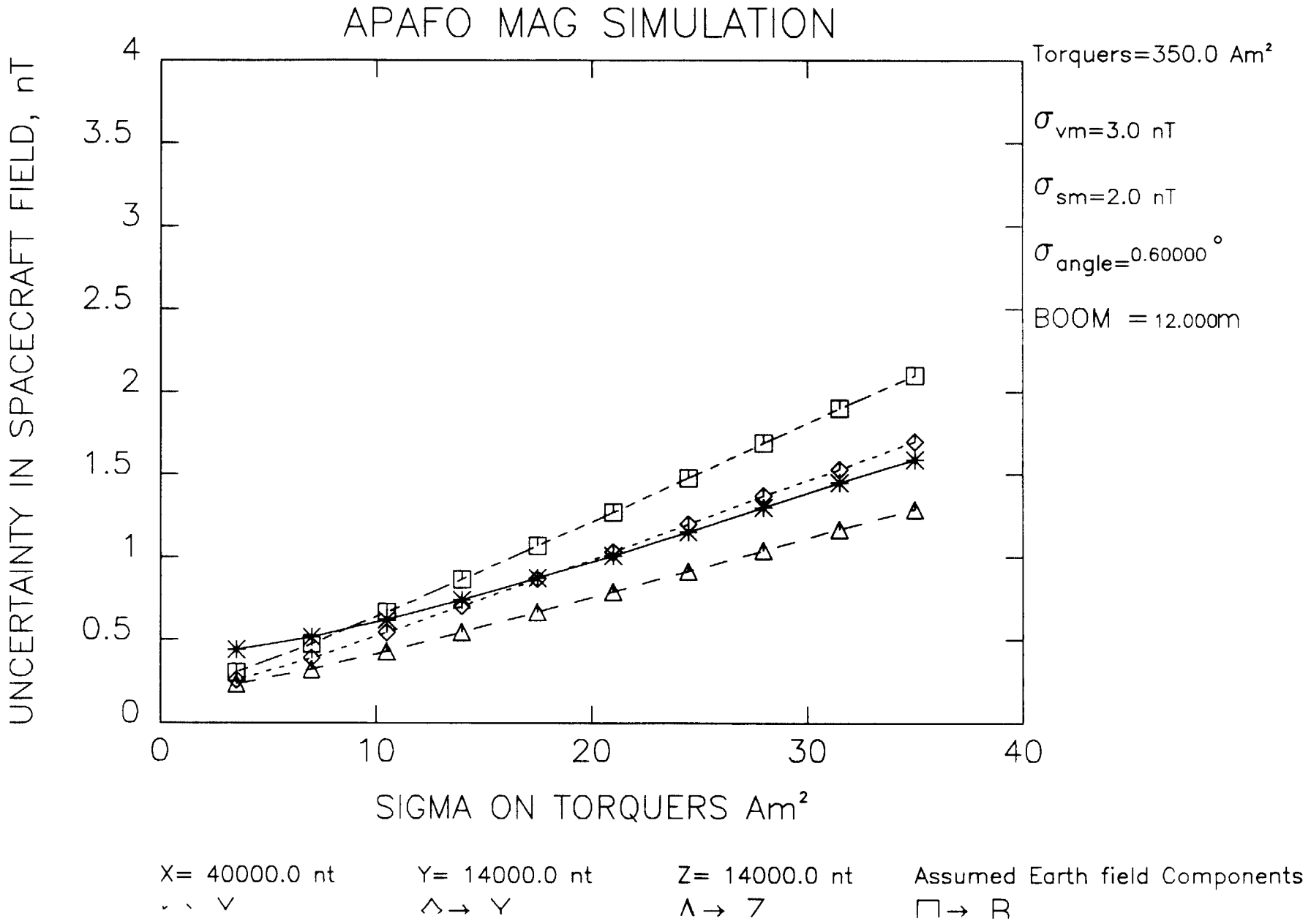

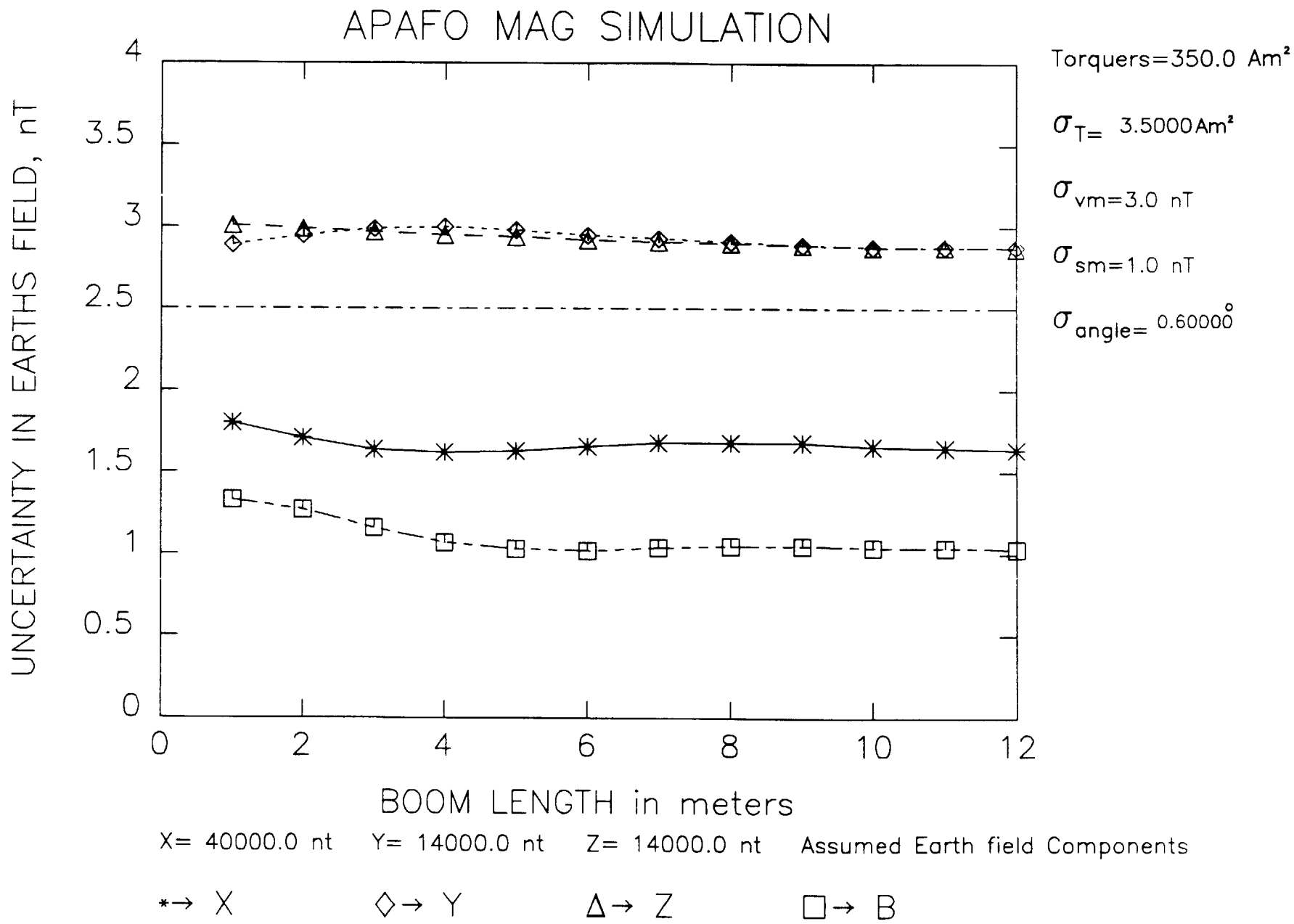
APAFO MAG SIMULATION
UNCERTAINTY IN EARTHS FIELD, nT
BOOM LENGTH in meters
0
0.5
1
1.5
2
2.5
3
3.5
4
0
2
4
6
8
10
12
Torquers=350.0 Am²
σT= 3.5000Am²
σvm=3.0 nT
σsm=1.0 nT
σangle= 0.60000°
X= 40000.0 nt
Y= 14000.0 nt
Z= 14000.0 nt
Assumed Earth field Components
*→ X
◇→ Y
Δ→ Z
□→ B

Figure 14.

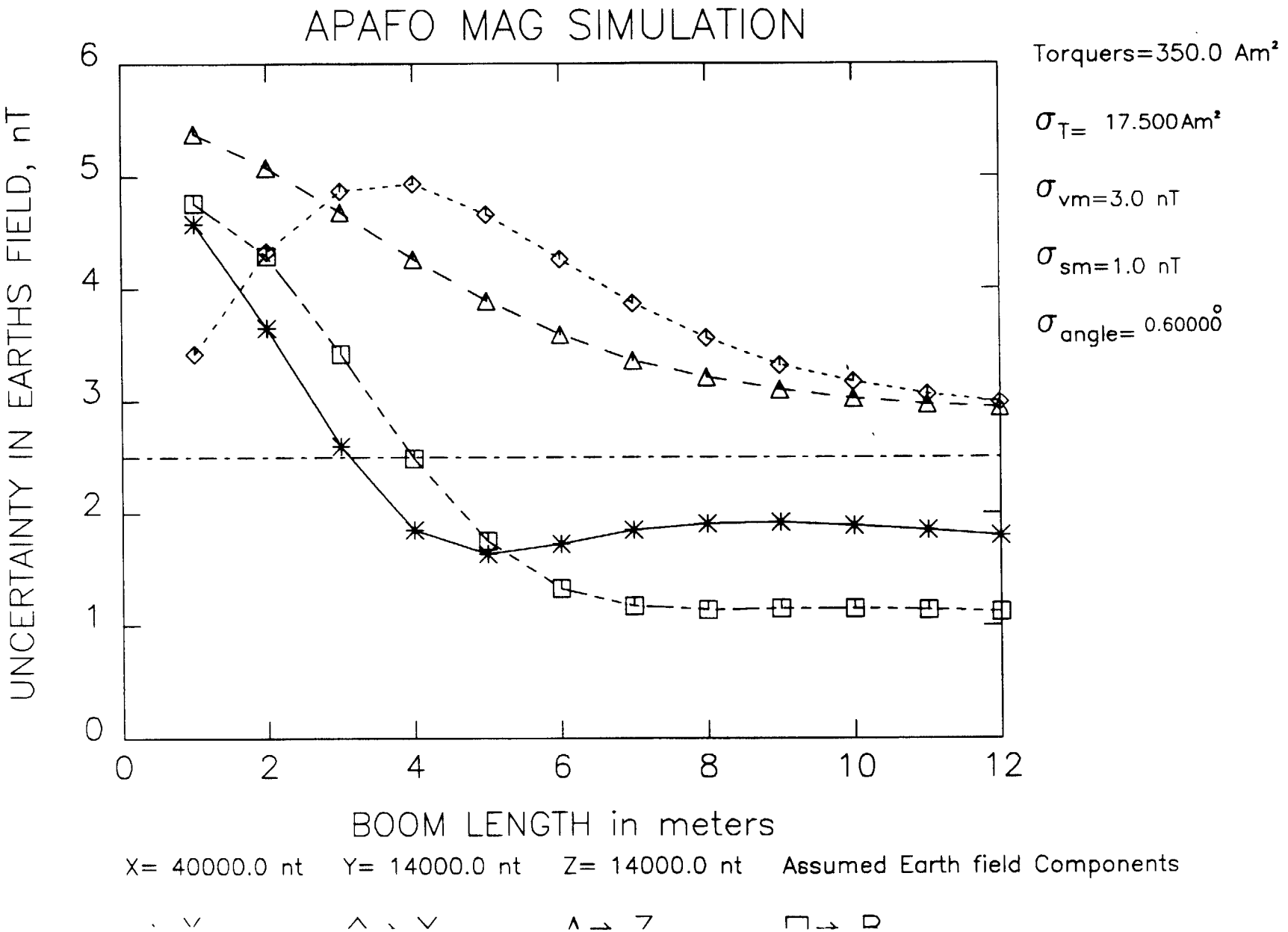

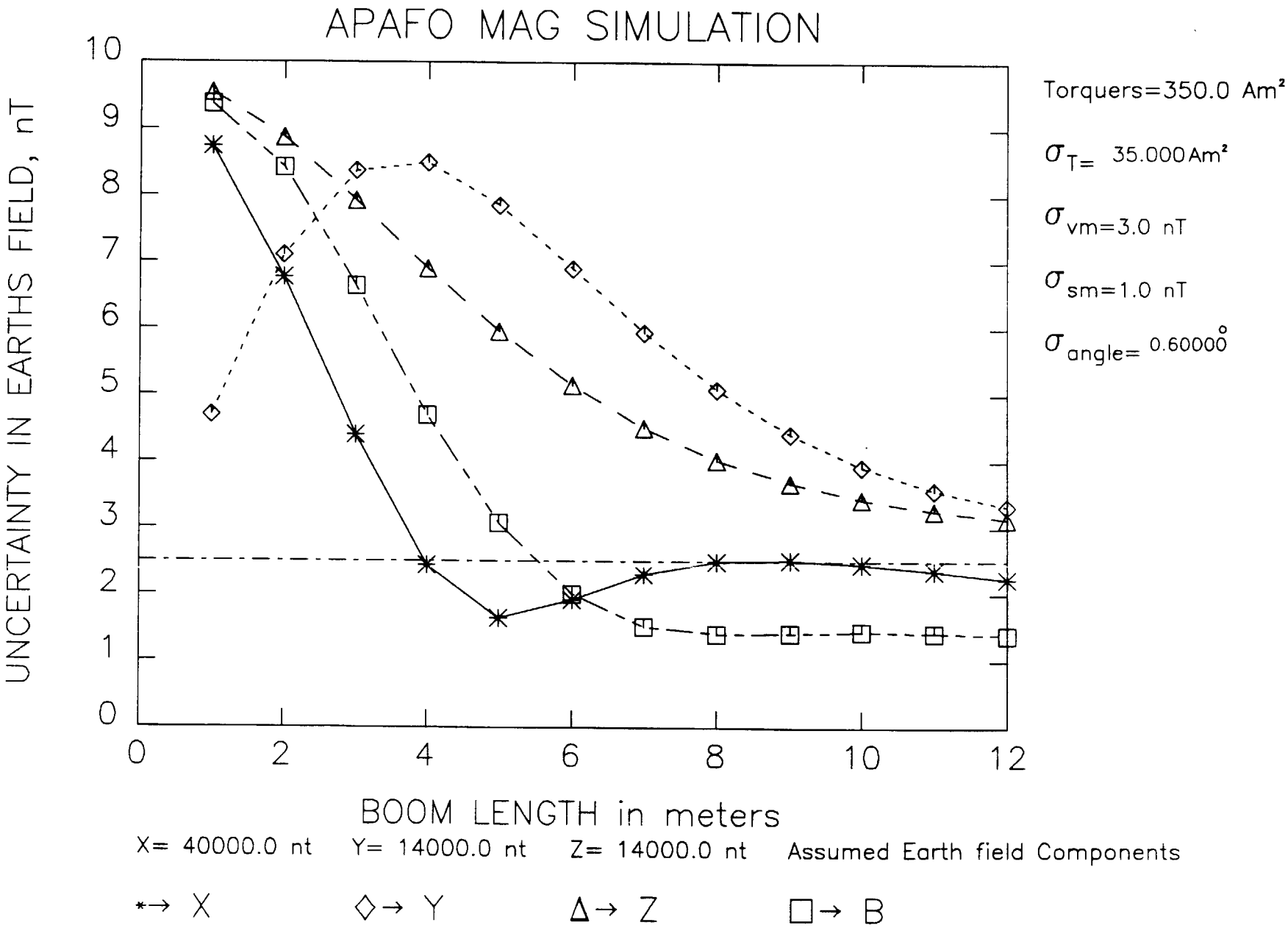
APAFO MAG SIMULATION
UNCERTAINTY IN EARTHS FIELD, nT
BOOM LENGTH in meters
0
1
2
3
4
5
6
7
8
9
10
0
2
4
6
8
10
12
Torquers=350.0 Am²
σT= 35.000Am²
σvm=3.0 nT
σsm=1.0 nT
σangle= 0.60000°
X= 40000.0 nt Y= 14000.0 nt Z= 14000.0 nt Assumed Earth field Components
*→ X
◇→ Y
Δ→ Z
□→ B

Figure 16.

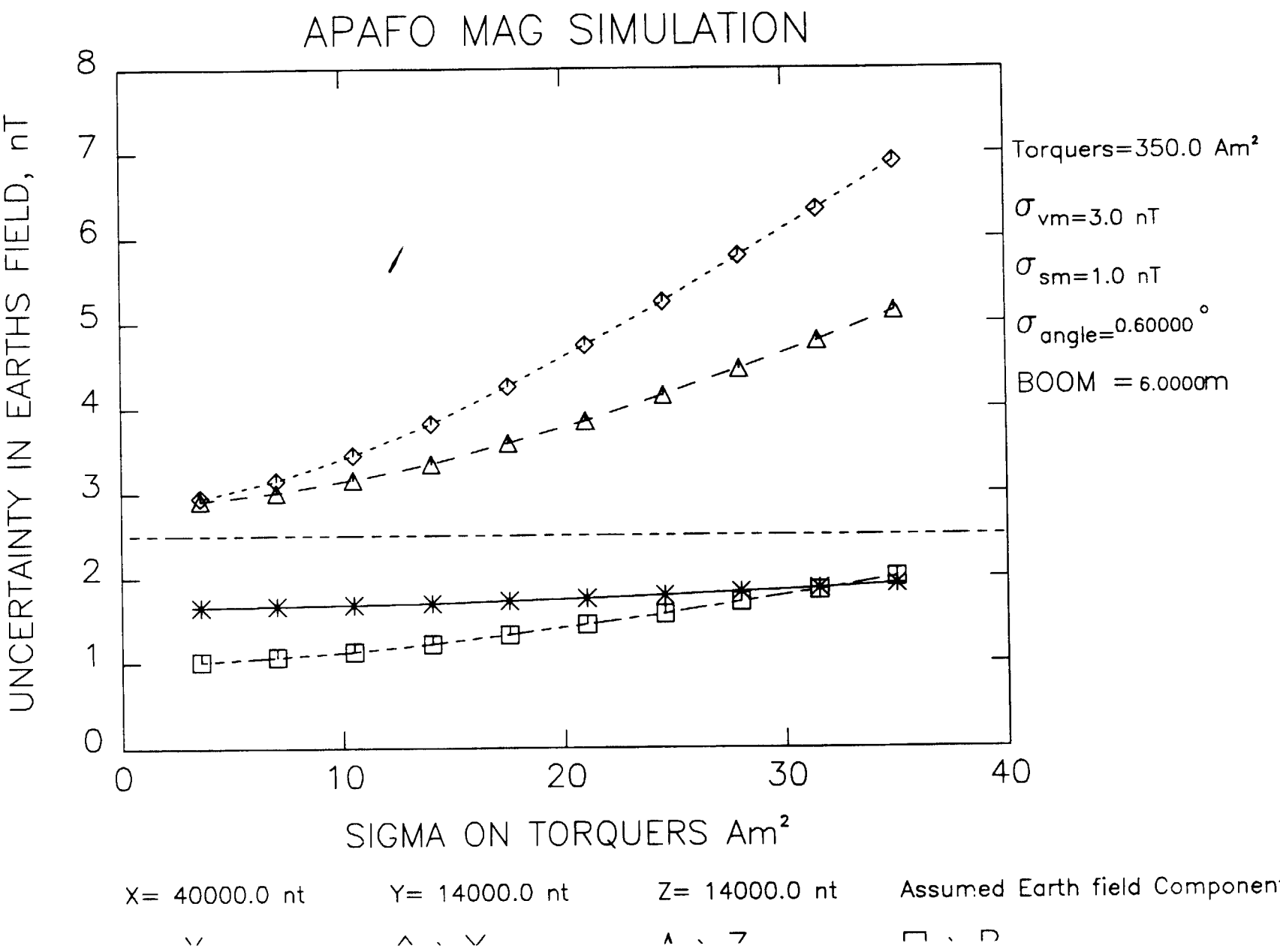
APAFO MAG SIMULATION
UNCERTAINTY IN EARTHS FIELD, nT
SIGMA ON TORQUERS Am²
0
1
2
3
4
5
6
7
8
0
10
20
30
40
Torquers=350.0 Am²
σ vm=3.0 nT
σ sm=1.0 nT
σ angle=0.60000 °
BOOM =6.0000m
X= 40000.0 nt
Y= 14000.0 nt
Z= 14000.0 nt
Assumed Earth field Components

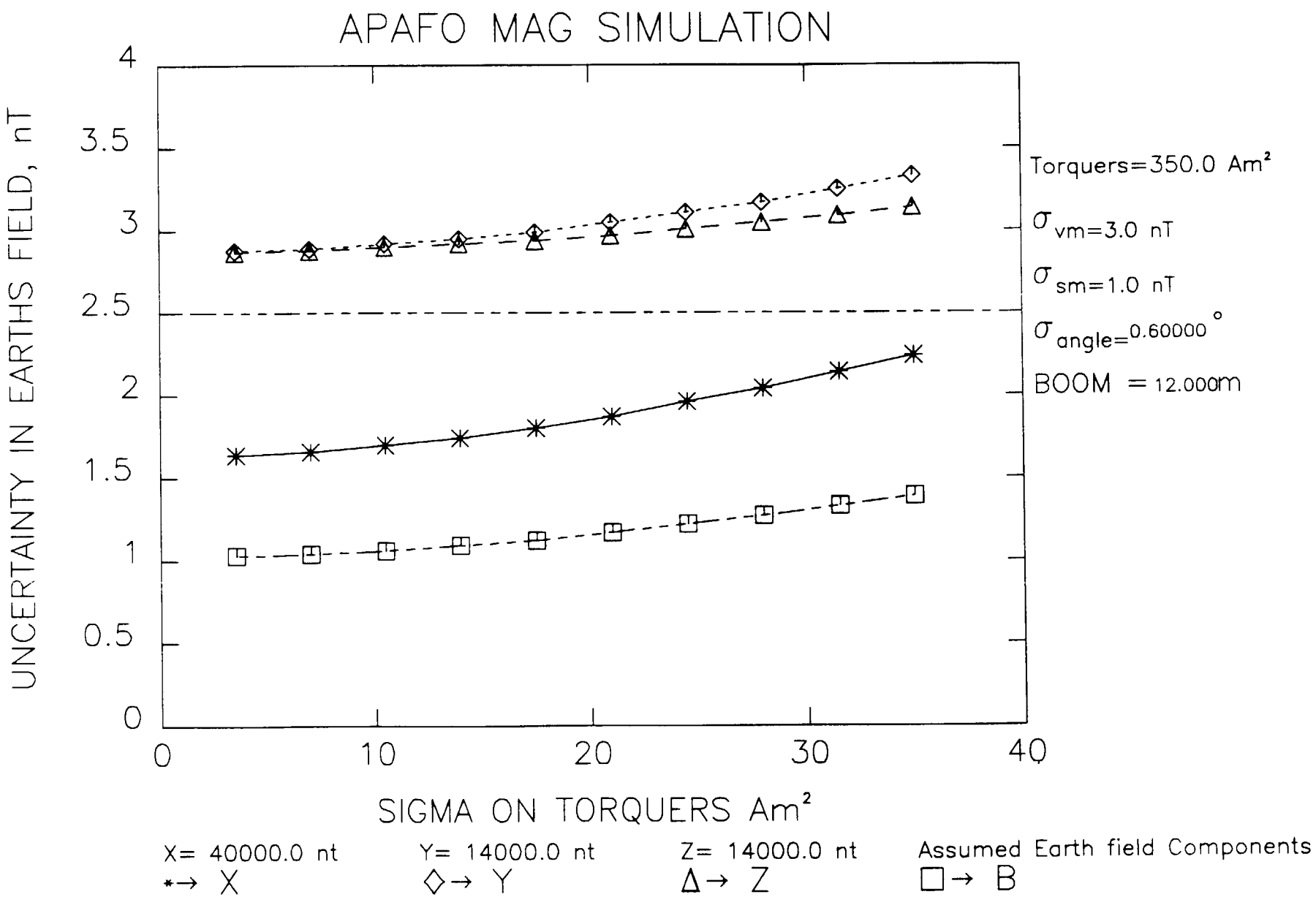
APAFO MAG SIMULATION
UNCERTAINTY IN EARTHS FIELD, nT
SIGMA ON TORQUERS Am²
0
0.5
1
1.5
2
2.5
3
3.5
4
0
10
20
30
40
Torquers=350.0 Am²
σvm=3.0 nT
σsm=1.0 nT
σangle=0.60000°
BOOM =12.000m
X= 40000.0 nt
*→ X
Y= 14000.0 nt
◇→ Y
Z= 14000.0 nt
Δ→ Z
Assumed Earth field Components
□→ B

Figure 18.

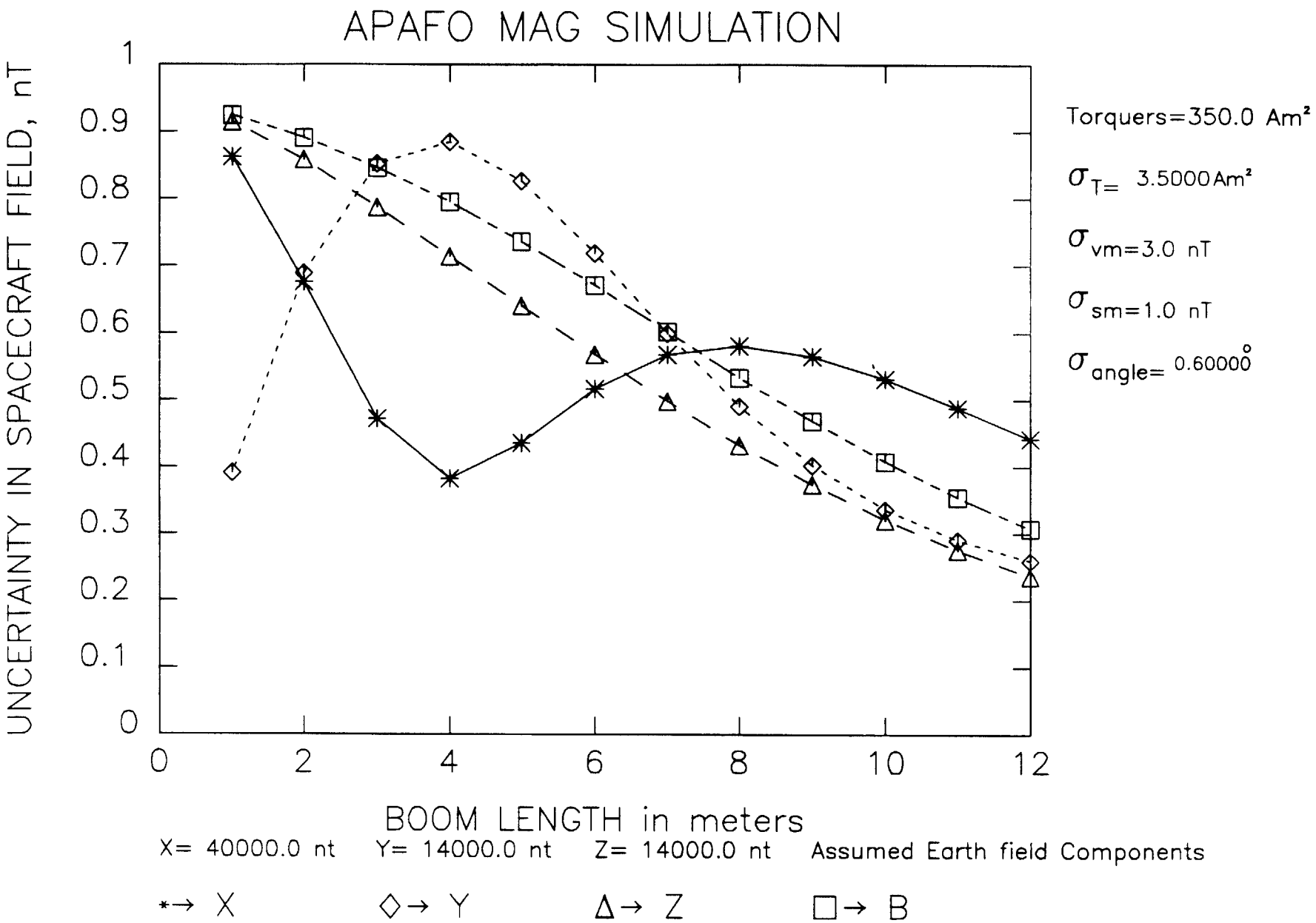
APAFO MAG SIMULATION
UNCERTAINTY IN SPACECRAFT FIELD, nT
1
0.9
0.8
0.7
0.6
0.5
0.4
0.3
0.2
0.1
0
0
2
4
6
8
10
12
BOOM LENGTH in meters
Torquers=350.0 Am²
σ T= 3.5000Am²
σ vm=3.0 nT
σ sm=1.0 nT
σ angle= 0.60000°
X= 40000.0 nt Y= 14000.0 nt Z= 14000.0 nt Assumed Earth field Components
*→ X
◇→ Y
Δ→ Z
□→ B

Figure 19

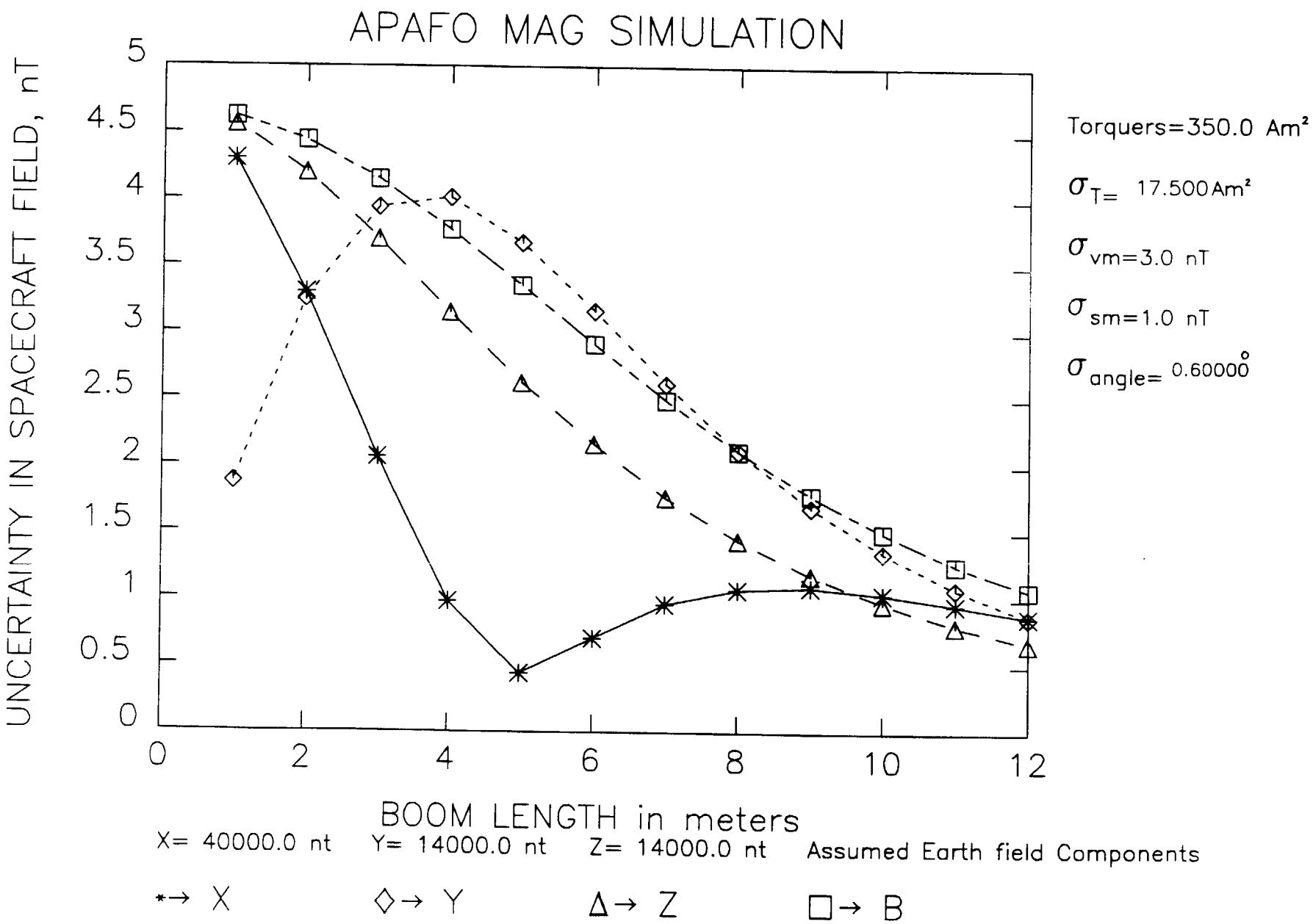
APAFO MAG SIMULATION
UNCERTAINTY IN SPACECRAFT FIELD, nT
0
0.5
1
1.5
2
2.5
3
3.5
4
4.5
5
0
2
4
6
8
10
12
BOOM LENGTH in meters
Torquers=350.0 Am²
σ T= 17.500Am²
σ vm=3.0 nT
σ sm=1.0 nT
σ angle= 0.60000°
X= 40000.0 nt
Y= 14000.0 nt
Z= 14000.0 nt
Assumed Earth field Components
→ X
→ Y
→ Z
→ B

Figure 20.

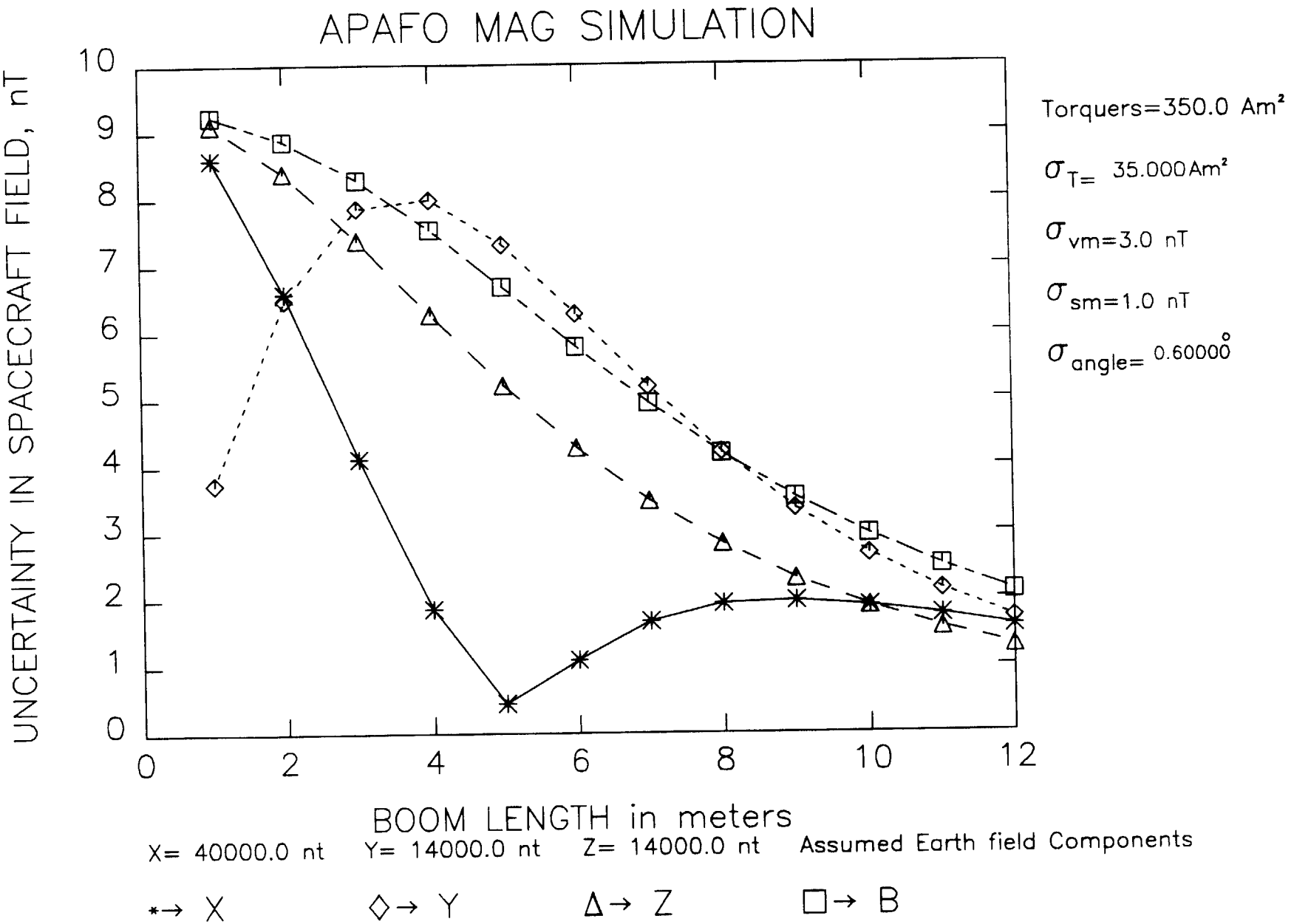
APAFO MAG SIMULATION
UNCERTAINTY IN SPACECRAFT FIELD, nT
BOOM LENGTH in meters
0
1
2
3
4
5
6
7
8
9
10
0
2
4
6
8
10
12
Torquers=350.0 Am²
σT= 35.000Am²
σvm=3.0 nT
σsm=1.0 nT
σangle= 0.60000°
X= 40000.0 nt Y= 14000.0 nt Z= 14000.0 nt Assumed Earth field Components
*→ X
◇→ Y
Δ→ Z
□→ B

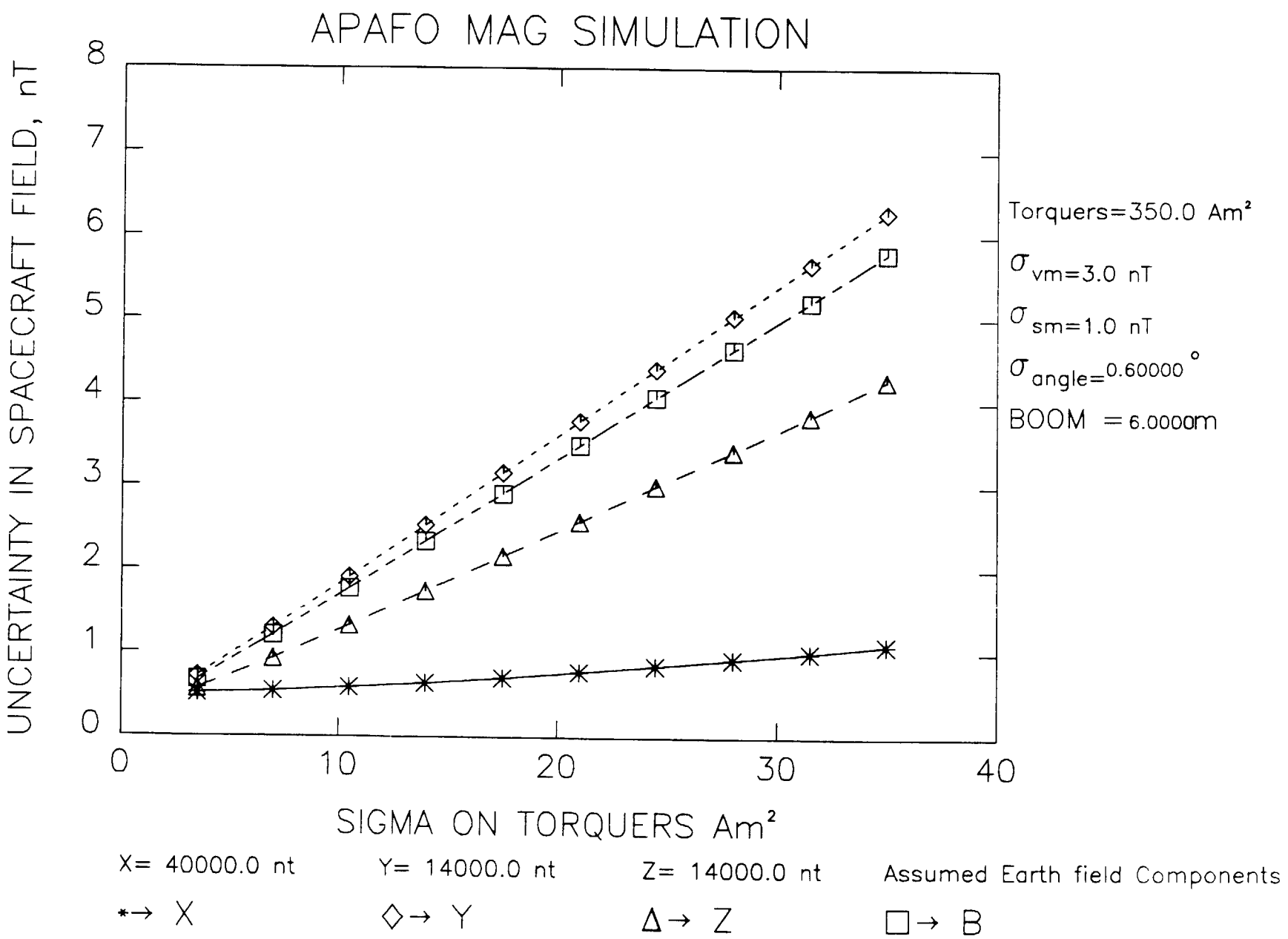
APAFO MAG SIMULATION
UNCERTAINTY IN SPACECRAFT FIELD, nT
0
1
2
3
4
5
6
7
8
0
10
20
30
40
SIGMA ON TORQUERS Am²
Torquers=350.0 Am²
σ vm=3.0 nT
σ sm=1.0 nT
σ angle=0.60000 °
BOOM =6.0000m
X= 40000.0 nt
Y= 14000.0 nt
Z= 14000.0 nt
Assumed Earth field Components
*→ X
◇→ Y
Δ→ Z
□→ B

Figure 22.

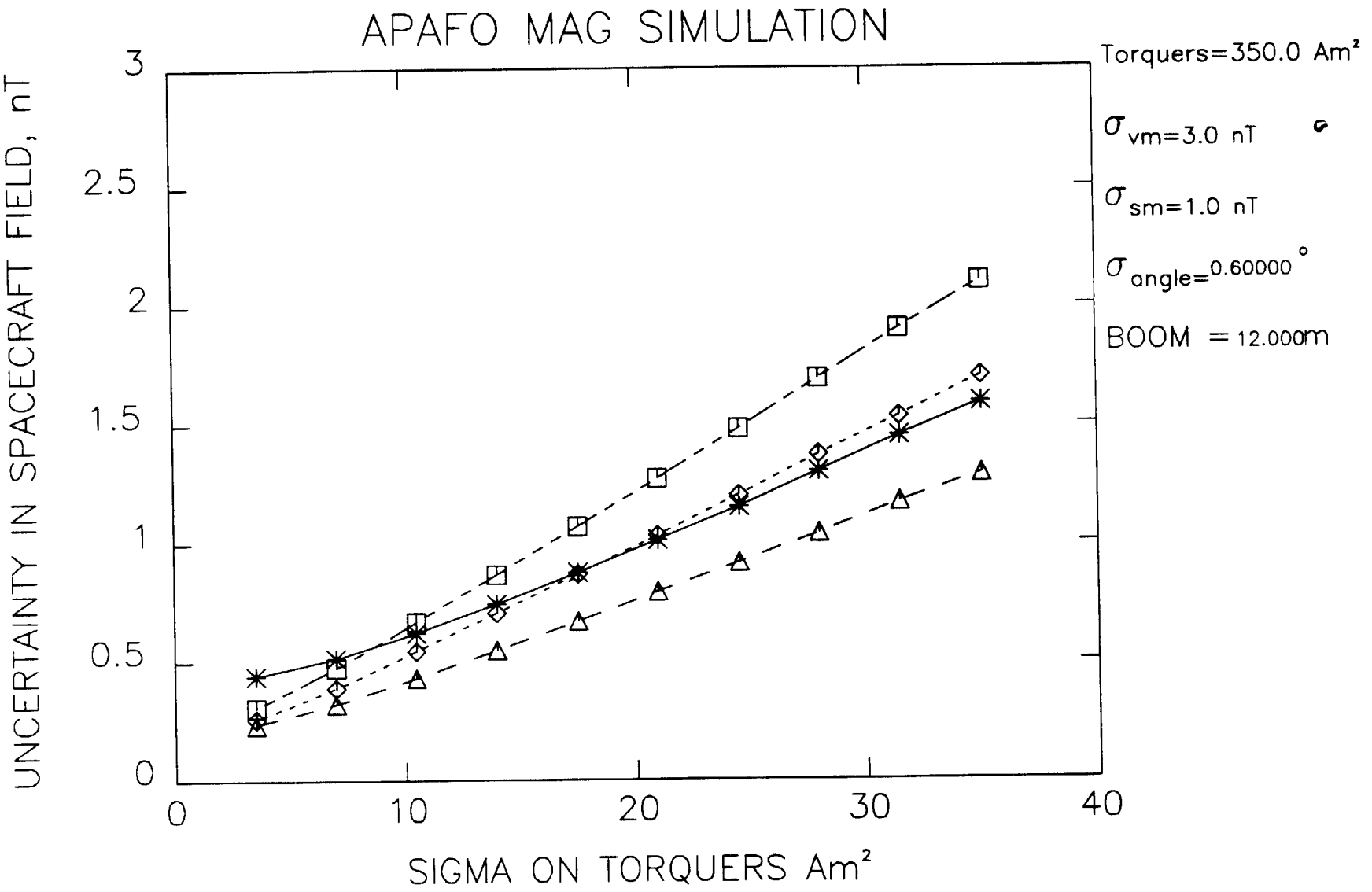
APAFO MAG SIMULATION
UNCERTAINTY IN SPACECRAFT FIELD, nT
SIGMA ON TORQUERS Am²
0
0.5
1
1.5
2
2.5
3
0
10
20
30
40
Torquers=350.0 Am²
σvm=3.0 nT
σsm=1.0 nT
σangle=0.60000°
BOOM = 12.000m
X= 40000.0 nt
*→ X
Y= 14000.0 nt
◇→ Y
Z= 14000.0 nt
Δ→ Z
Assumed Earth field Components
□→ B

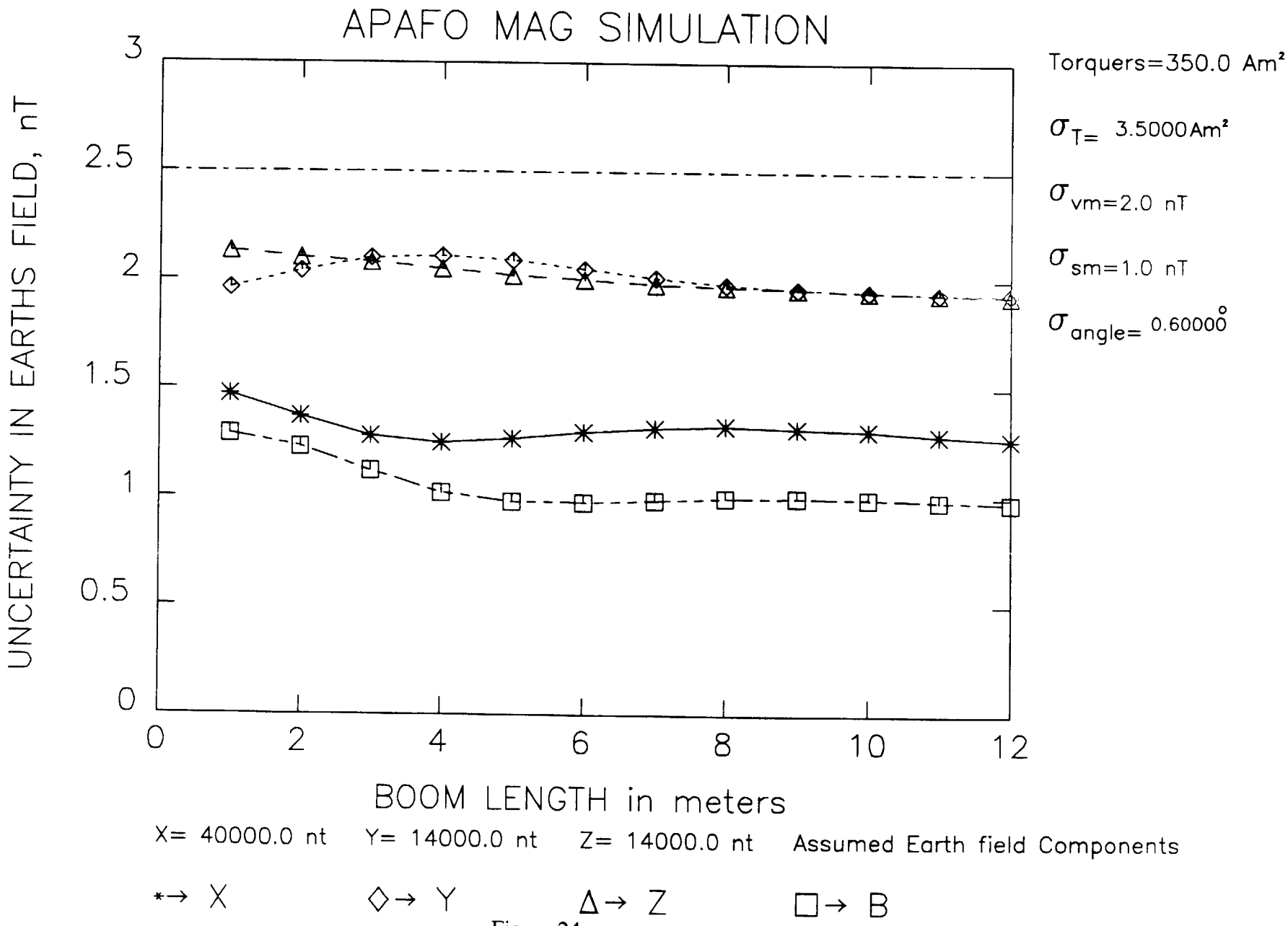
APAFO MAG SIMULATION
UNCERTAINTY IN EARTHS FIELD, nT
BOOM LENGTH in meters
0
0.5
1
1.5
2
2.5
3
0
2
4
6
8
10
12
Torquers=350.0 Am²
σT= 3.5000Am²
σvm=2.0 nT
σsm=1.0 nT
σangle= 0.60000°
X= 40000.0 nt
Y= 14000.0 nt
Z= 14000.0 nt
Assumed Earth field Components
*→ X
◇→ Y
Δ→ Z
□→ B

Figure 24.

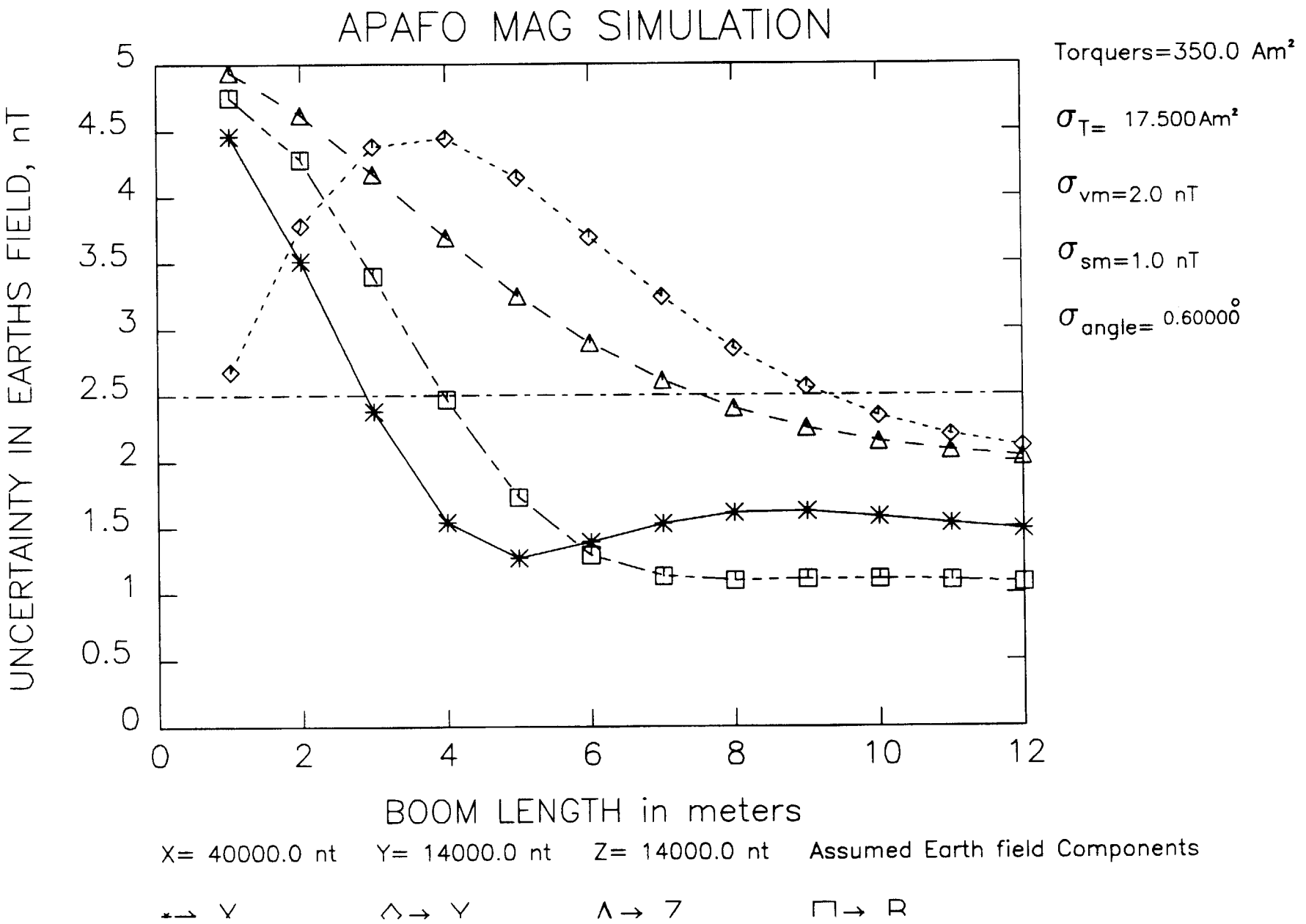
APAFO MAG SIMULATION
Torquers=350.0 Am²
σT= 17.500Am²
σvm=2.0 nT
σsm=1.0 nT
σangle= 0.60000°
UNCERTAINTY IN EARTHS FIELD, nT
0
0.5
1
1.5
2
2.5
3
3.5
4
4.5
5
0
2
4
6
8
10
12
BOOM LENGTH in meters
X= 40000.0 nt Y= 14000.0 nt Z= 14000.0 nt Assumed Earth field Components
→ Y
→ Y
→ Z
→ R

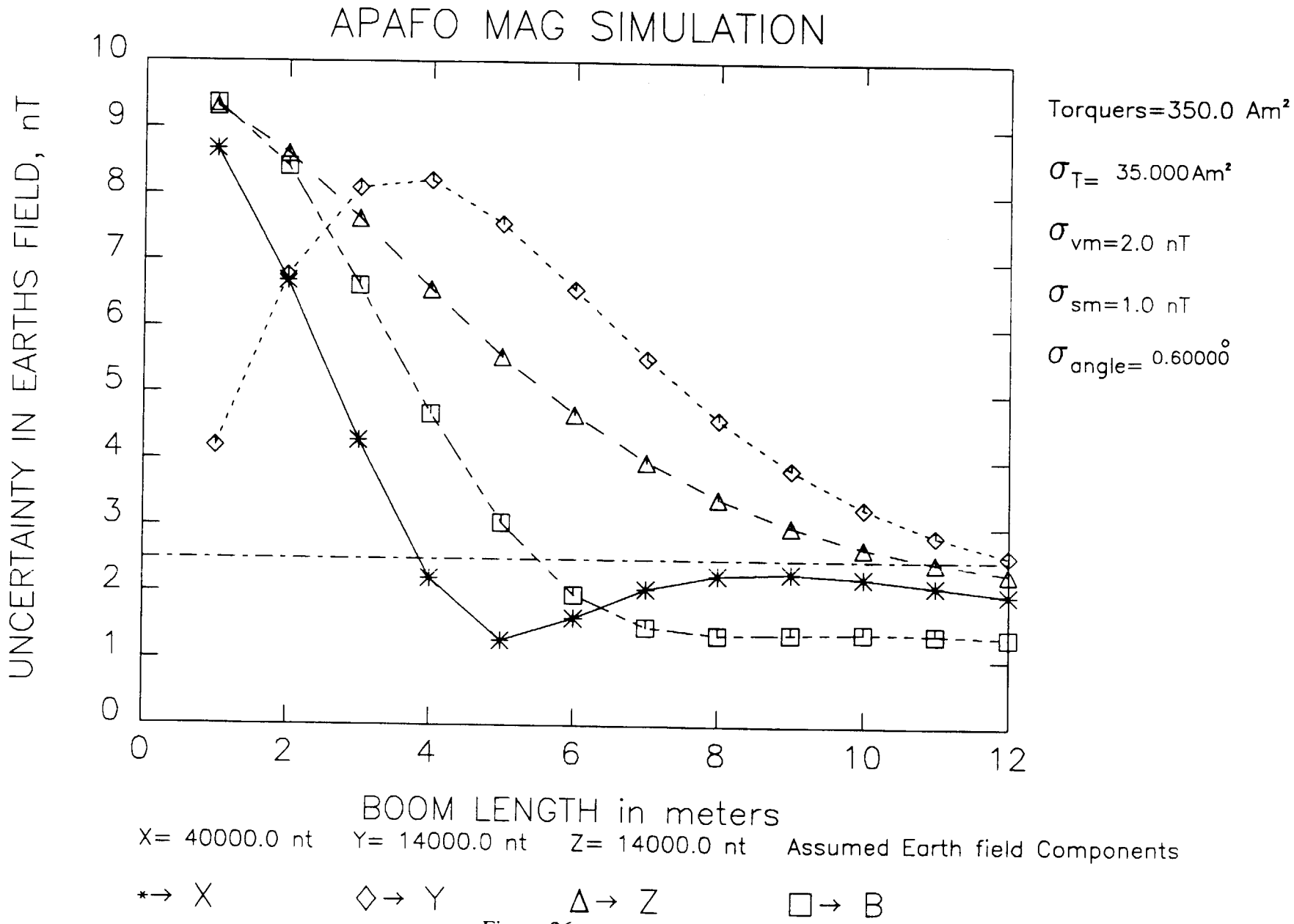
APAFO MAG SIMULATION
UNCERTAINTY IN EARTHS FIELD, nT
BOOM LENGTH in meters
0
1
2
3
4
5
6
7
8
9
10
0
2
4
6
8
10
12
Torquers=350.0 Am²
σT= 35.000Am²
σvm=2.0 nT
σsm=1.0 nT
σangle= 0.60000°
X= 40000.0 nt
Y= 14000.0 nt
Z= 14000.0 nt
Assumed Earth field Components
*→ X
◇→ Y
Δ→ Z
□→ B

Figure 26.

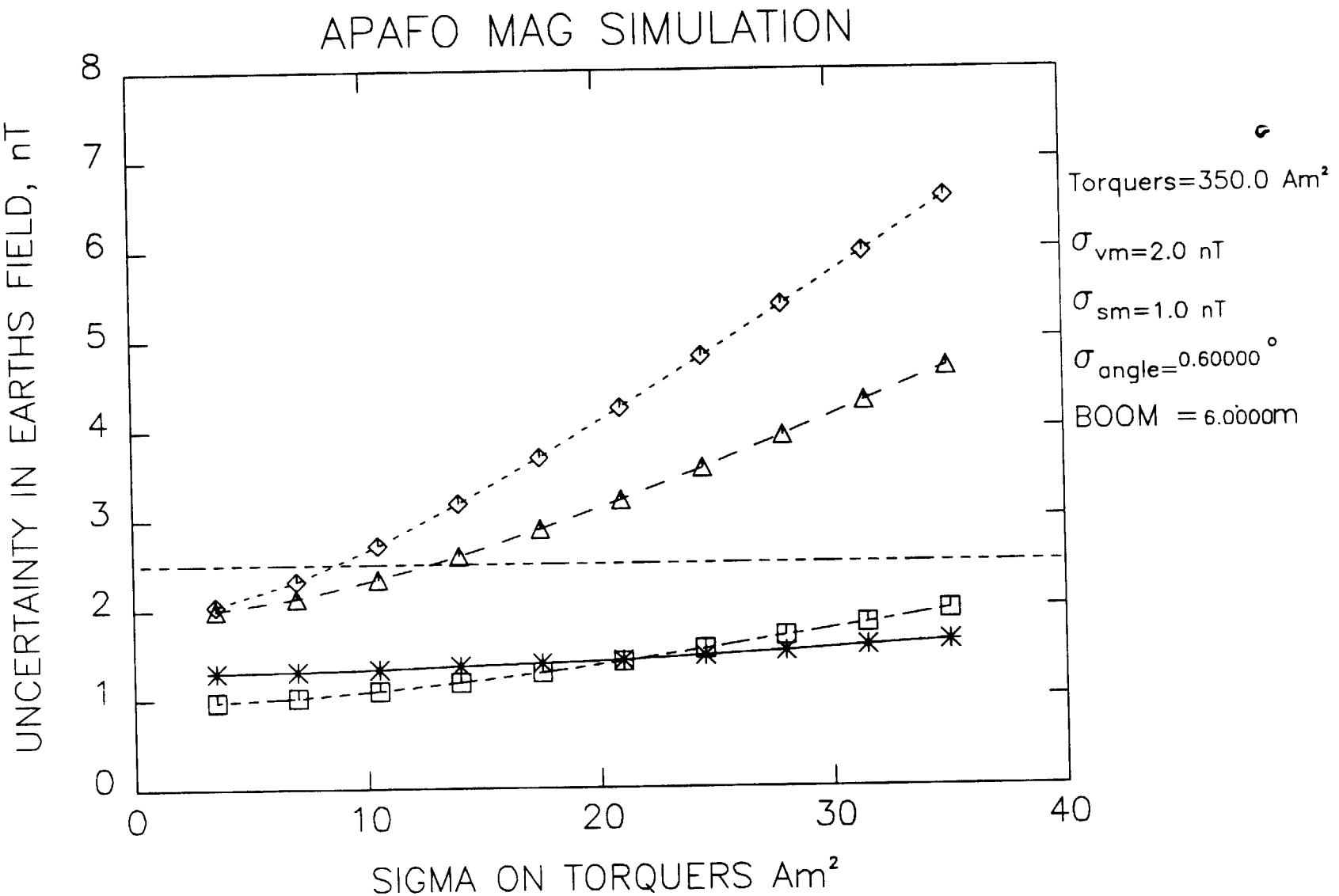
APAFO MAG SIMULATION
UNCERTAINTY IN EARTHS FIELD, nT
SIGMA ON TORQUERS Am²
0
1
2
3
4
5
6
7
8
0
10
20
30
40
Torquers=350.0 Am²
σ vm=2.0 nT
σ sm=1.0 nT
σ angle=0.60000 °
BOOM =6.0000m
X= 40000.0 nt
Y= 14000.0 nt
Z= 14000.0 nt
Assumed Earth field Components

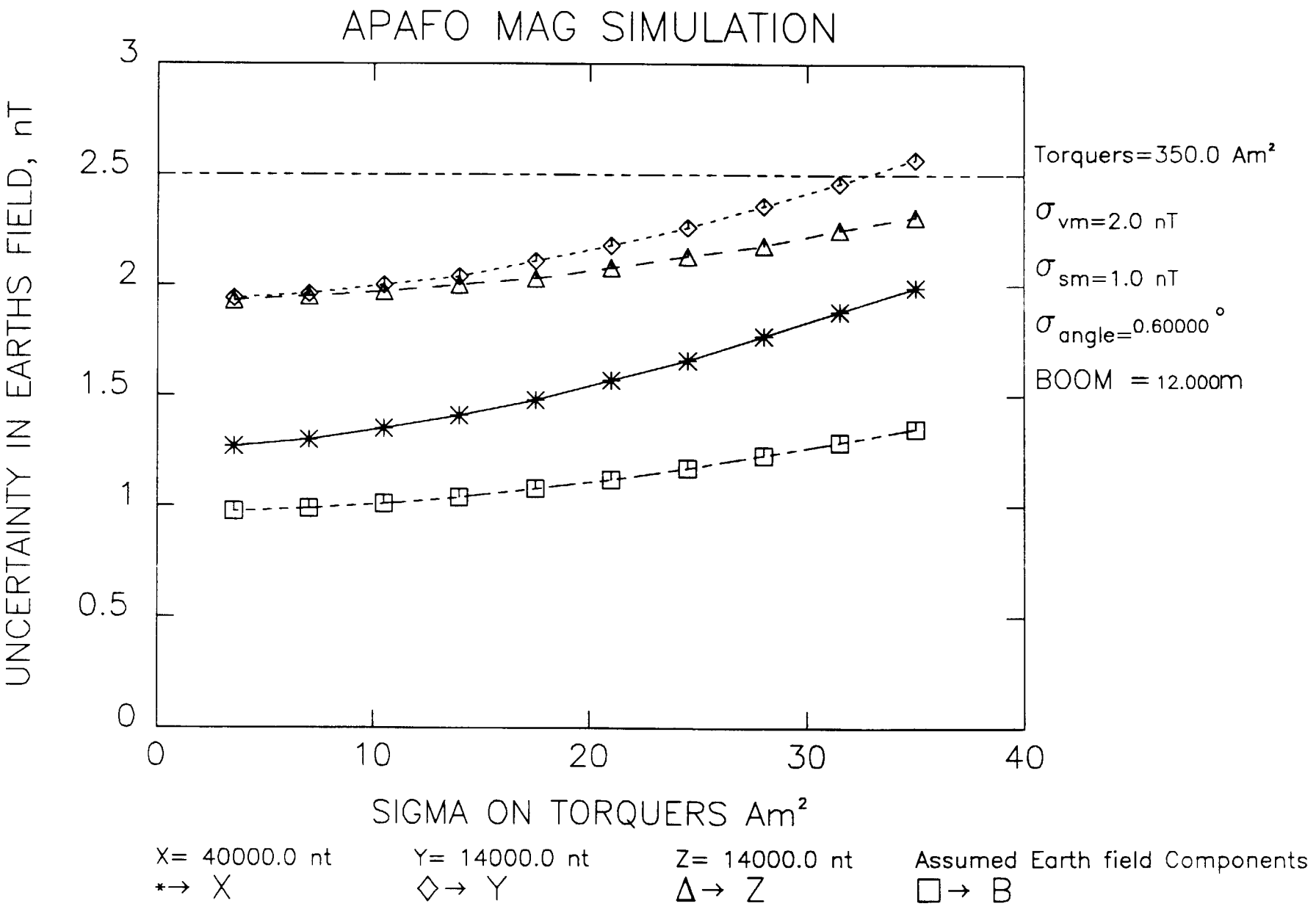
APAFO MAG SIMULATION
UNCERTAINTY IN EARTHS FIELD, nT
SIGMA ON TORQUERS Am²
0
0.5
1
1.5
2
2.5
3
0
10
20
30
40
Torquers=350.0 Am²
σvm=2.0 nT
σsm=1.0 nT
σangle=0.60000°
BOOM =12.000m
X= 40000.0 nt
*→ X
Y= 14000.0 nt
◇→ Y
Z= 14000.0 nt
Δ→ Z
Assumed Earth field Components
□→ B

Figure 28.

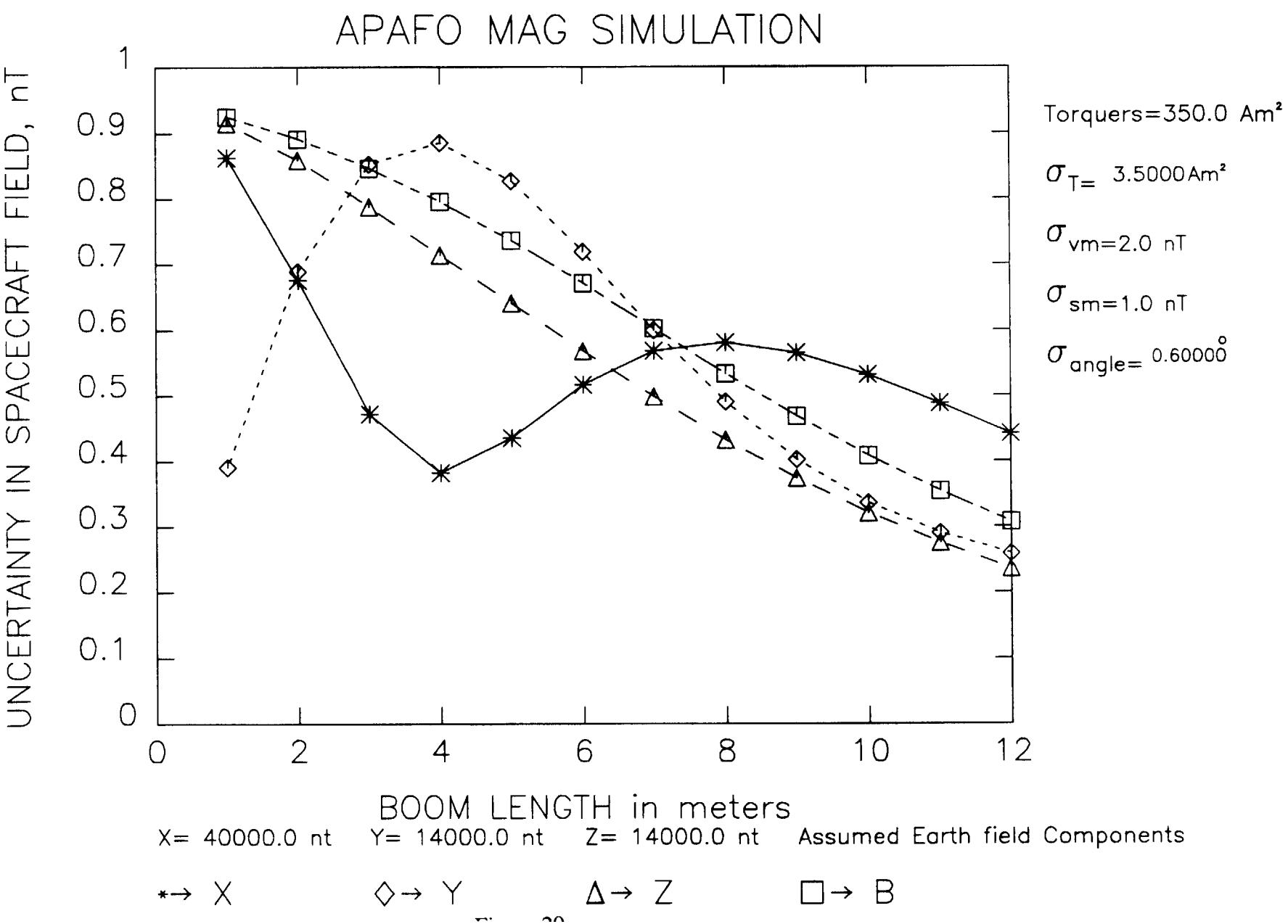
APAFO MAG SIMULATION
UNCERTAINTY IN SPACECRAFT FIELD, nT
1
0.9
0.8
0.7
0.6
0.5
0.4
0.3
0.2
0.1
0
0
2
4
6
8
10
12
BOOM LENGTH in meters
Torquers=350.0 Am²
σT= 3.5000Am²
σvm=2.0 nT
σsm=1.0 nT
σangle= 0.60000°
X= 40000.0 nt Y= 14000.0 nt Z= 14000.0 nt Assumed Earth field Components
*→ X
◇→ Y
Δ→ Z
□→ B

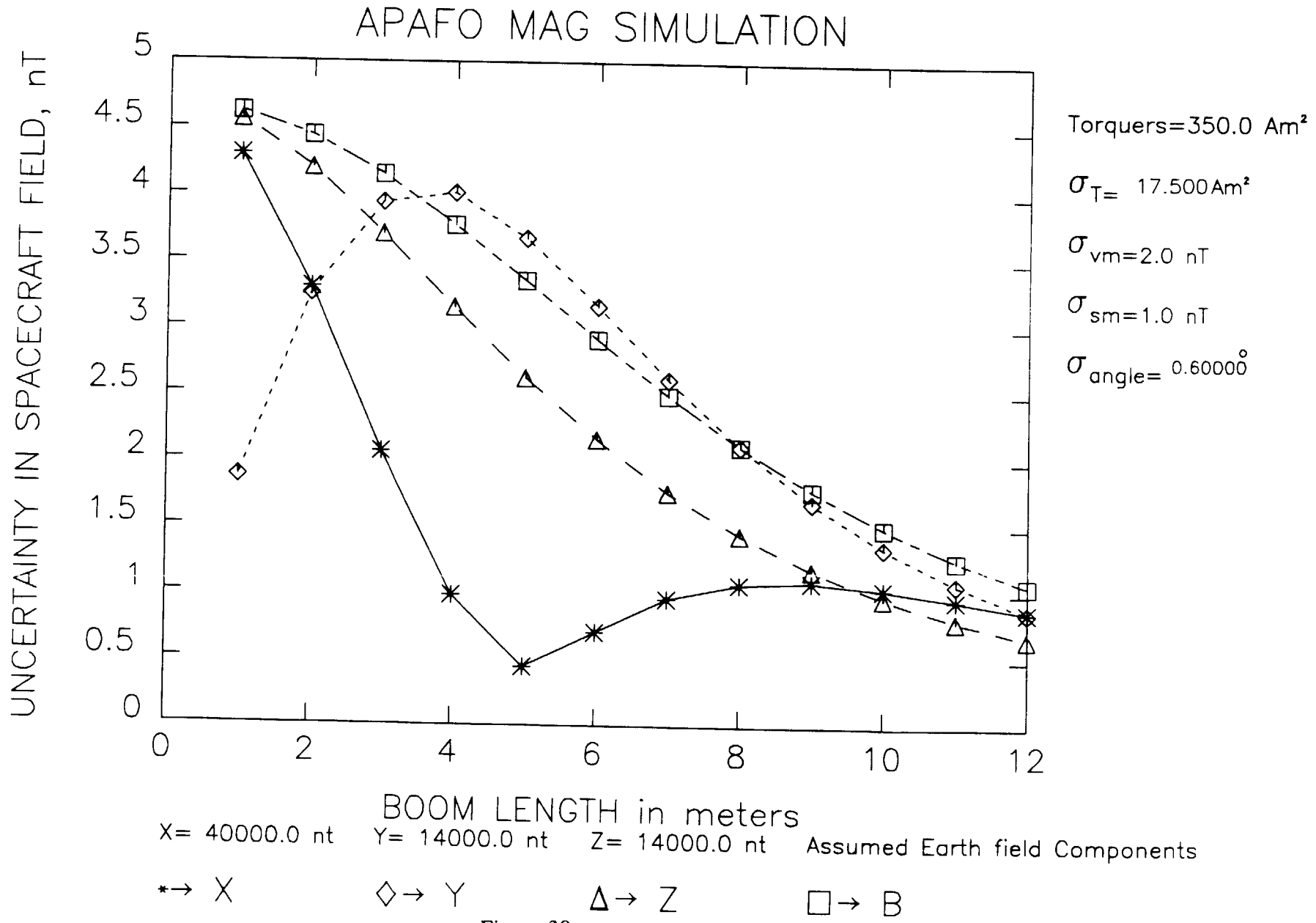
APAFO MAG SIMULATION
UNCERTAINTY IN SPACECRAFT FIELD, nT
0
0.5
1
1.5
2
2.5
3
3.5
4
4.5
5
0
2
4
6
8
10
12
BOOM LENGTH in meters
Torquers=350.0 Am²
σT= 17.500Am²
σvm=2.0 nT
σsm=1.0 nT
σangle= 0.60000°
X= 40000.0 nt
Y= 14000.0 nt
Z= 14000.0 nt
Assumed Earth field Components
*→ X
◇→ Y
Δ→ Z
□→ B

Figure 30.

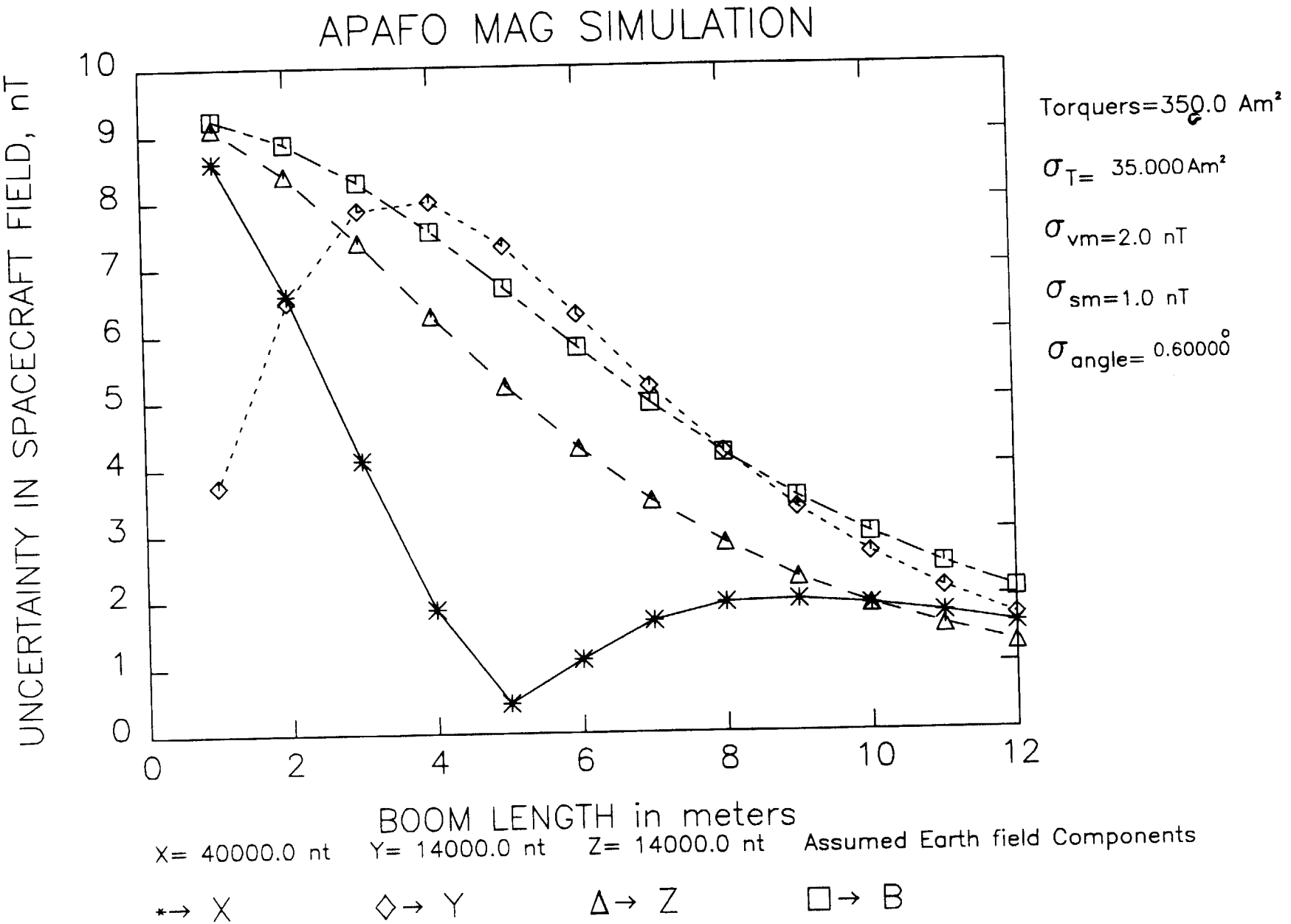
APAFO MAG SIMULATION
UNCERTAINTY IN SPACECRAFT FIELD, nT
BOOM LENGTH in meters
0
2
4
6
8
10
12
0
1
2
3
4
5
6
7
8
9
10
Torquers=350.0 Am²
σT= 35.000 Am²
σvm=2.0 nT
σsm=1.0 nT
σangle= 0.60000°
X= 40000.0 nt
Y= 14000.0 nt
Z= 14000.0 nt
Assumed Earth field Components
*→ X
◇→ Y
Δ→ Z
□→ B

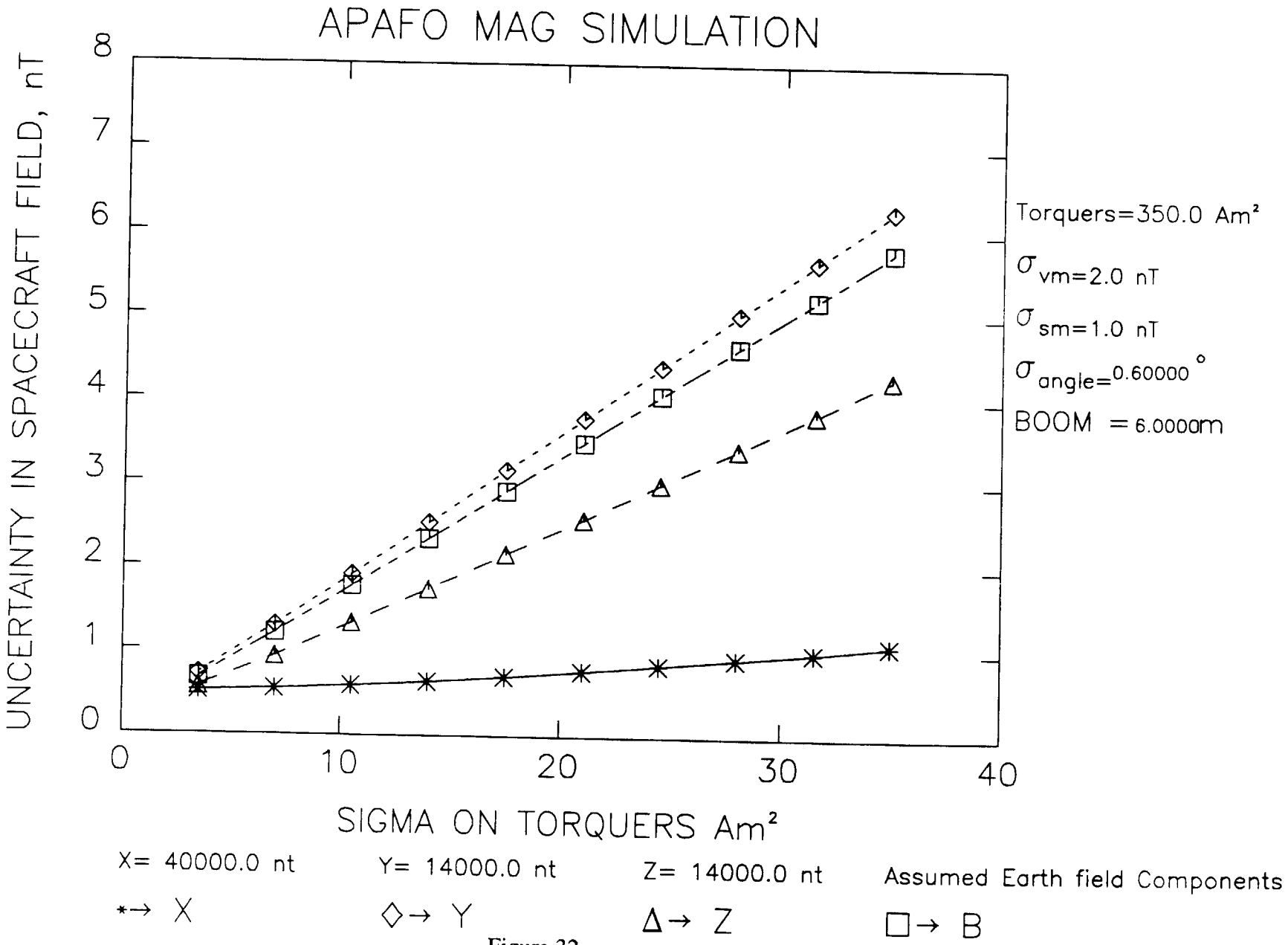
APAFO MAG SIMULATION
UNCERTAINTY IN SPACECRAFT FIELD, nT
SIGMA ON TORQUERS Am²
0
1
2
3
4
5
6
7
8
0
10
20
30
40
Torquers=350.0 Am²
σvm=2.0 nT
σsm=1.0 nT
σangle=0.60000°
BOOM =6.0000m
X= 40000.0 nt
Y= 14000.0 nt
Z= 14000.0 nt
Assumed Earth field Components
*→ X
◇→ Y
Δ→ Z
□→ B

Figure 32.

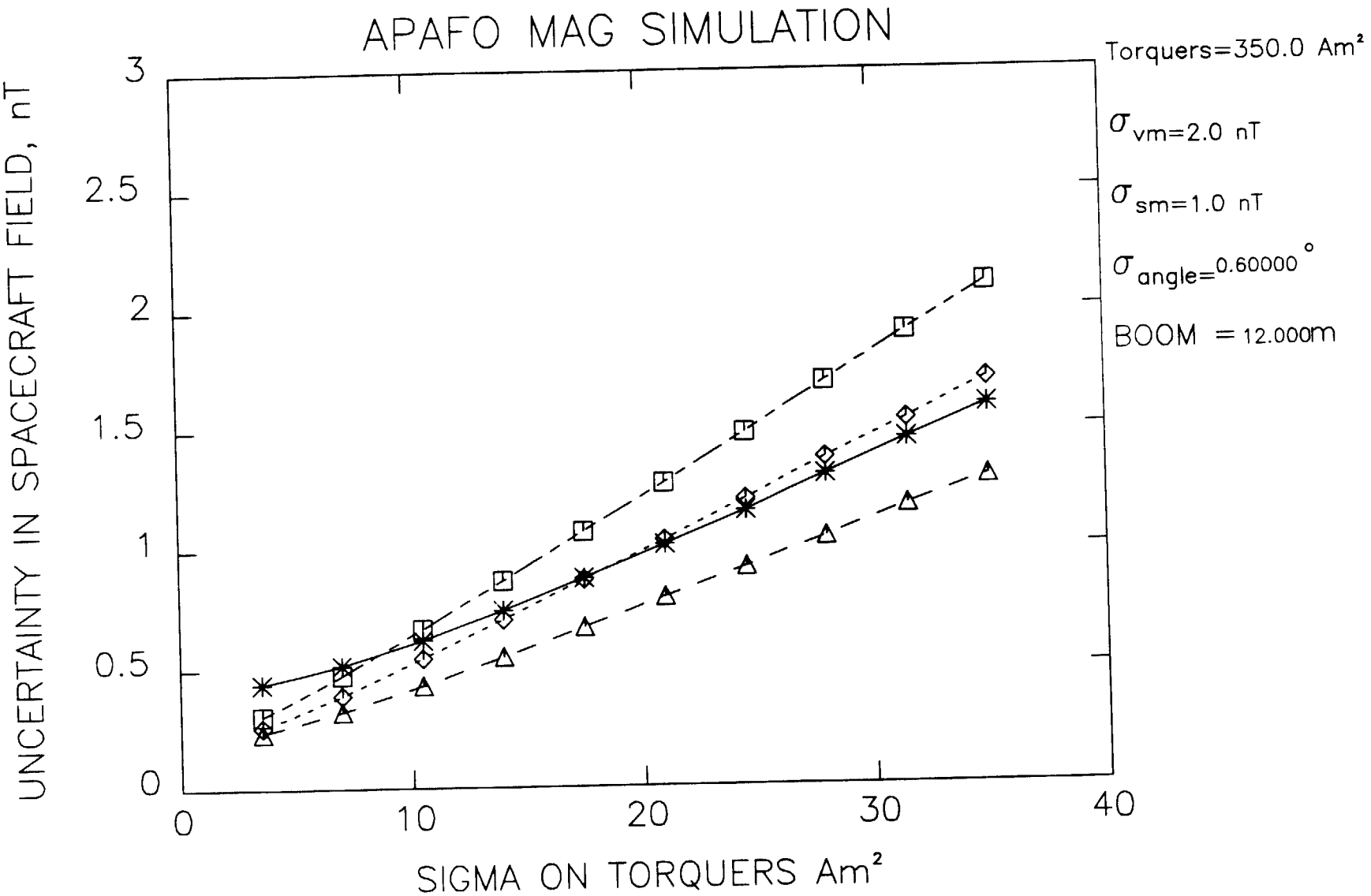
APAFO MAG SIMULATION
Torquers=350.0 Am²
σvm=2.0 nT
σsm=1.0 nT
σangle=0.60000°
BOOM =12.000m
UNCERTAINTY IN SPACECRAFT FIELD, nT
SIGMA ON TORQUERS Am²
0
0.5
1
1.5
2
2.5
3
0
10
20
30
40
X= 40000.0 nt
Y= 14000.0 nt
Z= 14000.0 nt
Assumed Earth field Components

NASA
National Aeronautics and Space Administration

Report Documentation Page

1. Report No.	2. Government Accession No.	3. Recipient's Catalog No.
NASA TM 104545		

4. Title and Subtitle	5. Report Date
Preliminary Calibration Plan for the Advanced Particles and Field Observatory (APAFO) Magnetometer Experiment	July 1991
	6. Performing Organization Code: 921.0

7. Author(s)	8. Performing Organization Report No.
C.V. Voorhies, R.A. Langel, J. Slavin, E.R. Lancaster, and S. Jones	91B00119
	10. Work Unit No.

9. Performing Organization Name and Address	11. Contract or Grant No.
Goddard Space Flight Center Greenbelt, Maryland 20771	

12. Sponsoring Agency Name and Address	13. Type of Report and Period Covered
National Aeronautics and Space Administration Washington, D.C. 20546-0001	Technical Memorandum
	14. Sponsoring Agency Code

15. Supplementary Notes

C.V. Voorhies and R.A. Langel: Geodynamics Branch, NASA-GSFC, Greenbelt, Maryland;
J. Slavin: Electrodynamics Branch, NASA-GSFC, Greenbelt, Maryland;
E.R. Lancaster and S. Jones: ST Systems Corporation, Lanham, Maryland.

16. Abstract

Pre-launch and post-launch calibration plans for the APAFO magnetometer experiment are presented. A study of trade-offs between boom length and spacecraft field is described; the results are summarized. The pre-launch plan includes: calibration of the Vector Fluxgate Magnetometer (VFM), Star Sensors, and Scalar Helium Magnetometer (SHM); optical bench integration; and acquisition of basic spacecraft field data. Post-launch calibration has two phases. In phase one, SHM data are used to calibrate the VFM, total vector magnetic-field data are used to calibrate a physical model of the spacecraft field, and both calibrations are refined by iteration. In phase two, corrected vector data are transformed into geocentric coordinates, previously undetected spacecraft fields are isolated, and initial geomagnetic field models are computed. Provided the SHM is accurate to the required 1.0 nT and can be used to calibrate the VFM to the required 3.0- nT accuracy, the trade-off study indicates that a 12-m boom and a spacecraft field model uncertainty of 5 percent together allow the 1.0-nT spacecraft field error requirement to be met.

17. Key Words (Suggested by Author(s))	18. Distribution Statement
APAFO, Magnetometer Calibration	Unclassified - Unlimited Subject Category 19

19. Security Classif. (of this report)	20. Security Classif. (of this page)	21. No. of pages	22. Price
Unclassified	Unclassified	81	